Universidade de Aveiro Departamento de Ciências Médicas

Universidade NOVA de Lisboa
2018

Faculdade de Ciências Médicas

Ana Rita Filgueiras Ferreira

Peroxissomas e infeções virais: para além da defesa antiviral

Peroxisomes and viral infections: antiviral defense and beyond

Universidade de Aveiro Departamento de Ciências Médicas

Universidade NOVA de Lisboa
2018 Faculdade de Ciências Médicas

Ana Rita Filgueiras Ferreira

Peroxissomas e infeções virais: para além da defesa antiviral

Peroxisomes and viral infections: antiviral defense and beyond

Thesis submitted at University of Aveiro to fulfil the requirements to obtain the Doctor degree in Biomedicine, held under the scientific guidance of Dr. Daniela Ribeiro, Post-Doctoral Researcher at the Department of Medical Sciences at University of Aveiro, and Dr. Jonathan Kagan, Associate Professor at Harvard Medical School.

Tese apresentada à Universidade de Aveiro para cumprimento dos requisitos necessários à obtenção do grau de Doutor em Biomedicina, realizada sob a orientação científica da Dra. Daniela Ribeiro, Investigadora em pós-doutoramento no Departamento de Ciências Biomédicas da Universidade de Aveiro, e pelo Dr. Jonathan Kagan, Professor Associado da Harvard Medical School

Dedico este trabalho aos meus pais e família pelo incansável apoio.

o júri

presidente   Professor Doutor Helmuth Robert Malonek
professor catedrático, Universidade de Aveiro

Doutor Markus Islinger
professor associado, Universidade de Heidelberg

Doutor Jorge Eduardo da Silva Azevedo
professor catedrático, Universidade do Porto

Doutora Maria João Lopes Gonçalves de Brito Amorim
investigadora auxiliar, Instituto Gulbenkian de Ciência

Doutora Ana Raquel Santos Calhôa Mano Soares
investigadora de pós-doutoramento, Universidade de Aveiro - Departamento
de Ciências Médicas

Doutora Daniela Maria Oliveira Gandra Ribeiro
investigadora de pós-doutoramento, Universidade de Aveiro - Departamento
de Ciências Médicas

agradecimentos

To Daniela, thank you for giving me this opportunity and for believing in me (even when I had my doubts). You have helped me grow as a scientist. I am so grateful. Thank you!

To Jon, thank you for receiving me at your lab. It was an incredible experience to work there. Thank you for all the knowledge that you shared. I am so grateful for the opportunity.

To all the other members and ex-members of ODID lab, thank you all for sharing so many moments at the lab and outside it. I have learned so much with you. A special thank you to Isabel, we started this journey together and because of it we have shared a lot of good and bad moments (or it would not be a PhD). And also to Mariana, for helping me with our crazy experiments and being there even at distance. Thank you both for your friendship.

To all the colleagues in Kagan's lab, thank you for having me on the team, for all the brainstorms and happy hours. To Megan, a special thank you for being there for all the questions that I had.

To all the new friends that I made in Boston, you made my stay in Boston unforgettable. Thank you for all the trips, dinners and nights. It was 9 months of amazing adventures!

To the "special ones", thank you for having my back in the good and bad moments, even with a 5 hours' time zone difference (6 in one case), and for reminding me that I have a life outside the lab.

Por ultimo, aos meus pais e à minha família,
sem vocês não estaria aqui, vocês são o meu suporte e eu sei que o vosso apoio é incondicional. Obrigada por acreditarem em mim!

"If you want to go fast, go alone. If you want to go far, go together."
"Se quer ir rápido, vá sozinho. Se quer ir longe, vá acompanhado."

palavras-chave

Peroxissomas, imunidade inata celular, defesa antiviral, MAVS, HCV, HCMV, NS3-4A, vMIA.

resumo

Os peroxissomas são organelos intracelulares multifuncionais, cruciais para diferentes processos fisiológicos e patológicos. Recentemente, a MAVS, proteína adaptadora mitocondrial essencial para a defesa antiviral mediada pelos recetores RLR, foi identificada nos peroxissomas.

Após infeção, o ácido ribonucleico viral é reconhecido pelos recetores RLRs que induzem uma cascata de sinalização que se inicia com a ativação da MAVS, tanto nas mitocôndrias como nos peroxissomas, culminando com a produção de efetores antivirais, tais como interferões do tipo I e genes induzidos pelos interferões (ISGs), que impedem a replicação e disseminação viral. Foi demonstrado que as MAVS peroxissomais e mitocondriais atuam de forma complementar: a MAVS peroxissomal induz uma resposta rápida, mas de curto prazo, enquanto que a MAVS mitocondrial leva a uma resposta antiviral tardia, porém duradoura.

O objetivo deste trabalho foi compreender a importância dos peroxissomas na defesa antiviral celular e nas infeções virais. Os resultados apresentados nesta tese provam que a NS3-4A do vírus da hepatite C (HCV) e a vMIA do citomegalovírus humano (HCMV) exploram os peroxissomas para inibir a sinalização antiviral dependente da MAVS, impedindo a produção dos ISGs. Mostramos que a NS3-4A inibe a sinalização dependente dos peroxissomas através da clivagem do domínio citosólico da MAVS e também mostramos que a vMIA interage com a MAVS peroxissomal, inibindo a sua oligomerização e impedindo a sinalização a jusante. Para além disso, a vMIA induz a fragmentação peroxissomal, que provamos ser independente da inibição da sinalização antiviral. Mostramos também que a vMIA é dependente da MFF, uma proteína adaptadora da fissão peroxissomal, e demonstramos que a MFF medeia a interação entre a vMIA e a MAVS peroxissomal. Finalmente, apresentamos um interatoma das interações proteína-proteína entre vírus humanos e peroxissomas, revelando que vírus distintos interagem com diferentes proteínas peroxissomais. Uma análise detalhada das interações identificadas revelou que o metabolismo lipídico pode ser a principal função peroxissomal explorada pelos vírus, possivelmente para aumentar a infeção viral, ou para a defesa do hospedeiro celular.

Em conjunto, estes resultados reforçam o papel dos peroxissomas como plataformas para a sinalização dos RLRs e, além disso, sugerem que a sua importância para a infeção viral pode ir além da defesa antiviral. Novos estudos são propostos para compreender melhor o papel dos peroxissomas na infeção viral, o que pode levar à descoberta de novos alvos para o desenvolvimento de terapias antivirais.

keywords

abstract

Peroxisomes are multifunctional intracellular organelles, crucial for different physiological and pathological processes. Recently, MAVS (mitochondrial antiviral signaling), the mitochondrial adaptor protein essential for the RLR (retinoic acid inducible gene I-like receptors)-mediated antiviral defense was identified at peroxisomes.

Upon infection, viral RNA is recognized by RLRs which induce a signaling cascade that initiates with MAVS activation at both mitochondria and peroxisomes. This culminates with the production of antiviral effectors, such as type I IFNs (interferons) and ISGs (IFN-stimulated genes) that prevent viral replication and dissemination. It has been demonstrated that peroxisomal and mitochondrial MAVS act together in a complementing manner: peroxisomal MAVS induces a rapid but short-term response, while mitochondrial MAVS leads to a delayed but long-lasting antiviral response.

The aim of this work was to understand the importance of peroxisomes in the cellular antiviral defense and in viral infections. The results presented in this thesis prove that HCV (hepatitis C virus) NS3-4A and HCMV (human cytomegalovirus) vMIA target peroxisomes to inhibit peroxisomal MAVS-dependent antiviral signaling, impairing the production of ISGs. We show that NS3-4A inhibits peroxisomal-dependent signaling through the cleavage of peroxisomal MAVS cytosolic domain. We also show that vMIA interacts with peroxisomal MAVS, inhibiting its oligomerization and impairing the downstream signaling. Additionally, vMIA induces peroxisomal fragmentation, which we prove to be independent of the vMIA-mediated peroxisomal MAVS inhibition. Moreover, we show that vMIA is dependent of MFF, an adaptor protein of peroxisomal fission machinery, and we demonstrate that MFF mediates the interaction between vMIA and peroxisomal MAVS. Finally, we present an interactome of protein-protein interactions between human viruses and peroxisomes, revealing that distinct viruses target peroxisomal proteins. A detailed analysis of the identified interaction revealed that lipid metabolism may be the main peroxisomal function exploited by viruses, possibly to enhance viral infection, or for cellular host defense.

Altogether, these results enforce the role of peroxisomes as platforms for RLR signaling and, moreover, suggest that their importance for viral infection may go beyond the antiviral defense. Further studies are proposed to better disclose the role of peroxisomes in viral infection, which can ultimately lead to the discovery of novel targets for the development antiviral therapeutics.

List of Abbreviations

(+)ssRNA	positive single strand RNA
5'pppRNA	5' triphosphate RNA
Acetyl-CoA	acetyl coenzyme A
ACOT8	acyl-coenzyme A thioesterase 8
ACOX	acyl-CoA oxidase
Acyl-CoA	long-chain fatty acid-Acyl-CoA
AGPS	Alkyldihydroxyacetonephosphate synthase
AP-1	activator protein 1
ATP	adenosine triphosphate
BCFA	branched-chain fatty acids
CARDIF	CARD adaptor inducing IFN- β
CARDs	caspase recruitment domains
CD81	cluster differentiation 81
cGAS	cyclic GMP-AMP synthase
CLDN1	claudin 1
DAI	DNA-dependent activator of interferon regulatory factor
DLP1	dynamin-like protein
DNA	deoxynucleic acids
dsDNA	double-stranded deoxyribonucleic acid
dsRNA	double-stranded RNA
E	early
ER	endoplasmic reticulum
ERIS	ER IFN stimulator
FAR	fatty Acyl-CoA Reductase
FIS1	mitochondrial fission factor 1
GAGs	glycosaminoglycans
GNPAT	glyceronephosphate O-Acyltransferase
GTPase	guanin triphosphate enzyme
HBV	hepatitis B virus
HCV	hepatitis C virus
HHV	human herpesvirus
HIV	human immunodeficiency virus
hrs	hours
HSD17B4	peroxisomal multifunctional enzyme type 2
HSV	herpes simplex virus

IAV	influenza A virus
IBV	influenza B virus
IE	immediate early
IFNAR	interferon alfa/beta receptor complex
IFNLR	interferon lambda receptor complex
IFNs	interferons
IKK	IκB kinase
IPS-1	IFN-β promoter stimulator-1
IRES	internal ribosomal entry site
IRFs	interferons regulatory factors
ISG	interferon-stimulated genes
KO	knock-out
L	late
LDL	lipoproteins
LDLR	low-density lipoprotein receptors
LDs	lipid droplets
LGP2	laboratory of genetics and physiology 2
LVPs	lipoviroproteins
MAM	mitochondria associated membranes
MAPKs	mitogen-activated protein kinases
MAVS	mitochondrial antiviral signaling
MDA-5	melanoma differentiation-associated gene-5
Mefs	mouse embryonic fibroblasts
MFF	mitochondrial fission factor
MHC1	major histocompatibility complex classe I
min	minutes
MITA	mediator of IRF3 activation
MPYS	methionine-proline-tyrosine-serine
mRNAs	mature RNAs
MyD88	myeloid differentiation primary response 88
NF-κB	nuclear factor kappa-light-chain enhancer of activated B cells
NLR	nucleotide oligomerization domain-like receptors
OAS	2',5'-oligoadenylate synthase
OCLN	occluding
PAMPs	pathogen-associated molecular patterns
PKR	protein kinase RNA-activated
PMPs	peroxisomal membrane proteins
PPIs	protein-protein interactions

PPRα	proliferator-activated receptor α
PRRs	pattern recognition receptors
RdRp	RNA-dependent RNA polymerase
RIG-I	retinoic acid-inducible gene I
RLRs	RIG-I-like receptors
RNA	ribonucleic acids
RNA pol III	RNA polymerase III
ROS	reactive oxygen species
SEM	standard error mean
SRB1	scavenger receptor class B type I
STING	stimulator of interferon genes
TBK1	TRAF family member associated NF-κB activator-binding kinase 1
TBSV	tomato bushy stunt virus
TIR	toll/interleukin-1 receptor
TLRs	toll-like receptors
TMEM173	transmembrane protein 173
TNF	tumor necrosis factor
TRAF	TNF receptor-associated factor
TRIF	TIR-domain-containing adapter-inducing interferon-β
TRIM25	tripartite motif-containing 25
UTR	untranslated regions
VISA	virus-induced signaling adaptor
VLCFA	very long-chain-fatty acids
VLDL	very low-density lipoproteins
vMIA	viral mitochondria-localized inhibitor of apoptosis
vRNA	viral ribonucleic acids
WT	wild-type

Table of Contents

Table of figures

Table of tables

Legal considerations

The author declares that part of the results presented in this thesis were published under the name of Ferreira, A. R., and that she has participated in the planning and execution, as well as in the preparation and interpretation of the data.

Ferreira, A. R.*, Magalhães, A. C., Camões, F., Gouveia, A., Vieira, M., Kagan, J. C. and Ribeiro, D. (2016). Hepatitis C virus NS3-4A inhibits the peroxisomal MAVS-dependent antiviral signaling response. J. Cell. Mol. Med. 20, 750–757.

Magalhães, A. C.*, **Ferreira, A. R.***, Gomes, S., Vieira, M., Gouveia, A., Valença, I., Islinger, M., Nascimento, R., Schrader, M., Kagan, J. C., and Ribeiro D. (2016). Peroxisomes are platforms for cytomegalovirus' evasion from the cellular immune response. Sci. Rep. 6, 26028.

Ferreira, A. R.*, Gouveia, A.*, Marques M., Valença, I., Kagan, J. C. and Ribeiro, D. Human Cytomegalovirus' vMIA controls peroxisome morphology and dampens antiviral signaling via MAVS and MFF. – soon to be submitted to Molecular Cell

Ferreira, A. R., Valença, I., Marques, M., Felgueiras, J., and Ribeiro, D. New insights on the interplay between viruses and peroxisomes: a protein-protein interaction analysis. – soon to be submitted to International Journal of Molecular Sciences

*Shared first authorship

I. General Introduction

1.1. Peroxisomes

Peroxisomes are intracellular organelles bounded by a single lipid bilayer membrane that surrounds a dense granular matrix, devoided of nucleic acids or protein synthesis machinery. Peroxisomal proteins are encoded by nuclear genes and synthesized in the cell cytoplasm by polyribosomes (Fujiki et al., 1984; Lazarow and Fujiki, 1985; Rachubinski, 1984). Their shape and size vary greatly in response to growth conditions or environmental stimulus, such as fatty acids, temperature alterations or even infection by pathogens (Ribeiro et al., 2012; Schrader and Fahimi, 2006). Peroxisomes can appear as spherical or rod-like, ranging from 0.1 to 0.5 micrometers (μm) in diameter, and also occasionally elongated with up to 5 μm in length (Islinger et al., 2012a; Litwin and Bilińska, 1995; Schrader et al., 1994). Peroxisomes are crucial organelles for mammalian cells and their main functions include β- and α-oxidation of fatty acids, decomposition of hydrogen peroxide, synthesis of ether-phospholipids and docosahexaenoic acids, among several others (Figure 1).
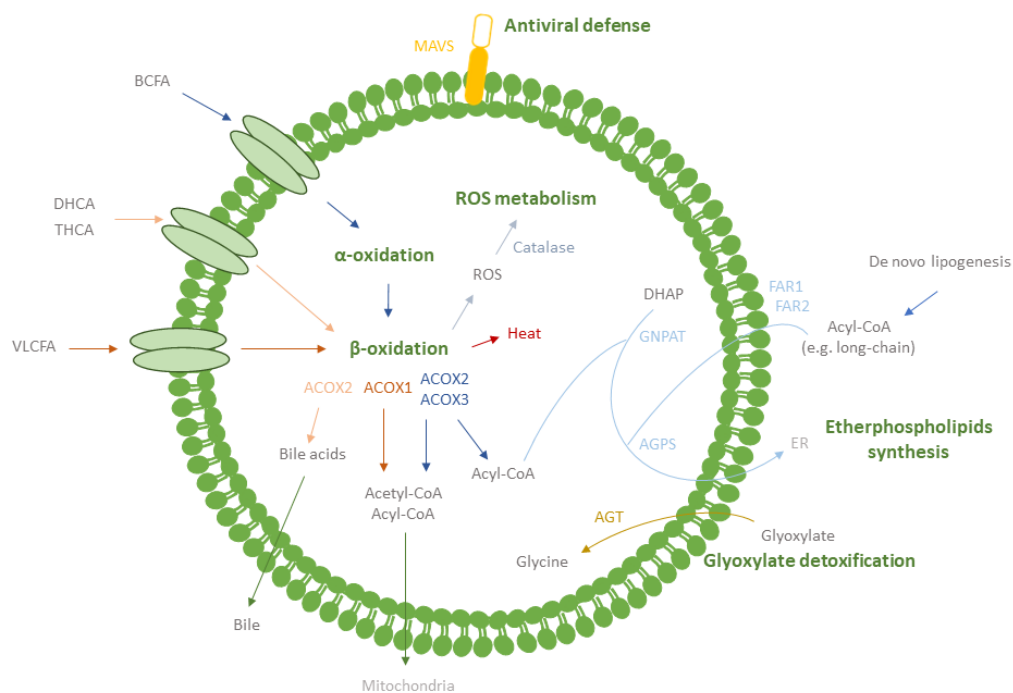
Figure 1. Schematic representation of peroxisomal main functions and interactions with other subcellular organelles. The main functions of peroxisomes are α-oxidation of BCFA, β-oxidation of VLCFA, synthesis of bile acids and etherphospholipids, glyoxylate detoxification, removal of ROS and antiviral defense. Some of the peroxisomal enzymes involved in each pathway are represented. BCFA - branched-chain fatty acids; VLCFA - very long-chain fatty acids; Acetyl-CoA - acetyl coenzyme A; Acyl-CoA - acyl coenzyme A; ACOX - acyl-CoA oxidase; AGPS - alkyldihydroxyacetonephosphate synthase ; FAR - fatty acyl-CoA reductase; GNPAT -glyceronephosphate O-acyltransferase ; ER – endoplasmic reticulum ; MAVS – mitochondrial antiviral signaling; ROS – reactive oxygen species

I. General Introduction

Most of the molecular processes behind these peroxisomal functions are shared with other organelles, with the exception of the oxidation of very long-chain fatty acids (VLCFA), which are solely metabolized at peroxisomes (further explored in section 1.1.3) (Schrader et al., 2015b; Wanders et al., 2016). Peroxisomes have been also described as essential for many physiological and pathological processes, as well as important signaling platforms in immunity, inflammation, ageing, cancer and in host-pathogen interactions (Cipolla and Lodhi, 2017; Dahabieh et al., 2018; Lazarow, 2011; Odendall and Kagan, 2013; Valença et al., 2015).

1.1.1. Peroxisome biogenesis

Peroxisome biogenesis consists in the formation of a membrane, which is followed by the insertion of peroxisomal membrane proteins (PMPs) necessary for the subsequent import of peroxisomal enzymes (Lazarow and Fujiki, 1985). Until now, 16 proteins involved in peroxisomal biogenesis, termed peroxins, which are encoded by *Pex* genes, were identified. Peroxisome biogenesis can be initiated from pre-existing peroxisomes – growth and division model - where lipids and proteins are imported from the cytosol, or be mediated by the endoplasmic reticulum (ER) – *de novo* model - where specialized areas form pre-peroxisomal vesicles and mediate the targeting of peroxisomal proteins, which, after fusion, originate mature peroxisomes (Costello and Schrader, 2018; Hettema et al., 2014). While this process has slower kinetics leading to the formation of new peroxisomes (Motley and Hettema, 2007), the growth and division pathway is a faster process that depends on the presence of pre-existing peroxisomes. Both models agree with the existence of signaling peptides that allow the specific targeting of peroxisomal proteins from the matrix (PTS1 and PTS2) and membrane proteins (mPTS), as well as specific systems for membrane translocation for matrix and membrane proteins (Francisco et al., 2017; Gould et al., 1989; Jones et al., 2001).

Growth and division model

The growth and division model is an asymmetric process that consists of peroxisomal polarization, which allows membrane protrusion and consequent elongation (Huybrechts et al., 2009). Subsequently, the import of the membrane and matrix proteins is initiated, the peroxisomal membrane constricts and final scission occurs, leading to the multiplication of these organelles (Costello and Schrader, 2018; Fahimi et al., 1993; Schrader et al., 1994).

These processes are regulated by the multifunctional protein PEX11β (Delille et al., 2010), and some proteins shared with the mitochondria division machinery: the guanin triphosphate enzyme (GTPase)

dynamin-like protein (DLP1) and its membrane adaptor proteins mitochondrial fission 1 (FIS1) and mitochondrial fission factor (MFF) (Kobayashi et al., 2007; Koch and Brocard, 2012; Koch et al., 2005; Koch et al., 2010).

After activation of PEX11β, the peroxisomal membrane expands due to the incorporation of lipids, forming a tubular structure (Opaliński et al., 2011; Schrader et al., 1998b). PEX11β recruits the anchoring proteins MFF and FIS1 to the peroxisomal membrane (Koch and Brocard, 2012), which in turn recruit DLP1 (Gandre-Babbe and van der Bliek, 2008; Itoyama et al., 2013; Kobayashi et al., 2007; Koirala et al., 2013; Losón et al., 2013; Otera and Mihara, 2011; Yoon et al., 2003). Consequently, PEX11β acts as a GTPase activating protein for DLP1, inducing membrane scission (Figure 2) (Bonekamp et al., 2013; Koch et al., 2003; Williams et al., 2015). Nevertheless, some controversy exists regarding which of these adaptors is the one that recruits DLP1 to peroxisomes. FIS1 was initially described as the main DLP1-adaptor at the peroxisomal membrane (Kobayashi et al., 2007; Koch et al., 2005; Yoon et al., 2003), but MFF was recently demonstrated to be essential for DLP1 recruitment to this organelle (Gandre-Babbe and van der Bliek, 2008; Itoyama et al., 2013; Koirala et al., 2013; Losón et al., 2013; Otera and Mihara, 2011).
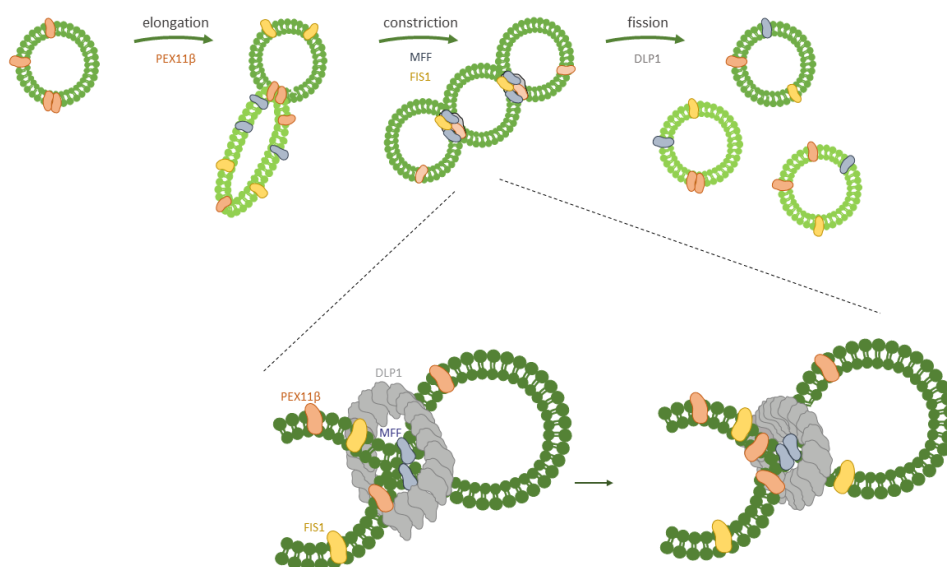
Figure 2. Growth and division model for peroxisome biogenesis. Peroxisomal proliferation starts with membrane elongation that is followed by constriction and final fission. Activation of PEX11β initiates the remodeling of the peroxisomal membrane in pre-existing peroxisomes inducing the elongation of one of their extremities. With membrane growth, FIS1 and MFF accumulate and recruit DLP1 allowing its assembling in a ring-like complex that hydrolyze guanosine-5'-triphosphate (GTP) and cleaves the peroxisomal membrane. MFF – mitochondrial fission factor; FIS1 – mitochondrial fission 1; DLP1 – dynamin like protein 1

Although the regulation of this process is still poorly understood, some studies performed in yeast have shown that PEX11β phosphorylation may be one form of regulation (Joshi et al., 2012; Knoblach

and Rachubinski, 2010; Thomas et al., 2015). Moreover, it was suggested that PEX11β self-interaction regulates membrane deformation (Bonekamp et al., 2013) and this self-interaction may be sensitive to redox metabolism, coordinating the division with the oxidative levels of peroxisomes (Marshall et al., 1996). Excess of PEX11 proteins can also inhibit the constriction of peroxisomes, leaving peroxisomes in an elongated state (Koch et al., 2010).

PMPs can be directly imported into the peroxisomal membrane, even in mutant cells with impaired peroxisomal matrix protein import, forming peroxisomal ghosts (Santos et al., 1988), or peroxisomal membrane remnants, and becoming functional peroxisomes after reintroducing the faulty *Pex* gene (Mayerhofer, 2016). However, in the absence of *Pex3*, *Pex16* or *Pex19*, PMPs targeting or import is not possible, as they encode key components for the post-translational targeting and insertion machinery, as well as for the peroxisomal membrane synthesis (Fang et al., 2004; Jones et al., 2004; Matsuzaki and Fujiki, 2008; Sacksteder et al., 2000).

PEX19 is a cytosolic chaperone that binds to a range of PMPs through recognition of their specific peroxisome targeting signal – mPTS. PEX19 binding to PMPs prevents their degradation and maintains their import-competent conformation (Jones et al., 2004; Sacksteder et al., 2000). Primarily, PMPs were sorted in two groups – class 1, which comprised the proteins that relied on PEX19 to be imported into peroxisomes, while class 2 consisted in the proteins that did not required targeting by PEX19 (Jones et al., 2004). After binding, PEX19 mediates the PEX19-PMP complexes docking to PEX3 at the peroxisomal membrane (Fang et al., 2004; Muntau et al., 2003). It was proposed that PEX3 has the capability to perturb the peroxisomal lipid bilayer, allowing the insertion of PMPs in the peroxisomal membrane (Pinto et al., 2009). On the other hand, PEX3 belongs to the class 2 of PMPs meaning that it is not trafficked to peroxisomes by PEX19, but rather by PEX16, where their direct interaction may be essential for the insertion of PEX3 into mature peroxisomes (Matsuzaki and Fujiki, 2008).

De novo model

The growth and division model was challenged when the formation of peroxisomes in mutant yeast cells that lacked peroxisomes due to a mutation in the biogenesis peroxins *Pex3* and *Pex19* was observed (Hoepfner et al., 2005), raising the question whether peroxisomes could originate from other organelles.

In mammalian cells, besides the genes *Pex3* and *Pex19*, *Pex16* was also observed to be essential for peroxisomal membrane biogenesis, as well as for segregation/inheritance of peroxisomes (Ghaedi et al., 2000; Sacksteder et al., 2000; South and Gould, 1999). An earlier study had also suggested that peroxisomes originate from ER based on electron microscopy analysis of mammalian cells (Novikoff

and Novikoff, 1972). Corroborating the involvement of ER in the peroxisomal biogenesis, evidence showing that different PMPs, before being transported to peroxisomes, are targeted to the ER where they accumulate in a specialized subdomain emerged from different studies (Aranovich et al., 2014; Geuze et al., 2003; Toro et al., 2009; Yonekawa et al., 2011). Moreover, it was shown that PEX16 mediates the trafficking and recruitment of several PMPs to the ER (Hua et al., 2015).

From these specialized or pre-peroxisomal subdomains at ER, peroxisomes are formed *de novo* in a SEC16B-dependent process. Additionally, it is speculated that from these subdomains, ER may also provide new PMPs and lipids to fuel the growth and division model, and maintain the pool of pre-existing peroxisomes (Mayerhofer, 2016). However, it is still unknown how this process is regulated or even the mechanisms behind the insertion of PMPs in the ER, it seems that mammalian PMPs after being synthesized can be routed to peroxisomes through two different pathways, either directly (explained in the previous subsection) or indirectly (Mayerhofer, 2016).

Recently, it was shown that during *de novo* formation in mammalian cells, after introduction of *Pex3* in deficient cells, the encoded protein was inserted in mitochondria, instead of ER or peroxisomes, and exited in vesicular structures. These vesicular structures, that derived from mitochondria, were also composed by PEX14, PMP70 and catalase, suggesting the maturation of these structures into import-competent peroxisomes. However, the partner for the membrane protein import machinery of PEX3, PEX16, was observed in a second class of vesicles derived from ER. These vesicles were seen targeting the PEX3/PEX14 enriched sites of mitochondrial surface (Sugiura et al., 2017). The same process was seen in yeast cells, when a PEX3 fusion protein with a mitochondrial targeting signal induced mitochondria-derived import-competent peroxisomes (Rucktäschel et al., 2010). Both findings lead to the speculation that *de novo* formation may be initiated by the targeting of PMPs to any endomembrane in the absence of peroxisomes (Costello and Schrader, 2018).

How peroxisomes coordinate both processes is still to be understood, however, since peroxisomes have an essential role on the metabolism of lipids and ROS, it is most likely that both pathways are regulated by the cellular state, which is in turn affected by the environment of the cell. The studies that tried to clarify the stimulus that induce each one of the routes for peroxisomes formation, showed contradictory results. In mammalian cells, it was shown that peroxisomes could rise from *de novo* pathway even in the presence of pre-existing peroxisomes (Kim et al., 2006), contrary to the initial belief that *de novo* formation occurred only in the absence of peroxisomes. Currently, it is accepted that both routes may cooperate to maintain the peroxisomal population homeostasis (Mayerhofer, 2016), however, further studies should address how *de novo* and fission generation of peroxisomes are regulated and coordinated.

I. General Introduction

The maturation process of peroxisomes into fully functional organelles is common to both processes of peroxisomal formation. Synthesis of peroxisomal matrix proteins occurs in free ribosomes in the cytosol, being then post-translationally imported into the organelle. Proteins that present one or two peroxisomal targeting signals (PTS1 or PTS2) are recognized by soluble receptors PEX5 or PEX5-PEX7 complex, which transport them to docking sites present at the peroxisomal membrane (Francisco et al., 2017). After recognition, cargo is released and receptors are shuttled back to the cytosol (reviewed in (Dias et al., 2016)).

1.1.2. Peroxisome dynamics

Peroxisomes are highly dynamic organelles that due to alterations on the cellular environment, such as starvation, infection or cell death, change their shape, number, enzyme content and distribution to compensate the metabolic needs of the cell (Camões et al., 2009; Islinger et al., 2012b; Ribeiro et al., 2012; Smith and Aitchison, 2013).

Peroxisome motility

Such as other organelles, peroxisomes traffic through the cell taking advantage of the cytoskeletal tracks. Peroxisomes' motility involves oscillations, short-range and long-distance motions. Whereas in plants and yeast peroxisomes move through the actin cytoskeleton with the aid of type-V myosins (Fagarasanu et al., 2010; Sparkes and Gao, 2014), in mammalian cells peroxisomes use microtubules to perform their long-distance bidirectional movements (Schrader et al., 1996; Schrader et al., 2000) (reviewed in (Neuhaus et al., 2016)). MIRO1, an Ras GTPase known to link mitochondria to the motor proteins kinesin and dynein, was recently identified as a possible adaptor for peroxisomal motility in microtubules (Castro et al., 2018; Okumoto et al., 2018). They show that this protein alters peroxisomes distribution and motility and mediates the pulling forces needed for peroxisomal distribution and proliferation (Castro et al., 2018).

Peroxisome proliferation

The regulation of peroxisomal proliferation is achieved through the induction, by external stimuli, of transcription factors that are able to enhance the expression of peroxisomal genes (Schrader et al., 2016). However, the knowledge on the signaling pathways behind the regulation of peroxisome proliferation in mammals is still poor and most of the studies have been performed in yeast, where peroxisomes are the sole organelle responsible for β-oxidation and the transcriptional control system

is less complex (Gurvitz and Rottensteiner, 2006; Schrader et al., 2016). In mammals, the best described mechanism for regulation of peroxisome proliferation is mediated by the peroxisome proliferator-activated receptor α (PPRα). In rats, several fibrates have been reported to induce peroxisomal proliferation and to be agonists of PPARα (Guo et al., 2006; Hess et al., 1965; Lazarow and De Duve, 1976), although having a very mild effect in humans (Lawrence et al., 2001). However, in HepG2 cells, several genes that code for peroxisomal enzymes were identified as having peroxisome proliferator response elements that are regulated by PPARα (van der Meer et al., 2010). Nevertheless, the mechanisms behind the stimulation of peroxisome proliferation by PPARα in humans are controversial, since no correlation between PEX11β, essential for peroxisome proliferation, and PPARα has been observed.

PPAR-independent mechanisms of regulation of peroxisome proliferation have been described, although their mechanisms of action are still unknown (Schrader et al., 2016). Growth factors, arachidonic acid, UV light and ROS induce peroxisomes elongation in HepG2 cells, which are resistant to treatment with fibrates (Schrader et al., 1998a; Schrader et al., 1998b).

Peroxisome degradation

The specific removal of the excess of peroxisomes by autophagy is designated as pexophagy. Three pathways for the degradation of peroxisomes are accepted: (1) p62 recognizes an unknown ubiquitinated PMP which leads to the recruitment of an autophagosome after interaction with LC3-II (Kim et al., 2008); (2) LC3-II interacts directly with PEX14 by competing with PEX5 for the interaction with PEX14, depending on the nutrient conditions (Hara-Kuge and Fujiki, 2008); (3) binding of NBR1 to an ubiquitinated PMP or directly to the peroxisomal membrane, which can be also mediated by p62 (Deosaran et al., 2013). It has been shown that DLP1 may be recruited and activated prior to pexophagy, suggesting that peroxisomal fragmentation is required for the selective process of autophagy (Mao et al., 2014; Twig and Shirihai, 2011). PEX3, has also been recently linked to peroxisomal degradation by pexophagy (Nazarko, 2017; Zientara-Rytter et al., 2018). Nevertheless, the regulation of peroxisomes number and size is still poorly understood and a better understanding on how these proteins cooperate to regulate peroxisomes dynamics is still required.

1.1.3. Peroxisomes and other organelles

Organelle interaction is essential for the integration of different functions, such as metabolism, cellular maintenance or cell fate. Peroxisomes cooperate with other organelles in the cells, such as ER,

I. General Introduction

lipid droplets (LD) and mitochondria (Lodhi and Semenkovich, 2014; Schrader et al., 2015b).The interplay between these organelles is accomplished through direct contact, diffusion of molecules or metabolites, or vesicular transport (Cohen et al., 2018; Schrader et al., 2015b). Besides the *de novo* formation of peroxisomes, interaction with the ER was also associated to the delivery of the phospholipids necessary for the formation of peroxisomal membranes, although the few studies that have addressed this issue were performed in yeast and the mechanisms behind this process are not yet fully understood (Guo et al., 2007; Raychaudhuri and Prinz, 2008). Other signaling pathways may be shared between ER and peroxisomes, such as antiviral defense or lipid metabolism, but more research on this topic is needed. A recent work uncovered new membrane contact sites between peroxisomes and ER in mammalian cells, associated to the regulation of the biosynthesis of plasmalogens and peroxisome motility (Costello et al., 2017a): peroxisomal Acyl-CoA binding domain containing protein 5 and 4 (ACBD5 and ACBD4) interact with VAPA/B, ER-resident tail-anchored proteins (Costello et al., 2017b; Costello et al., 2017c).

Peroxisomes are also in close contact with mitochondria, and they share several morphological and metabolic functions (Camões et al., 2009; Schrader and Yoon, 2007; Schrader et al., 2015a). Both organelles change their morphology to modulate cellular and tissue physiology, oscillating from a small and spherical to tubular and long nets (Schrader et al., 2000; Tilokani et al., 2018). Supporting this proximity at the morphological level, it was found that both organelles share the components of their fission machinery, DLP1, FIS1 and MFF, as discussed above. However, the reason for this dual targeting is still poorly understood. Adding to the morphological similarities, peroxisomes and mitochondria also have a strong metabolic connection (Camões et al., 2009; Wanders et al., 2016). Both mitochondria and peroxisomes perform β-oxidation, although the enzymes involved in this process are specific for each organelle (Osumi and Hashimoto, 1980). In both organelles the process of β-oxidation is similar and involves four main reactions: 1) dehydrogenation, 2) hydration, 3) dehydrogenation, and 4) thiolytic cleavage (Lodhi and Semenkovich, 2014; Wanders et al., 2016). In each cycle, fatty acids are shortened by two carbons atoms which are released as acetyl-coenzyme A (acetyl-CoA). Both pathways have substrate specificities: mitochondria degrades long-chain fatty acids derived from the diet, where peroxisomes are responsible for the oxidization of more complex lipids, such as VLCFA, long- and medium-chain dicarboxylic acids, prostaglandins, bile acid precursors, leukotrienes and mono- and poly-unsaturated fatty acids (Lodhi and Semenkovich, 2014; Poirier et al., 2006). While mitochondria metabolizes lipids to supply acetyl-CoA for adenosine triphosphate (ATP) production and anabolic reactions, peroxisomes mostly prevent the toxic effects of their accumulation in the cell and also supply acetyl-CoA for the biosynthesis of cholesterol and bile acids (Lodhi and Semenkovich, 2014). Although peroxisomes perform β-oxidation, they cannot fully metabolize acetyl-

CoA, thus acetyl-CoA esters produced in peroxisomes are shuttled to mitochondria for further oxidation (Osumi and Hashimoto, 1980; Vanhove et al., 1993).

Peroxisomes and mitochondria are also responsible for the metabolism of ROS and reactive nitrogen species (RNS), which consist in by-products of metabolic reactions (Dan Dunn et al., 2015; Fransen et al., 2012). At peroxisomes, these by-products are manly formed during lipid oxidation, while at mitochondria, they are produced in the electron transport chain. To counterbalance the production of negative molecules and protect cells, both organelles have mechanisms that maintain redox homeostasis. At peroxisomes, catalase acts by converting H_2O_2 into water and O_2, and it is present in the matrix of peroxisomes to participate in cell response to stress. Additionally to catalase, other antioxidant enzymes exist in peroxisomes to metabolize different ROS or RNS (Fransen et al., 2012). Although until recently it was thought that ROS were merely undesirable cell products, it is now accepted that they are essential to several physiological and pathological pathways as immune signaling regulation and autophagy, acting as cellular anti-microbial compounds (Di Cara et al., 2017; Nathan and Shiloh, 2000)

In 2010, it was found that peroxisomes, together with mitochondria, coordinate the antiviral response induced by retinoic acid-inducible gene I (RIG-I)-like receptors (RLRs) upon the recognition of viral ribonucleic acids (RNA). Both organelles share an antiviral signaling adaptor, designated as mitochondrial antiviral signaling protein (MAVS) (Dixit et al., 2010) (described in section 1.2.1).

1.1.4. Peroxisomes in health and disease

Peroxisome dysfunctions have been associated to severe neurological and developmental disorders. Specific peroxisomal disorders represent a group of genetic diseases where one or more peroxisomal functions are impaired and have been subdivided into three subgroups: peroxisome biogenesis disorders, single peroxisomal enzyme deficiencies and single peroxisomal substrate transport deficiencies (Wanders, 2014). The Zellweger syndrome is an example of an important disease caused by a dysfunction of peroxisomal functions, where there is the accumulation of VLCFA but no plasmalogens and phospholipids synthesis due to the absence of peroxisomes (Braverman et al., 2013). These molecular alterations lead to neural impairment, as well as lipid composition on several tissues as in erythrocytes (Klouwer et al., 2015).

Dysfunction of peroxisomal functions on ROS and ether phospholipids metabolism was also associated to several neurodegenerative diseases as Parkinson's or Alzheimer's disease, as well as cancer and ageing (Cipolla and Lodhi, 2017; Dorninger et al., 2017; Scherz-Shouval and Elazar, 2011; Wanders,

2014). As indicated above (and further described below), peroxisomes also play an important role during innate immunity against viral infection.

1.2. Cellular Antiviral signaling

The innate immune system is responsible for identifying threats and initiating a sequence of responses that will allow the elimination of the potential infectious pathogens (Janeway, 1989). It presents two main characteristics: the capacity to distinguish between infectious non-self- from self-molecules and the capacity to stimulate the adaptive immune system for a specific response (Janeway and Medzhitov, 2002). The innate immunity relies on different pattern recognition receptors (PRRs) which recognize, at the intracellular or extracellular space, specific compounds of the pathogens, designated as pathogen-associated molecular patterns (PAMPs) (Janeway, 1989).

Antiviral PRRs can be subdivided according to their location: they can be bound to a membrane or circulate freely in the cytosol. At the extracellular space, pathogens will encounter toll-like receptors (TLRs) which are bound to plasma membrane (Kawai and Akira, 2011). TLRs, that can recognize viral RNA or deoxynucleic acids (DNA), can also be bound to endosomes. Furthermore, several types of cytosolic receptors are responsible for recognizing viral nucleic acids: viral RNA is recognized by the RLRs (Yoneyama et al., 2015) and the NLRs (nucleotide oligomerization domain-like receptors) (Lupfer and Kanneganti, 2013); viral DNA is recognized by different cytosolic sensors that induce the stimulator of interferon (IFN) genes (STING)-dependent antiviral signaling (Paludan and Bowie, 2013).

Although PRRs are located in different regions of the cells and signal through different types of adaptor proteins, when activated, they initiate similar and tightly regulated signaling cascades (Chow et al., 2015). These signaling cascades lead to the activation of transcription factors, such as IFN regulatory factors (IRFs), nuclear factor kappa-light-chain enhancer of activated B cells (NF-κB) and activator protein 1 (AP-1), which control a set of genes that potentially lead to the production of proinflammatory cytokines and IFNs. Furthermore, PRRs also induce non-transcriptional responses that consist in cytokine processing, autophagy, phagocytosis and cell death (Beachboard and Horner, 2016).

1.2.1. RIG-I-like receptors in cellular antiviral signaling

The RLR family consists in a DExD/H-box family of helicases which recognize different species of viral RNA (Dixit and Kagan, 2013; Loo and Gale, 2011; Yoneyama et al., 2015). RIG-I and melanoma

differentiation-associated gene-5 (MDA5) have two caspase recruitment domains (CARDs) at their N-terminal, a central helicase domain and a C-terminal regulatory domain (Kang et al., 2002; Yoneyama et al., 2004). Laboratory of genetics and physiology 2 protein (LGP2), another member of this family, lacks the two CARDs at the N-terminal and, while it can also bind to double-stranded RNA (dsRNA), it seems to act as a dominant-negative regulator of RIG-I and MDA5 and not as a promoter of innate immune defense (Malur et al., 2012; Parisien et al., 2018; Thiagarajan et al., 2007; van der Veen et al., 2018; Yoneyama et al., 2005). However, LGP2 role on innate immunity is still controversial and some studies have shown that LGP2 is necessary for antiviral response against viruses that induce RIG-I- and MDA5-dependent signaling (Childs et al., 2013; Hei and Zhong, 2017; Satoh et al., 2010; Thiagarajan et al., 2007). Currently, it is established that RIG-I is responsible for the recognition 5' triphosphate RNA (5'pppRNA) present in several viral genomes and short blunt-ends in dsRNA (Hornung et al., 2006; Pichlmair et al., 2006; Saito and Gale, 2008; Schlee et al., 2009; Schmidt et al., 2009). Moreover, RIG-I seems to have a specificity for smaller sequences of dsRNA. These structures are essential for RIG-I to discriminate between non- from self-RNA, although several others motifs may be also necessary for viral RNA recognition by RIG-I (Schlee, 2013). In contrast, MDA5 agonists are not so well characterized and it is accepted that it may recognize long sequences of dsRNA and positive single strand RNA ((+)ssRNA) (Fredericksen et al., 2008; Gitlin et al., 2006; Kato et al., 2006; Loo et al., 2008; McCartney et al., 2008; Melchjorsen et al., 2010; Roth-Cross et al., 2008; Saito and Gale, 2008).

Additionally to RNA viruses, several reports have shown that RLRs may be also required against infections by DNA viruses. This is supported by the existence of viral proteins coded by different DNA viruses, which target RIG-I- and/or MDA5-dependent signaling (Castanier et al., 2010; Inn et al., 2011; Jin Choi et al., 2018; Marques et al., 2018; Zhao et al., 2012). Additionally, RIG-I was identified as an indirect sensor for cytosolic DNA through recognition by RNA polymerase III (RNA pol III) (Ablasser et al., 2009; Chiu et al., 2009; Melchjorsen et al., 2010). Moreover, it has been shown that synthetic or pathogen-derived double-stranded DNA (dsDNA) can activate RLR-induced immune responses independent of RNA pol III (Choi et al., 2009), and in herpes simplex virus (HSV) infection of human primary macrophages, MDA5 was reported to be responsible for the early recognition of HSV (Melchjorsen et al., 2010). These results suggest that RLR-sensing receptors may not be restricted to the recognition of RNA viruses but be able to respond to foreign DNA, enforcing their importance in both RNA- and DNA- viral infections.

At resting state, RIG-I presents a closed conformation where the CARD domains are autoinhibited through a stable interaction with the helicase domain (Civril et al., 2011). To be activated, RIG-I recognizes the RNA structure, which triggers the helicase domain to bind to the RNA backbone, inducing a change of conformation (Leung and Amarasinghe, 2012; Luo et al., 2012). When CARD

domains are exposed they are polyubiquitinated by tripartite motif-containing 25 (TRIM25) and RIPLET, which prompts the aggregation of RIG-I (Gack et al., 2007; Jiang et al., 2012; Oshiumi et al., 2009). This sequence of events allows the activation of MAVS and the following downstream signaling (Figure 3) (Jiang et al., 2012; Kowalinski et al., 2011; Seth et al., 2005). In contrast to RIG-I, MDA5 presents an open conformation in steady state, and the inhibition is accomplished by the phosphorylation of serine and threonine residues on the C-terminal and CARD domains. These phosphorylations are also common on RIG-I (Chan and Gack, 2015). Although the activation mechanisms of RIG-I and MDA5 have been elucidated in the last years, the mechanisms for LGP2 activation stay uncharacterized.
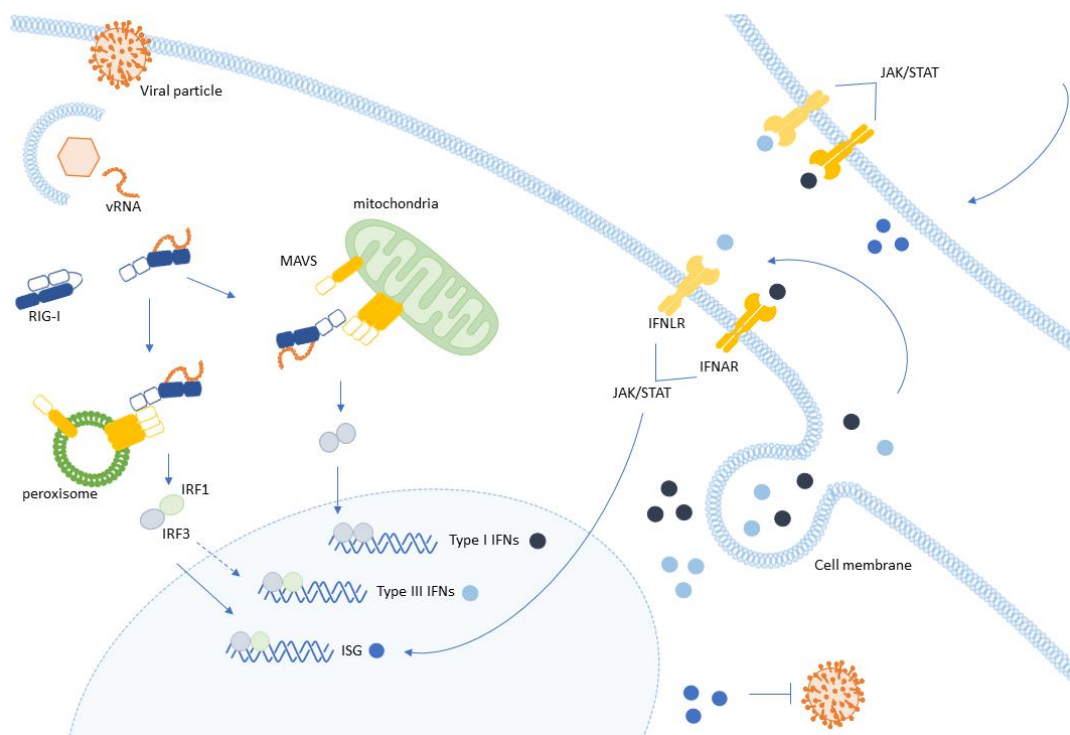
Figure 3. RIG-I-like receptor antiviral signaling pathway. Upon infection, viral RNA is released into the cytosol which is sensed by RIG-I and/or MDA5. Both receptors travel to peroxisomes and mitochondria to activate MAVS, inducing a downstream signaling cascade that culminates with the production of type I IFNs and ISGs. Peroxisomal MAVS induces a rapid production of ISGs, and type III IFNs in some types of cells, via activation of IRF1 and IRF3, while at mitochondria it leads to a delayed but sustained IFN response through IRF3. Once secreted, IFNs bind to specific receptors on the cell surface, activating the JAK-STAT pathway and generating an amplifying loop that results in the accumulation of RIG-I and other ISGs. The conjugation of these responses leads to the restriction of viral replication and spreading to neighboring cells. RIG-I – retinoic inducible gene I; vRNA – viral RNA; MAVS – mitochondrial antiviral signaling protein; IRF – interferon regulatory factor; IFN – interferon; IFNAR – interferon alfa/beta receptor complex; IFNLR – interferon lambda receptor complex

Both RIG-I and MDA5 require MAVS [also known as IFN-β promoter stimulator-1 (IPS-1), CARD adaptor inducing IFN- β (CARDIF) and virus-induced signaling adaptor (VISA)], to pass the signal to IRF3 which leads to the expression of IFNs, cytokines and IFN-stimulated genes (ISGs) (Kawai et al., 2005; Meylan et al., 2005; Seth et al., 2005; Xu et al., 2005). MAVS localizes at the membranes of mitochondria,

peroxisomes and mitochondria associated membranes (MAM) and is composed of an N-terminal CARD domain, a central proline-rich region, and a C-terminal transmembrane domain (Dixit et al., 2010; Horner et al., 2011a; Meylan et al., 2005; Seth et al., 2005; Xu et al., 2005). The CARD-CARD interaction between RIG-I/MDA5 and MAVS induces a conformational change on MAVS leading to the formation of resistant prion fiber-like active aggregates, which allows a large amplification of the activation signal to other MAVS that were not directly activated (Hou et al., 2011). MAVS polymerization recruits the tumor necrosis factor (TNF) receptor-associated factors (TRAF), TRAF2, TRAF5 and TRAF6, which are required for TRAF family member associated NF-κB activator-binding kinase 1 (TBK1) protein and the IκB kinase (IKK) complex activation (Liu et al., 2013; Xu et al., 2005). These kinases are then responsible for the phosphorylation of IRF3, as well as the NF-κB, respectively. IRF3 is a transcription factor that dimerizes and translocates to the nucleus where it activates the expression of IFNs (Meylan et al., 2005; Seth et al., 2005; Xu et al., 2005). The secreted IFNs induce, in a autocrine and paracrine manner, the JAK/STAT pathway leading to the expression of ISGs, such as RIG-I, MDA5, protein kinase RNA-activated (PKR), 2',5'-oligoadenylate synthase (OAS), major histocompatibility complex class I (MHC1) among several others (Dixit and Kagan, 2013; Leung et al., 2012; Yoneyama et al., 2005).

Dixit et al. described differences on the signaling kinetics, as well as the signaling products expressed after activation of RLR, depending on the subcellular localization of MAVS: peroxisomal MAVS activates a rapid but short-termed expression of ISGs, while mitochondria MAVS triggers a delayed but long lasting ISGs production (Dixit et al., 2010). Later, the same group described that the RLR signaling, in addition to induce the production of type I IFNs and ISGs, it also induces the expression of type III IFNs, a class of IFNs that has tissue-specific roles in antiviral immunity. Moreover, they show that these can be induced by a variety of viruses and identified peroxisomes as being the signaling organelles that induce their expression, complementing the type I IFNs induced from mitochondria (Odendall et al., 2014). The role of each organelle as a platform on the RLR antiviral response is still controversial, as one other study has shown no such differences in terms of IFN production, although using distinct experimental setups (Bender et al., 2015).

1.2.2. Cytosolic DNA sensors in cellular antiviral signaling

The first DNA sensor to be described was DNA-dependent activator of IFN regulatory factor (DAI). After binding, DAI interacts with IRF3, TBK-1 and activates NF-κB, inducing the expression of type I IFNs. STING is an adaptor transmembrane protein localized at the ER and essential for the induction of type I IFNs in response to viral DNA (Ishikawa and Barber, 2008; Jin et al., 2008; Sun et al., 2009;

Zhong et al., 2008). Upon activation, STING translocates from the ER to punctate perinuclear compartments through the Golgi complex (Ishikawa and Barber, 2008; Ishikawa et al., 2009). It was also reported that STING localizes upstream of TBK1, and their interaction leads to the phosphorylation of IRF3 (Ishikawa and Barber, 2008; Sun et al., 2009; Tanaka and Chen, 2012; Zhong et al., 2008). As MAVS, STING is the adaptor protein of different DNA sensors, such as DDX41, IFI16 and, the most studied one, cyclic GMP-AMP synthase (cGAS), (Pu et al., 2011; Sun et al., 2013; Unterholzner et al., 2010; Wu et al., 2013). Chen's group reported that cytosolic DNA leads to the production of cyclic-di-GMP-AMP (cGAMP) after being sensed by cGAS, inducing IFN production through the STING-dependent pathway (Sun et al., 2013; Wu et al., 2013).

STING was also associated to the recognition of RNA viruses, after some studies reported that STING interacts with MAVS and that STING absence in RNA virus-infected cells lead to decreased levels of IFN expression (Ishikawa and Barber, 2008; Ishikawa et al., 2009; Jin et al., 2008; Sun et al., 2009; Zhong et al., 2008). However, other studies have not found any differences on the antiviral response against RNA viruses in the absence of STING (Chen et al., 2011; Sauer et al., 2011). These differences may be justified due to other unknown STING function that can lead to the induction of IFNs and ISGs in a RIG-I-independent manner (Holm et al., 2013; Holm et al., 2016). Also, it has been proposed that cGAS is capable of detecting some viral RNA species leading to the production of cGAMP, the trigger that activates STING-dependent pathway (Schoggins et al., 2014). Contrary to this, Franz et al. reported that in RNA virus-infected fibroblasts, STING is not required to prompt IFN expression, being however responsible for the restriction of viral replication (Franz et al., 2018).

1.2.3. Toll-like receptors in cellular antiviral signaling

TLRs are type I transmembrane proteins and are the most studied and well-known class of PRRs. Up to this date, ten different TLRs have been described in humans but only six are involved in antiviral immunity. TLR2 and TLR4 are responsible for recognizing viral structural proteins and localize at the plasma membrane, while the endosomal TLR3, TLR7 and TLR8 recognize viral RNA and TLR9 recognizes viral DNA (Kawai and Akira, 2010; Kawai and Akira, 2011). TLRs activate two different adaptor proteins activating two different signaling pathways. Most TLRs, when activated directly or indirectly, recruit the adaptor protein myeloid differentiation primary response 88 (MyD88), with the exception of TLR3, which recruits Toll/interleukin-1 receptor (TIR)-domain-containing adapter-inducing interferon-β (TRIF), as well as TLR4 that is able to activate both adaptor proteins (Yamamoto, 2003). MyD88-dependent signaling pathway leads to the activation of NF-κB and mitogen-activated protein kinases (MAPKs) to induce inflammatory cytokines (Adachi et al., 1998; Medzhitov et al., 1998; Thompson et

al., 2011). TRIF-dependent signaling pathway is responsible for activating the transcription factors IRF3 and NF-κB, consequently inducing the production of type I IFNs and inflammatory cytokines (Thompson et al., 2011; Yamamoto, 2003).

1.5. Hepatitis C virus

Hepatitis C virus (HCV) is an hepatotropic virus that may lead to chronic hepatitis, liver fibrosis and cirrhosis, which can progress to hepatocellular carcinoma (Chen and Morgan, 2006; Thrift et al., 2017). Besides infecting hepatocytes, HCV has also the capacity to spread to immune cells such as mononuclear cells, lymphocytes and T cells, and gastrointestinal mucosa (Artini et al., 1995; Crovatto et al., 2000; Gill et al., 2016; Petrovic et al., 2011; Zignego et al., 1992). HCV is an enveloped (+)ssRNA virus that belongs to the *Hepacivirus* genus from the *Flaviviridae* family (Kim and Chang, 2013; Manns et al., 2017; Simmonds, 2013). Its viral particle presents a diameter that ranges from ~45 to 100 nanometer (nm) and is formed by an enveloped lipid bilayer where two enveloped glycoproteins, E1 and E2, are attached. Inside, the C protein forms a non-icosahedral nucleocapsid, which contains the viral genome. HCV's genome is approximately 9.6 kilobases long and its open reading frame encodes a single polyprotein with 3000 amino acids. HCV is characterized by its 5' and 3' untranslated regions (UTRs), which are essential for its replication and translation, respectively. The 5' UTR allows the formation of a stable pre-initiation complex through binding between its internal ribosomal entry site (IRES) and the 40S ribosomal subunit (Appel et al., 2006; Manns et al., 2017; Moradpour et al., 2007; Niepmann et al., 2013; Otto and Puglisi, 2004; Shi and Lai, 2006).

HCV has a high replication rate and a low fidelity RNA-dependent RNA polymerase (RdRp). Seven different genotypes have been identified, being subdivided in a high number of subtypes (Simmonds, 2013). HCV differs from the other members from the *Flaviviridae* family, since normally they present a constant diameter of approximately 50 nm with a smooth surface and an icosahedral symmetry (Catanese et al., 2013; Mukhopadhyay et al., 2005). Additionally, HCV particles also differ between viral particles produced in cell culture or isolated from infected patients, suggesting that the host plays a role in the make-up of the viral structure and composition (Bartenschlager et al., 2011; Catanese et al., 2013).

1.5.1. Life cycle

I. General Introduction

When in the liver, HCV is already associated with lipoproteins with different densities forming lipoviroproteins (LVPs). At the cell membrane, the LVPs are captured by glycosaminoglycans (GAGs) and low-density lipoprotein receptors (LDLR), which induce alterations on HCV surface, allowing the recognition by different cell receptors (Figure 4) and the internalization by clathrin-mediated endocytosis (Miao et al., 2017; Timpe et al., 2007). Following internalization, the endosomes mature, leading to the fusion of the endosomal membrane with the HCV envelop and to the release of the nucleocapsid into the cytosol (Bartosch and Cosset, 2006; Manns et al., 2017; Miao et al., 2017). Here, decapsidation of viral particles releases the HCV genome, which serve as template for the synthesis of the HCV polyprotein in the rough ER. When processed, the polyprotein results in three structural proteins (E1, E2 and C) and seven non-structural proteins (p7, NS2, NS3, NS4A, NS4B, NS5A and NS5B). C, NS4A and NS5B regulate translation, as well as the 3' UTR and cellular factors (Chevaliez and Pawlotsky, 2006; Hoffman and Liu, 2011; Niepmann et al., 2013).
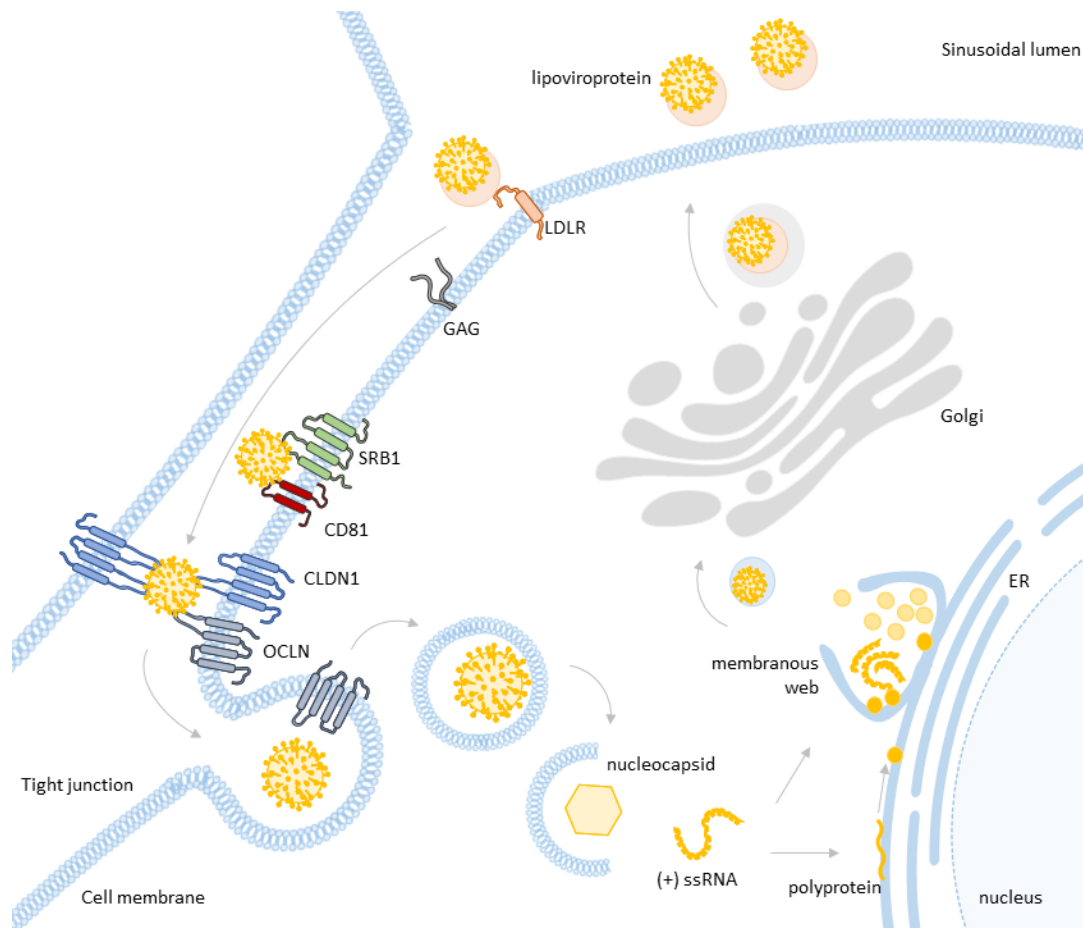
Figure 4. Schematic representation of the hepatitis C virus life cycle. Hepatitis C virus (HCV) reaches the cell surface conjugated with lipoproteins, which are recognized by LDLR and glycosaminoglycans (GAGs). Upon viral recognition, the viral particle is transported along the tight junctions through interaction with several receptors (CD81, SRB1, CLDN1 and OCLD), triggering internalization by clathrin-mediated endocytosis. Cellular and viral membranes fuse and the capsid is disorganized, releasing the viral RNA into the cytosol. At the ER, HCV genome is translated into a polyprotein that is further processed by host and viral proteases releasing single viral

proteins. A membranous web is formed during this process to harbor the viral genome replication and viral assembly. The assembly of new virions is dependent of lipid metabolism and occurs at the membranous web and ER. New virions suffer maturation becoming associated with lipoproteins and being then released by exocytosis. LDLR - low density lipoprotein receptors; GAG – glycosaminoglycans; SRB1- scavenger receptor class B type I; CD81 – cluster differentiation 81; CLDN1 – claudin 1; OCLN – occluding; (+)ssRNA – positive single-strand ribonucleic acid; ER – endoplasmic reticulum

After being target to the ER, the precursor polyprotein is processed by host peptidases (e.g. signal peptidases) and viral auto-proteases (NS2, NS3-4A) given form to the mature viral proteins, identified above (Wu, 2001). It has been reported that, during processing, viral proteins induce membrane alterations culminating with the formation of a 'membranous web', which consists of a double-membrane vesicle, and where it was identified HCV non-structural proteins and genome, as well as LDs and ERs membranes (Egger et al., 2002; Gosert et al., 2003; Itabe, 2010). Moreover, it was reported that these webs are required for viral RNA replication by NS5B and translation (Ishii et al., 1999; Lohmann et al., 1997; Niepmann et al., 2013).

The assembly and release of HCV are strictly associated with lipid metabolism (Lavie and Dubuisson, 2017; Targett-Adams et al., 2010). During infection, LDs suffer a profound intracellular redistribution, and accumulate in perinuclear regions associated to HCV proteins and genome (Boulant et al., 2008; Kim and Chang, 2013). The HCV C protein seems to be essential for the assemble of virions, as well as p7 and NS2 (Popescu et al., 2011). It was observed that HCV structural proteins and the replication complex assemble in lipid-rich environment of membranous webs. The mature virions are similar to very low density lipoproteins (VLDL) and low density lipoproteins (LDL) and associate to different apolipoproteins before being released (Lavie and Dubuisson, 2017; Popescu et al., 2011).

1.5.2. NS3-4A as a tool for HCV to evade cellular antiviral signaling

The non-structural protein NS3-4A is a non-covalent heterodimer complex formed by the HCV non-structural proteins, NS3 and NS4A. NS3 is a serine protease and RNA helicase and its function is activated and stabilized by NS4A (Koch et al., 1996; Morikawa et al., 2011). NS4A has also the capability of targeting and anchoring the complex to intracellular membranes (Foy et al., 2003; Lin, 2006; Morikawa et al., 2011). NS3-4A is vital for viral replication, and it is also critical for viral persistence and pathogenesis (Morikawa et al., 2011). NS3-4A is responsible for the processing of HCV polyprotein and for the formation of a replication complex in the membranous web (Moradpour and Penin, 2013; Morikawa et al., 2011).

NS3-4A was shown to block both RIG-I and TLR3 pathways, disrupting the IFN-dependent antiviral response (Li et al., 2005a; Li et al., 2005b; Meylan et al., 2005). The blockage occurs due to cleavage

of the protein adaptors of each pathway, MAVS and TRIF, respectively. Mitochondrial MAVS has been shown to be cleaved at its Cys-508, adjacent to the C-terminal transmembrane domain, thus resulting in its release from the membrane and inhibiting its oligomerization (Li et al., 2005b; Meylan et al., 2005). TRIF is cleaved at its Cys-372 leading to the separation of TIR domain from the TBK-1 binding domain, which impairs the activation of the downstream effectors (Li et al., 2005a).

Besides impairing the cellular innate immune response, it was reported that NS3-4A inhibits the systemic innate immunity through the cleavage of C4, a component of the complement system (Mawatari et al., 2013).

1.6. Human cytomegalovirus

Human cytomegalovirus (HCMV) belongs to the *Herpesviridae* family and is responsible for a lifelong latent infection in humans, affecting 40% to 60% of the adult population (Cannon et al., 2010; Mocarski et al., 2007). The infection is normally asymptomatic in healthy individuals, however, when reactivation occurs during pregnancy can lead to congenital infection and birth defects. In most of the cases, HCMV remains silent, suffering cycles of periodical reactivation with shedding of the infectious virions allowing its efficient transmission. This virus has a wide cell tropism being able to infect from epithelial to immune cells among others, and stablishes latency in myeloid cells of the bone marrow (Reeves and Sinclair, 2008).

HCMV is an enveloped virus with a symmetric icosahedral capsid that surrounds a complex non-segmented dsDNA genome. HCMV genome contains ~192 open reading frames that encode a vast number of proteins and micro RNAs (Stern-Ginossar et al., 2012). Its envelope is formed by a lipid bilayer where glycoprotein complexes are attached. The tegument layer, composed of viral phosphoproteins attached to the capsid, and to host and viral mature RNAs (mRNAs), separates the envelop from the capsid, which encloses the viral genome.

HCMV, through evolution, has developed a broad range of strategies to counteract and escape the human immune response, which lead to a high capacity of infection and dissemination (Biolatti et al., 2018; Christensen and Paludan, 2017; Marques et al., 2018; Noriega et al., 2012).

1.6.1. Life cycle

HCMV infection starts when its complexes of glycoproteins attach to the cell-surface's proteoglycans. The gB and gH glycoproteins are crucial for this process since they drive the fusion of the viral envelop with the cellular membrane, and the release into the cytosol of the capsid (Figure 5), as well as tegument proteins and virion mRNAs (Isaacson and Compton, 2009; Wille et al., 2013). Tegument proteins, attached to the capsid, are thought to interact with host microtubule machinery inducing the transport of the nucleocapsid into the nucleus, where it fuses with the nuclear membrane, releasing HCMV genome (Kalejta, 2008; Ogawa-Goto et al., 2003).
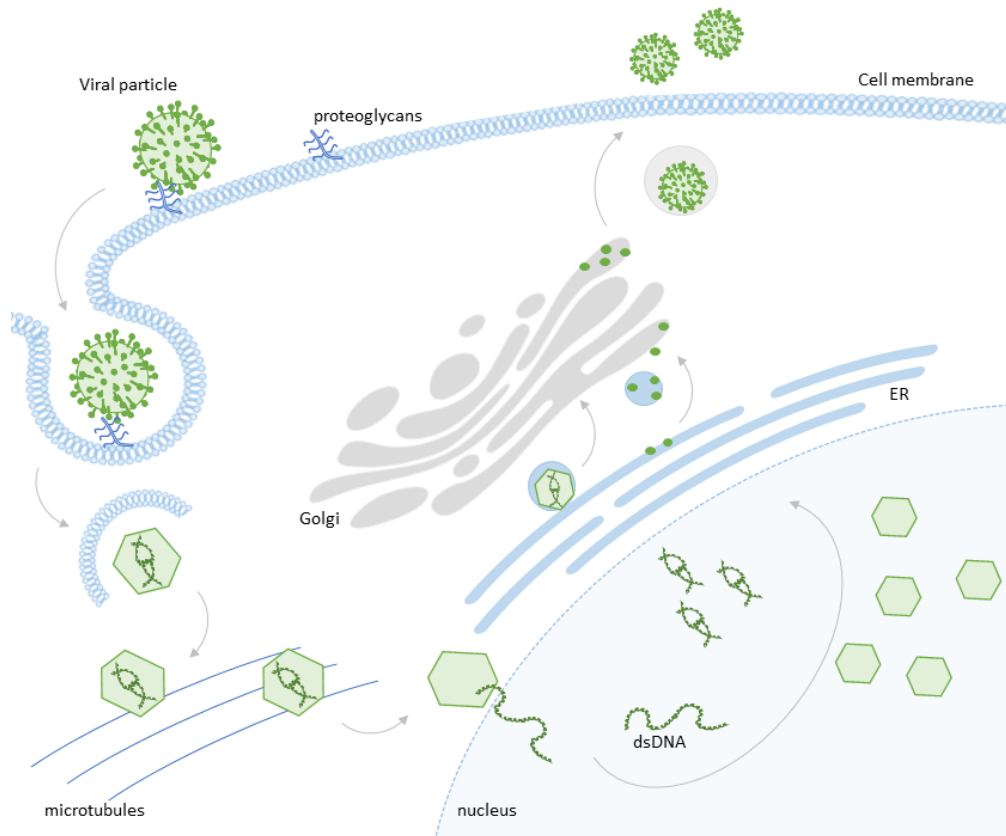
Figure 5. Schematic representation of the human cytomegalovirus life cycle. Human cytomegalovirus (HCMV) attaches to the cell surface through the interaction with specific cell receptors, like proteoglycans, which trigger fusion or endocytosis. After entering, the nucleocapsids are released into the cytosol and viral tegument proteins assist the use of the microtubule network to move towards the nucleus. Here, the release of viral DNA induces viral replication and translation. New capsids assemble in the nucleus and suffer envelopment at the ER-Golgi compartments. Then, fully mature virions are released through exocytosis at cell surface. dsDNA – double-stranded deoxyribonucleic acid; ER – endoplasmic reticulum

Viral DNA transcription and replication occurs in the nucleus, and is temporally controlled by different set of viral genes (Chambers et al., 1999). HCMV replication is divided in three phases: immediate early (IE), early (E), and later (L) phases. The IE transcripts are required to stimulate the transcription of E genes, which regulate viral replication and modulate cellular immune activation, and protect the virus against the host innate immunity (Torres and Tang, 2014). The transcripts produced during L phase induce viral capsids assembly, which occur in nuclear factories, and their release into the cytosol

(Reeves and Sinclair, 2008). During latent infection, the viral genome acquires the form of closed circular episomes, and has the capacity to replicate using the cellular replication machinery while maintaining the expression of a small number of viral genes (Jarvis and Nelson, 2002; Sinclair and Sissons, 2006).

In the cytosol, the non-enveloped capsids acquire the tegument proteins and then go through the viral assembly complex, that consists of the ER, Golgi apparatus and endosomes (Alwine, 2012). It is believed that a second envelopment occurs, where the lipid composition of the envelop of new virions is modified to resemble synaptic vesicles, leading to the release of virions with distinct envelop comparing with primary viral particles. The export of the new virions by exocytosis culminates with cell enlargement and consequential cell lysis (Liu et al., 2011).

1.6.2. vMIA as a tool for HCMV to evade the cellular antiviral signaling

The viral mitochondria-localized inhibitor of apoptosis (vMIA) protein is encoded by the HCMV IE gene UL37 exon 1 (hence it is also recognized as pUL37x1) and it was firstly described at mitochondria, as being a suppressor of apoptosis induced by different stimuli (Goldmacher et al., 1999).

As an anti-apoptotic protein, vMIA forms a complex with the adenine nucleotide translocator, a component of the mitochondrial transient pore, and inhibits apoptosis through the blockage of mitochondrial outer membrane permeabilization (Goldmacher, 2002; Goldmacher, 2005). vMIA has two domains, that are essential for its anti-apoptotic function: a mitochondrial localization domain located at its N-terminal, and a BAX-binding site at its at its C-terminal domain (Goldmacher, 2002). Moreover, vMIA disrupts mitochondrial networks through the modulation of the fusion and/or fission processes, and this was suggested to be associated to its anti-apoptotic function since mitochondrial fission has been implicated in the induction of apoptosis (McCormick et al., 2003). However, later, Castanier et al. have shown that the modulation of mitochondrial network by vMIA is also a mechanism of interfering with RIG-I/MDA-5 signaling at mitochondria (Castanier et al., 2010). They describe that mitochondria dynamics affects mitochondrial MAVS downstream signaling, since the induction of mitochondrial fragmentation impairs the production of IFNs and ISGs.

To corroborate the function of vMIA in the evasion of the cellular innate immunity during HCMV infection, vMIA was also found to interact with Viperin, an interferon inducible protein that is known to inhibit the replication of different viruses through a variety of mechanisms (Seo et al., 2011a; Seo et al., 2011b). vMIA induces Viperin translocation from the ER to the mitochondria, leading to the impairment of fatty acids β-oxidation and ATP generation, and to the disruption of actin cytoskeleton, thus increasing virion production (Seo et al., 2011a).

1.7. Peroxisomes in viral infections

Interactions between viruses and peroxisomes have been reported through the years and while some are associated with specific peroxisomal functions (Lazarow, 2011), some others are related to evasion of the peroxisome-dependent innate immune signaling.

The plant viruses belonging to the tombusvirus family, such as the tomato bushy stunt virus (TBSV), induce extensive inward vesicular alterations at peroxisomal membranes designated as peroxisome multivesicular bodies, which are thought to be the replication loci of TBSV (Jonczyk et al., 2007).

Several viruses were reported to modulate the peroxisomal-dependent antiviral response. The Dengue and West Nile virus, which belong to the *Flaviviruses* family, were reported to impair peroxisome biogenesis and dampen the early innate immune signaling from peroxisomes through PEX19 sequestration by their capsid (You et al., 2015). As introduced above, PEX19 is critical for peroxisomal biogenesis, since it is necessary for the import of PMPs, showing that viruses have developed evasion strategies that target essential pathways for peroxisome formation and proliferation. HSV-1 also evades the peroxisomal MAVS-dependent signaling through the viral protein VP16, though the mechanisms involved have not been disclosed (Zheng and Su, 2017). N[pro] from pestivirus was also reported to inhibit the IRF3 signaling, due to its recruitment to peroxisomes (Jefferson et al., 2014).

Interestingly, in human immunodeficiency virus (HIV) infection, secondary structured HIV-derived RNA was also detected at peroxisomes and induced IRF1 and IRF3 activation, as well as NF-κB, however with low expression of type I and III IFNs (Berg et al., 2012). Hepatitis B virus (HBV) was also described to produce the HBx viral protein, inducing NF-κB due to its targeting to peroxisomes. Nevertheless, it seems that the localization of this viral protein at peroxisomes is required to increase the invasiveness capacity of cells, by increasing ROS levels and facilitating ROS-mediated hepatocellular carcinoma (Han et al., 2014). Recently, it was shown that vFLIP, an oncogenic protein from the human herpesvirus 8 (HHV-8), is targeted to peroxisomes, where it interacts with MAVS. This interaction allows the stabilization of vFLIP's function, leading to the maintenance of HHV-8 latency (Choi et al., 2018). Mohan et al. identified the PTS1 domain that targets peroxisomal proteins to the matrix of peroxisomes in rotavirus' VP4 protein and reported that the localization at peroxisomes renders advantage for viral propagation (Mohan et al., 2002).

The association between viral infections and peroxisome metabolism has also been reported in several studies. It was shown that NS1 from IAV and influenza B virus (IBV) interact with the peroxisomal multifunctional enzyme type 2 (HSD17B4) protein (Wolff et al., 1996), a peroxisomal enzyme that acts

on β-oxidation of both unbranched and branched fatty acids (Möller et al., 1999). HIV's Nef was also found to interact with acyl-coenzyme A thioesterase 8 (ACOT8) protein (Cohen et al., 2000), which is essential for the regulation of acyl-CoAs, fatty acids and coenzyme A levels, and it is also involved in the metabolic regulation of peroxisomes proliferation (Hunt et al., 2012). Although these interactions between viral proteins and metabolic peroxisomal proteins have been identified, their effect still has to be further clarified. Recently, several high throughput studies have enforced this association. In a lipidomic study, Tanner et al. reported that influenza A virus (IAV) infection requires peroxisomal metabolism of ether lipids for efficient replication and spreading. Integrated systems biology has also been applied in Karposi's sarcoma associated herpesvirus (KSHV) infection revealing that this oncogenic herpesvirus increases peroxisome numbers and modulates peroxisomal lipid metabolism during infection (Sychev et al., 2017). Contrary to this, in a interactome study, it was reported that Zika virus decreases peroxisome numbers, and its replication is dependent of peroxisomes function, since viral replication was significantly impaired in peroxisome-deficient cells (Coyaud et al., 2018).

II. Aims

Viral infections pose a prominent and persistent threat to human health and most of the existing antiviral therapeutics are prone to resistance due to the high frequency of viral mutations. Furthermore, these are mainly directed to specific viruses or strains and not applicable for emerging or engineered viral hazards. The required development of broad-spectrum antiviral therapeutics may imply the discovery of common mechanisms shared by different viruses, e.g. as part of their life cycle or interaction with the host intracellular organelles. (Debing et al., 2015).

The exciting discovery that peroxisomes act as signaling platforms in early antiviral defense (Dixit et al., 2010; Odendall and Kagan, 2013) has not only revealed a novel function for this organelle but may possibly lead to the uncovering of one or more target mechanisms for the development of broad-spectrum antiviral strategies.

To contribute to a better understanding of the role of peroxisomes on the viral life cycle, establishment of the infection process, as well as on the cellular antiviral defense mechanisms, we proposed the following aims:

Aim 1. Characterize the role of peroxisomes in antiviral immunity against HCV (Section 3.1.)

      1.1. Study the effect of NS3-4A in the peroxisome-dependent antiviral signaling

Aim 2. Characterize the role of peroxisomes in antiviral immunity against HCMV (Section 3.2.)

      2.1. Study the effect of vMIA on the peroxisome-dependent antiviral signaling (Section 3.2.1)

      2.2. Unravel the mechanisms behind the role of vMIA within the peroxisome-dependent antiviral signaling (Section 3.2.2)

Aim 3. Construction and analysis of an interaction network between viral and peroxisomal proteins (Section 3.3.)

III. Results

3.1. Hepatitis C virus NS3-4A inhibits the peroxisomal MAVS-dependent antiviral signaling response

III. Results

Abstract

HCV is the cause of one of the most prevalent viral infections worldwide. Upon infection, the HCV genome activates the RIG-I-MAVS signaling pathway leading to the production of direct antiviral effectors which prevent important steps in viral propagation.

MAVS localizes at peroxisomes and mitochondria and coordinate the activation of an effective antiviral response: peroxisomal MAVS is responsible for a rapid but short-termed antiviral response, while the mitochondrial MAVS is associated with the activation of a stable response with delayed kinetics. The HCV NS3-4A protease was shown to specifically cleave the mitochondrial MAVS, inhibiting the downstream response.

In this study, we have analyzed whether HCV NS3-4A is also able to cleave the peroxisomal MAVS and whether this would have any effect on the cellular antiviral response. We show that NS3-4A is indeed able to specifically cleave this protein and release it into the cytosol, a mechanism that seems to occur at a similar kinetic rate as the cleavage of the mitochondrial MAVS. Under these conditions, RLR signaling from peroxisomes is blocked and antiviral gene expression is inhibited. Our results also show that NS3-4A is able to localize at peroxisomes in the absence of MAVS. However, mutation studies have shown that this localization pattern is preferred in the presence of a fully-cleavable MAVS.

These findings present evidence of a viral evasion strategy that disrupts RLR signaling on peroxisomes and provide an excellent example of how a single viral evasion strategy can block innate immune signaling from different organelles.

Introduction

HCV is a positive single stranded RNA virus belonging to the *Flaviviridae* family. HCV infection is one of the most prevalent worldwide affecting 130-170 million people (Chevaliez and Pawlotsky, 2006). With no effective vaccine, the current anti-HCV therapies often lead to significant side effects and result in viral resistance (Sarrazin et al., 2012).

Upon HCV infection, the virus is quickly sensed in the cytosol by soluble RNA helicases, RIG-I and/or MDA5 (Cao et al., 2014; Saito et al., 2008; Yoneyama et al., 2004), which dimerize and interact with MAVS through their CARD domains (Kawai et al., 2005; Meylan et al., 2005; Seth et al., 2005; Xu et al., 2005). This leads to a signaling cascade that culminates with the induction of IFNs and ISGs that

function as direct antiviral effectors, preventing important steps in viral propagation (Moore and Ting, 2008).

HCV has developed different mechanisms of evasion from the cellular immune response (Chen et al., 2013; Ding et al., 2013; Garaigorta and Chisari, 2009; Gokhale et al., 2014; Li et al., 2005b; Petrovic et al., 2011). The viral serine protease NS3-4A, besides being essential for HCV replication and assembling (Moradpour et al., 2007), is a key factor by which HCV is able to efficiently disrupt antiviral response (Foy et al., 2003). This complex is composed by two proteins: NS3, that contains the catalytic domain, and NS4A that acts as a cofactor stabilizing NS3 function and allowing the binding to organelle membranes (He et al., 2012; Hijikata et al., 1993; Morikawa et al., 2011). NS3-4A is able to efficiently cleave MAVS at the mitochondria membrane, leading to the blockage of IFNs production (Li et al., 2005b).

Although initially assumed to localize exclusively at the mitochondria outer membrane (Seth et al., 2005), MAVS was also found to be present at peroxisomes (Dixit et al., 2010), as well as at the MAM (Horner et al., 2011). The peroxisomal and mitochondrial MAVS-dependent pathways result in different but complementing responses: the peroxisomal MAVS is associated to a rapid but short-termed (type I IFN-independent and type III IFN-dependent) protection through the induction of ISGs, while the mitochondrial pathway leads to an type I IFN-dependent production of ISGs, with delayed kinetics and amplifying the peroxisome-dependent response (Dixit et al., 2010).

Peroxisomes are ubiquitous and essential subcellular compartments with a critical role in a variety of metabolic processes (Islinger et al., 2012b; Ribeiro et al., 2012; Schrader and Fahimi, 2006; Schrader and Fahimi, 2008). The novel role as signaling platforms in antiviral defense underlies their importance in health and disease.

In this study we have shown that HCV NS3-4A is also able to cleave the peroxisomal MAVS and affect the cellular antiviral response.

Results and Discussion

HCV NS3-4A is able to specifically cleave the peroxisomal MAVS

Mitochondria and peroxisomes act in concert to establish the RLR-dependent cellular response to viral infections (Dixit et al., 2010; Horner et al., 2011; Odendall et al., 2014). HCV NS3-4A was shown to cleave the mitochondrial MAVS, leading to the dislocation of the N-terminal fragment of MAVS from

the mitochondria to the cytosol and inhibiting the MAVS-dependent immune response (Li et al., 2005b; Meylan et al., 2005). Also the MAM-localized MAVS was shown to be cleaved by this viral protein (Horner et al., 2011). To investigate whether NS3-4A would also cleave the peroxisomal MAVS, we created a myc-tagged mutant of MAVS that localizes solely to peroxisomes, named myc-MAVS-PEX (Figure 6A). This construct was overexpressed in mouse embryonic fibroblasts (Mefs) cells where MAVS had been previously knocked-out (Mefs MAVS-KO cells, described in (Dixit et al., 2010)) and, upon immunolocalization with antibodies against myc and the peroxisomal marker PMP70, its peroxisomal localization was confirmed by confocal microscopy (Figure 6B a-c). The specific cleavage site from MAVS that is recognized by NS3-4A has been mapped to the Cys-508 (Li et al., 2005b; Meylan et al., 2005). We have also created a myc-tagged version of the peroxisomal MAVS that does not contain this cleavage site, which we named myc-MAVS500-PEX (Figure 6A). This construct was similarly overexpressed in Mefs MAVS-KO cells and its peroxisomal localization was confirmed by immunofluorescence (with antibodies against myc and PMP70) and confocal microscopy (Figure 6B d-f). Additionally, we have created a GFP-tagged version of NS3-4A (based on the construct described in (Breiman et al., 2006)), GFP-NS3-4A.
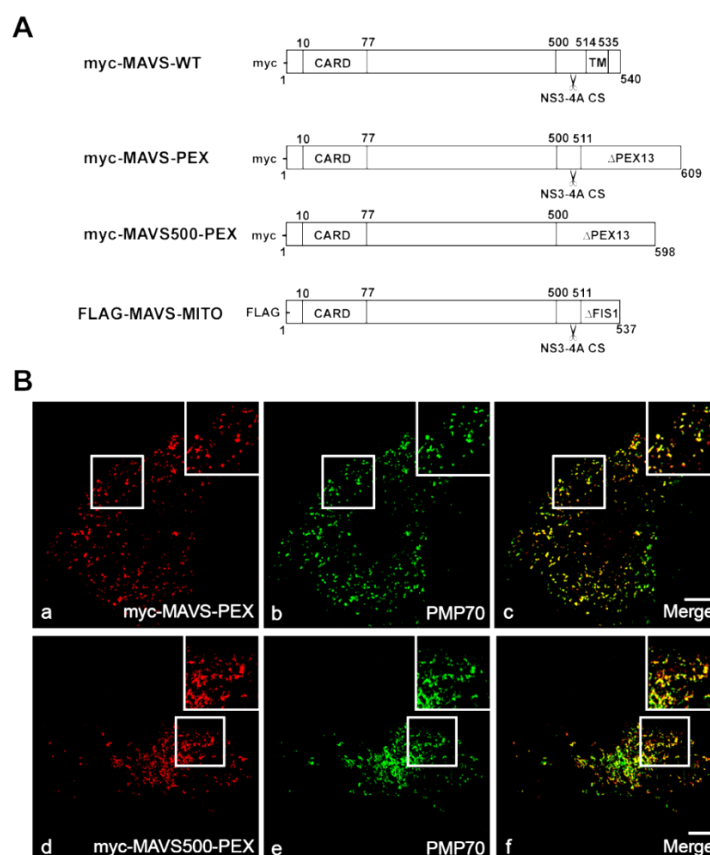
Figure 6. Localization pattern of the different peroxisomal MAVS used in this study. (A) Schematic representation of MAVS-WT and mutant MAVS constructs used in this study. The cleavage site is represented by a scissors. (B) (a-c) MAVS-PEX intracellular localization in Mefs MAVS-KO cells (a) myc-MAVS-PEX, (b) PMP70,

(c) merge image of a and b. (d-f) MAVS500-PEX intracellular localization in Mefs MAVS-KO cells (d) myc-MAVS500-PEX, (e) PMP70, (f) merge image of d and e. Arrows indicate co-localization loci. Bars represent 10 µm. Representative images of three independent experiments.

To analyze the possible cleavage of the peroxisomal MAVS by NS3-4A, we co-transfected myc-MAVS-PEX and GFP-NS3-4A in Mefs MAVS-KO cells. As shown in Figure 7A a-d, in the presence of NS3-4A, MAVS-PEX localizes at the cytoplasm, confirming that NS3-4A was able to traffic to peroxisomes and specifically cleave MAVS. As shown by the arrows in Figure 7A a-d, some MAVS-PEX remains localized at the peroxisomes. This is due to the fact that, at the time-point that the cells where collected (24 hours (hrs) post-transfection) not all the MAVS had yet been cleaved. This is supported by the presence of both myc-MAVS-PEX and GFP-NS3-4A at the same peroxisomes (as shown by the arrows in Figure 7A a-d), where the cleavage has not yet occurred. It is important to notice the presence of NS3-4A at some peroxisomes that do not contain MAVS-PEX. Whether this represents NS3-4A that remains attached to the peroxisomes after cleavage of MAVS-PEX or NS3-4A that simply migrated to peroxisomes that did not contain MAVS-PEX will be further investigated and discussed below in this section. As expected, myc-MAVS500-PEX was not cleaved by GFP-NS3-4A (Figure 7A e-h).
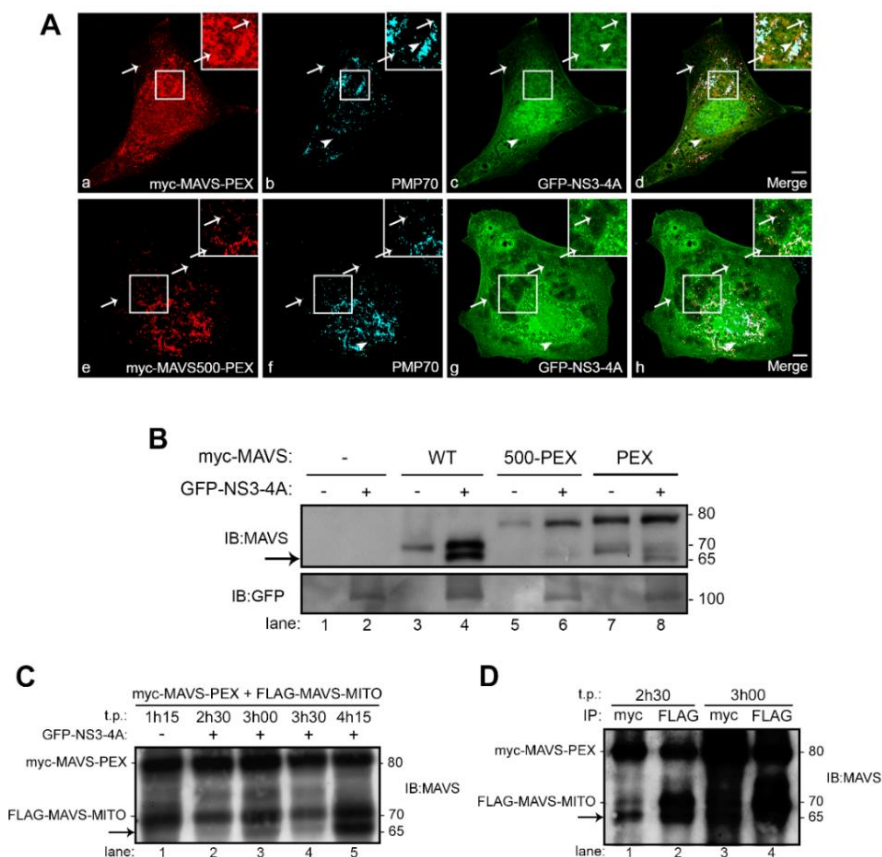
Figure 7. NS3-4A cleaves the peroxisomal MAVS with similar kinetics as the mitochondrial MAVS. (A) (a-d) MAVS-PEX is cleaved by NS3-4A in Mefs MAVS-KO cells. (a) myc-MAVS-PEX, (b) PMP70, (c) GFP-NS3-4A, (d)

merge image of a, b and c. (e-h) MAVS500-PEX is not cleaved by NS3-4A (e) myc-MAVS500-PEX, (f) PMP70, (g) GFP-NS3-4A, (d) merge image of e, f and g. Arrows indicate co-localization loci between MAVS-PEX or MAVS500-PEX with peroxisomes and NS3-4A. Full-head arrows indicate co-localization loci between peroxisomes and NS3-4A. Bars represent 10 µm. (B) Western blot analysis of NS3-4A cleavage of WT and mutant MAVS in Mefs MAVS-KO cells. Arrow indicates the cleavage product of MAVS. (C) Time course of myc-MAVS-PEX and FLAG-MAVS-MITO cleavage by GFP-NS3-4A in Mefs MAVS-KO cells. Arrow indicates the cleavage product of MAVS. (D) Pull-down analysis of the myc-MAVS-PEX and FLAG-MAVS-MITO in Mefs MAVS-KO cells. Immunoprecipitation was performed with antibodies against myc and FLAG. Arrow indicates the cleavage product of MAVS. Representative images of three independent experiments.

To confirm the cleavage of MAVS-PEX by NS3-4A, we performed western blot analyses of lysates from Mefs MAVS-KO cells expressing MAVS-PEX, MAVS500-PEX or wild-type (WT) MAVS (described in (Dixit et al., 2010)) in the presence or absence of NS3-4A. As shown in Figure 7B, a band corresponding to the expected size of the cleaved N-terminal fragment of MAVS appears when either MAVS-WT or MAVS-PEX were co-transfected with NS3-4A (indicated by the arrow, lanes 4 and 8 in Figure 7B), confirming that both proteins were cleaved by the viral protease.

The cleavage of the peroxisomal and mitochondrial MAVS by NS3-4A seems to occur with similar kinetics

The peroxisome-dependent RLR response to viral infections occurs faster than the mitochondrial one, which is slower but long-lasting, stabilizing the response initiated at peroxisomes (Dixit et al., 2010). We wondered whether the virus would somehow kinetically distinguish MAVS targeting at these two different organelles, more specifically, whether NS3-4A would cleave the peroxisomal MAVS faster than the mitochondrial one, to initially counteract the faster RLR response. To answer this question, we have constructed a mitochondria-targeted version of MAVS (FLAG-MAVS-MITO). The myc-MAVS-PEX and FLAG-MAVS-MITO were co-transfected into Mefs MAVS-KO cells and the lysates where collected at different time-points and analyzed by western blot. As shown in Figure 2C, as early as 2 hrs 30 min post-transfection, it is already possible to observe a band that corresponds to the cleaved N-terminal of MAVS (lane 2, indicated by the arrow). As it is not possible, with this experiment, to distinguish whether this band corresponds to the peroxisomal or mitochondrial MAVS, we have performed pull-down analyses of these lysates with antibodies against myc or FLAG at the two lower time-points where the cleavage was observed. As shown in Figure 2D, at 2 hrs 30min both myc-tagged and FLAG-tagged N-terminals of MAVS were pulled-down, indicating that both peroxisomal and mitochondrial MAVS had already been partially cleaved. At these low post-transfection time-points it is extremely difficult to obtain the necessary amount of protein to perform these analyses (cells are still recovering from the transfection procedure and the produced protein level in each cell is still low), which precluded the analyses at even lower time-points. Our results show that at 2 hrs 30 min post-

transfection both MAVS are cleaved but does not allow any specific conclusion concerning which one is the first to be cleaved. However, if at this time-point we can already clearly observe this cleavage, it is tempting to extrapolate that NS3-4A will cleave MAVS at both organelles with similar kinetics. Nevertheless, these results show that the virus does not preferentially cleave the mitochondrial MAVS, confirming the relevance of the peroxisome-dependent pathway and the importance of its inhibition by HCV for viral propagation.

NS3-4A cleavage of peroxisomal MAVS strongly inhibits the peroxisome-dependent antiviral cellular response

To analyze whether the cleavage of the peroxisomal MAVS by NS3-4A would cause the inhibition of the RLR signaling, we have co-transfected myc-MAVS-PEX and GFP-NS3-4A in Mefs MAVS-KO cells. RLR-dependent signaling events were stimulated in these cells by overexpressing a constitutively active version of RIG-I (GFP-RIG-I-CARD, (Yoneyama et al., 2004)). Twenty-four hours after the co-transfection, GFP-RIG-I-CARD was transfected and, 6 hrs after, the production of mRNA of two ISGs (IRF1 and Viperin) was quantified by RT-qPCR. As shown in Figure 8, there was a clear increase on the production of IRF1 and Viperin upon GFP-RIG-I-CARD overexpression when compared with control cells solely transfected with myc-MAVS-PEX. In the presence of NS3-4A, however, the production of IRF1 and Viperin decreased, clearly demonstrating that the cleavage of MAVS-PEX by NS3-4A disrupts MAVS signaling transduction from peroxisomes.
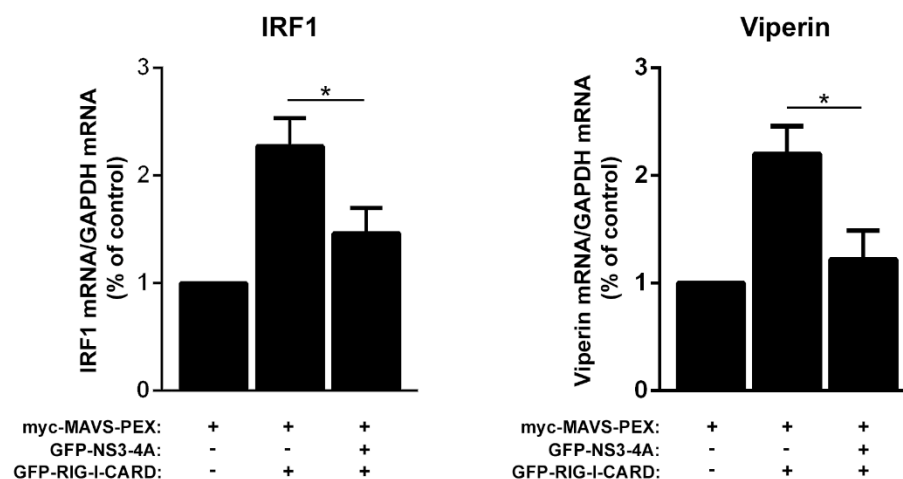
Figure 8. Cleavage of the peroxisomal MAVS by NS3-4A inhibits the peroxisomal-dependent production of antiviral compounds. RT-qPCR analysis of IRF1 and Viperin mRNA expression in Mefs MAVS-KO cells expressing myc-MAVS-PEX and stimulated with GFP-RIG-I-CARD in the presence or absence of GFP-NS3-4A. GAPDH was used as control. Data represents the means ± SEM of three independent experiments. Error bars represent SEM. *$p<0.05$ in one-way ANOVA, with Bonferroni's post-test, conditions were compared with the control myc-MAVS-PEX condition

III. Results

NS3-4A is able to traffic to peroxisomes in the absence of MAVS but preferentially targets this organelle in the presence of a fully cleavable version of this protein

The observation that NS3-4A can be present at peroxisomes containing MAVS without the specific cleavage site (Figure 7A), led us to wonder whether NS3-4A would be attracted to this organelle by the specific presence of MAVS at its membranes or due to the specific characteristics or the organelle itself. Up to now, this study has never been performed for any cellular organelle where NS3-4A is present.

To perform these analyses, we have expressed GFP-NS3-4A in Mefs MAVS-KO cells, in the presence or absence of myc-MAVS-PEX. As shown in Figure 9A, even in the absence of the peroxisomal MAVS, the NS3-4A can be partially found at peroxisomes. To statistically compare the level of NS3-4A at peroxisomes in the presence or absence of MAVS at this organelle, we have analyzed the co-localization level in about 45 cells per condition (from three independent experiments). We have also compared our results with the level of co-localization between NS3-4A and peroxisomes in cells where the non-cleavable myc-MAVS500-PEX was present. Figure 9B shows a quite high co-localization level between NS3-4A and peroxisomes when no MAVS are present at the organelle. However, this level increases when peroxisomal MAVS are present, especially if these MAVS contain the cleavage site.
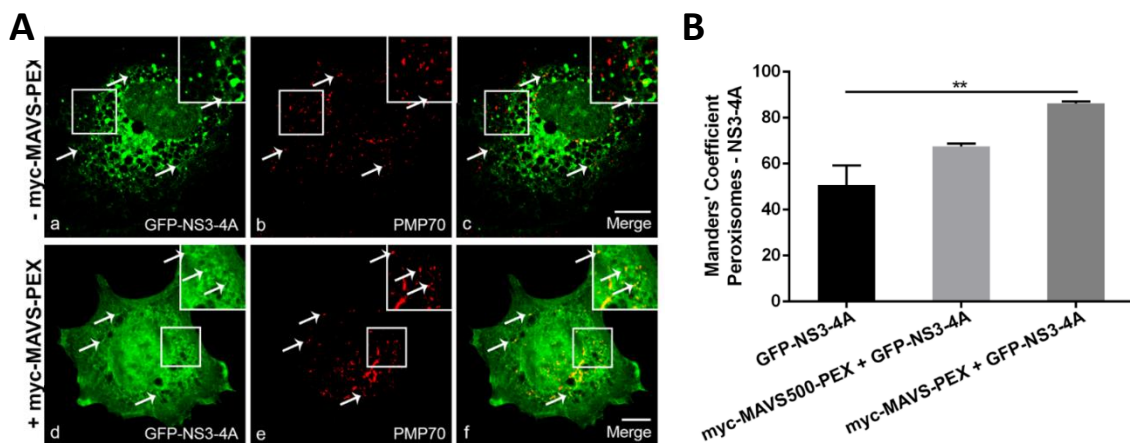
Figure 9. NS3-4A intracellular localization analysis in Mefs MAVS-KO cells. (A) (a-c) NS3-4A intracellular localization in the absence of MAVS-PEX (a) GFP-NS3-4A, (b) PMP70, (c) merge image of a and b. (d-f) NS3-4A intracellular localization in the presence of MAVS-PEX (d) GFP-NS3-4A, (e) PMP70, (f) merge image of d and e. Arrows indicate co-localization loci. Bars represent 10 µm. Representative images of three independent experiments. (B) Co-localization between NS3-4A and peroxisomes was analyzed using Manders' coefficient. Data represents the means ± SEM of three independent experiments, 45 cells were analyzed for each condition. Error bars represent SEM. **$p<0.01$ in one-way ANOVA, with Bonferroni's post-test.

Previous studies have shown that NS4A, besides stabilizing NS3, is responsible for the localization of the NS3-4A complex at the organelle's membranes (Hijikata et al., 1993; Tanji et al., 1995; Wölk et al.,

2000). Tanji et al (Tanji et al., 1995) have shown that, in their system, in the absence of NS4A, more than 50% of the NS3 was localized in the cytosol fraction, while when co-produced with NS4A, most of it was found in the membrane fraction. On the other hand, one other study has shown that NS4A alone was not sufficient enough to confer the membrane association and stability of NS3 protein and have stressed the importance of the NS3 helix α0 for these processes (He et al., 2012). Nevertheless, up to now, no study has tackled the possibility that NS3-4A would be attracted to the organelle's membranes by some specific membrane characteristics or by the presence of other (interacting) proteins in these membranes.

Our results suggest a model by which NS3-4A traffics to peroxisomes by itself but remains longer at these organelle's membranes when it encounters its interacting partner MAVS (Figure 5). The presence of NS3-4A at the peroxisomal membranes seems to be even less transient when the MAVS possesses the original cleavage site. More studies should be performed in order to better dissect the NS3-4A trafficking mechanisms, as well as the characteristics of the organelle's membranes that are responsible for attracting this viral protein complex.

Our findings have not only uncovered an additional mechanism for HCV evasion from the host antiviral defenses but also contribute to the unravelling of important antiviral signaling mechanisms that may affect many different viruses. Hence, these results may not only lead to the discovery of specific cellular targets for combat strategies against HCV, but also to the potential development of broad-spectrum antiviral therapeutics.
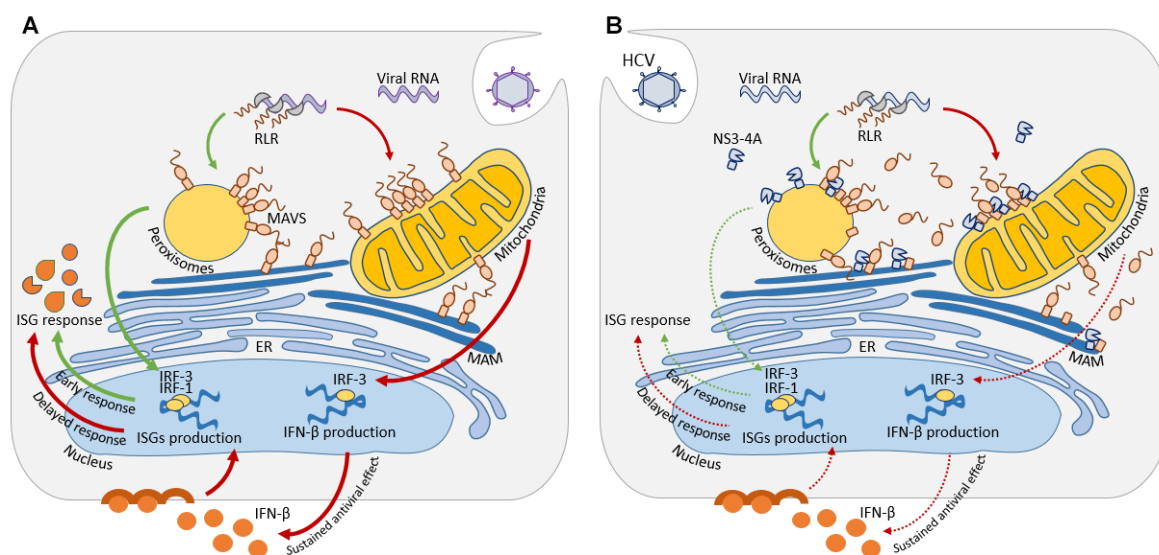
Figure 10. Model of organelle specific MAVS antiviral defense and HCV NS3-4A effect. (A) During infection, viral RNA is released into the cytosol where it is recognized by RLR receptors. RLR receptors activate MAVS present at peroxisomes, mitochondria and MAM. Peroxisomal MAVS induces an early antiviral response through

III. Results

IFN-independent ISGs expression. This rapid response is complemented by mitochondrial MAVS activation that mediates the expression of ISG through the secretion of type I IFN, promoting a delayed but sustained response. (B) HCV produces NS3-4A, non-structural protein for its life cycle that, among other functions, allows cellular antiviral defenses evasion. To accomplish this, HCV NS3-4A cleaves the adaptor protein MAVS at peroxisomes, mitochondria and MAM. MAVS cleavage leads to its release into the cytosol impairing the downstream signaling from peroxisomal and mitochondrial MAVS.

Materials and Methods

Plasmids and Antibodies

Myc-MAVS-PEX was generated by replacing the previously described localization motif of MAVS (Seth et al., 2005) with the localization motif of the peroxisomal protein PEX13 (Fransen et al., 2001) and adding a myc-tag to the N-terminal of the protein. This was performed using the MAVS-WT and MAVS500-PEX sequences (MAVS500-PEX was based on the construct previously described by Dixit et al (2010), where it was named MAVS-PEX (Dixit et al., 2010)) as templates and cloning into the pCMV-3C (Agilent Technologies, La Jolla, California, USA) vector. FLAG-MAVS-MITO was generated by replacing the PEX13 part of the myc-MAVS-PEX construct by the localization motif of the protein FIS1 (as described in (Dixit et al., 2010)) as well as the myc-tag by a FLAG-tag. This was performed using the MAVS-WT and MAVS500-MITO sequences (MAVS500-MITO was generated by cloning MAVS-MITO, described in (Dixit et al., 2010), as templates and it was cloned into the pCMV-2A (Agilent Technologies, La Jolla, California, USA) vector. NS3-4A was kindly provided by Dr. Meurs (Institut Pasteur, France), and it was cloned into a pEGFP-C1 vector (Clontech Laboratories, Mountain View, California, USA). GFP-RIG-I-CARD was kindly provided by Dr. Weber (Philipps-University Marburg, Germany).

In immunofluorescence, anti-PMP70 (Sigma-Aldrich, St. Louis, Missouri, USA) and anti-myc (71D10, Cell Signaling Technology, Beverly, Massachusetts, USA) were used to detect peroxisomes and Myc-MAVS-PEX, respectively. In immunoblotting, anti-MAVS (E-3, Santa Cruz Biotechnology, Dallas, Texas, USA), anti-GFP (Invitrogen, Waltham, Massachusets, USA), anti-myc (9E10, Santa Cruz Biotechnology, Dallas, Texas, USA) and anti-FLAG (Sigma-Aldrich, St. Louis, Missouri, USA) were used to detect MAVS, Myc-MAVS-PEX, FLAG-MAVS-MITO, respectively. Species-specific anti-IgG antibodies conjugated to HRP (BioRad Hercules, California, USA) and the fluorophores TRITC (Jackson Immunoresearch, West Grove, Pennsylvania, USA), Alexa 488 and Alexa 647 (both from Invitrogen, Waltham, Massachusetts, USA) were used as secondary antibodies.

40

Cell culture and transfections

Mefs MAVS-KO cells (described in (Dixit et al., 2010)) were cultured in Dulbecco's modified Eagle's medium supplemented with 100 U/mL, 100mg/mL streptomycin and 10% fetal bovine serum (all from PAA Laboratories GmbH, Germany) and incubated at 37°C in atmosphere containing 5% CO_2. These cells were transfected by microporation using the Neon Transfection System, under the manufacture recommendations (Invitrogen, Waltham, Massachusetts, USA). Cells were harvested and fixed from 2 hrs 30min to 24 hrs after transfection.

Immunofluorescence and microscopy analyses

Cells were processed for immunofluorescence as in (Valença et al., 2015) and photos were acquired with a Leica HCS A confocal microscope, using a Plan-Apochromat 63x water objective (Leica Microsystems CMS GmbH, Mannheim, Germany), and a Zeiss LSM 510 confocal microscope, using a Plan-Apochromat 63x and 100x/1.4 NA oil objectives (Carl Zeiss, Oberkochen, Germany). The lasers used were the 488 nm Argon-ion laser, the 561 nm DPSS laser and the 642 nm HeNe. Digital images were optimized for contrast and brightness using Adobe Photoshop (Adobe Systems, San Jose, CA, USA). Co-localization analysis were performed using the JACoP software (ImageJ, Bethesda, MD, USA) (Bolte and Cordelières, 2006).

Gel Electrophoresis and Immunoblotting

Cells lysates and protein quantification were performed as in (Valença et al., 2015) . After 15 min incubation at 65°C, protein samples were separated by SDS-PAGE in 7% polyacrylamide gels and transferred to a nitrocellulose membrane (PROTAN, Whatman, Dassel, Germany) by wet transfer. Immunoblots were treated with specific antibodies and enhanced chemiluminescence reagents (GE Healthcare, Waukesha, Wisconsin, USA).

Immunoprecipitation

For immunoprecipitation of myc-MAVS-PEX and FLAG-MAVS-MITO, the Protein G Magnetic beads kit (Millipore, Massachusetts, USA) was used. At indicated time-points, microporated cells were harvested and lysed as described. After protein quantification, protein samples were incubated with anti-myc (9E10, Santa Cruz Biotechnology, Dallas, Texas, USA) and anti-FLAG (Sigma-Aldrich, St. Louis,

III. Results

Missouri, USA) for 2 hrs at 4°C on a rotary mixer, before adding the beads to the mixture and incubating for 10 min. at room temperature. After washing, proteins were eluted in 3x laemmli sample buffer for 10 min. at 95°C. Immunoprecipitated samples were separated by running in a 7% SDS-polyacrylamide gel.

RNA extraction, cDNA synthesis and quantitative real-time polymerase chain reaction

Total RNA was isolated using TriFast reagent (Peqlab, VWR International GmbH, Erlangen, Germany) and quantified using NanoDrop 1000 (Thermo Scientific, Waltham, Massachussetts, USA). cDNA synthesis was obtained using 2 µg RNA and M-MuL V reverse transcriptase (New England Biolabs, Ipswich, Massachusetts, USA). RT-qPCR was performed in duplicate using iTaq Universal SYBR Green Master Mix (BioRad, Hercules, California, USA) and reactions were run on Applied Biosystems 7500 Real Time PCR System (Applied Biosystems, Walthman, Massachussetts, USA). Primer sequences used for quantification of IRF1 were 5' GGTCAGGACTTGGATATGGAA 3' and 5' AGTGGTGCTATCTGGTATAATGT 3', for Viperin were 5' TGTGAGCATAGTGAGCAATGG 3' and 5' TGTCGCAGGAGATAGCAAGA 3' and for GAPDH were 5' AGTATGTCGTGGAGTCTA 3' and 5' CAATCTTGAGTGAGTTGTC 3', and were designed using the Beacon Designer 7 (Premier Biosoft, Palo Alto, California). GAPDH was used as a reference gene and data analysis was performed using the 2−ΔΔCT method.

Statistical analyses

Statistical analysis was performed in Graph Pad Prism 5 (GraphPad Software, Inc., La Jolla, California, USA). Data represent the mean ± standard error mean (SEM). To determine the statistical significance between the experimental groups the one-way ANOVA followed by Bonferroni's multiple comparison tests. P values of P≤0.05 were considered as significant.

3.2. Human cytomegalovirus' vMIA controls evasion of the peroxisome-dependent cellular immune response via MAVS and MFF

Part of the results presented in this section were published as:

Ana Cristina Magalhães[1]*, <u>Ana Rita Ferreira</u>[1]*,Sílvia Gomes[1], Marta Vieira[1], Ana Gouveia[1], Isabel Valença[1], Markus Islinger[2], Rute Nascimento[3], Michael Schrader[4], Jonathan C. Kagan[5] and Daniela Ribeiro[1]* "**Peroxisomes are platforms for cytomegalovirus' evasion from the cellular immune response**". Scientific Reports. 2016. 6:26028.

Part of the results presented in this section are included in a manuscript which will soon be submitted for publication as:

<u>Ana Rita Ferreira</u>[1,5]*, Ana Gouveia[1]*, Ana Cristina Magalhães[1], Isabel Valença[1], Mariana Marques[1], Jonathan C. Kagan[5], Michael Schrader[4] and Daniela Ribeiro[1], "**Human Cytomegalovirus' vMIA controls peroxisome morphology and dampens antiviral signaling via MAVS and MFF**" (soon to be submitted to Molecular Cell)

[1]Institute for Research in Biomedicine – iBiMED, Department of Medical Sciences & Department of Biology, University of Aveiro, Aveiro, Portugal. [2]Neuroanatomy, Center for Biomedicine and Medical Technology Mannheim, University of Heidelberg, Heidelberg, Germany. [3]Infections and Immunity Laboratory, Instituto Gulbenkian de Ciência, Oeiras, Portugal. [4]College of Life and Environmental Sciences, Biosciences, University of Exeter, Exeter, Devon, UK. [5]Division of Gastroenterology, Boston Children's Hospital and Harvard Medical School, Boston, MA, USA. * co-authorship

Abstract

The human cytomegalovirus developed distinct evasion mechanisms from the cellular antiviral response involving vMIA, a virally-encoded protein that is not only able to prevent cellular apoptosis but also to inhibit signaling downstream from mitochondrial MAVS. vMIA has been shown to localize at mitochondria and to trigger their fragmentation, a phenomenon proven to be essential for the signaling inhibition. Here, we demonstrate that vMIA is also localized at peroxisomes, induces their fragmentation and inhibits the peroxisomal-dependent antiviral signaling pathway. Importantly, we demonstrate that peroxisomal fragmentation is not essential for vMIA to specifically inhibit signaling downstream the peroxisomal MAVS. Moreover, we show that vMIA depends on the interaction with MFF, adaptor protein from the fission machinery, to impair the peroxisomal-dependent antiviral signaling. We also show that vMIA interacts with the cytosolic chaperone PEX19, suggesting that the virus has developed a strategy to highjack the peroxisomal membrane proteins' transport machinery. Furthermore, we show that vMIA is able to specifically interact with the peroxisomal MAVS, inhibiting its oligomerization, which has been proven to be essential for the activation of the downstream signaling. Our results demonstrate that peroxisomes constitute a platform for evasion of the cellular antiviral response and that the human cytomegalovirus has developed a mechanism by which it is able to specifically evade the peroxisomal MAVS-dependent antiviral signaling.

Introduction

The HCMV is a large enveloped virus with dsDNA genome that belongs to the *Herpesviridae* family (Mocarski et al., 2007). HCMV is a highly widespread pathogen that has been described as one of the major causes of birth defects, when acute infection occurs during pregnancy, and opportunistic diseases in immunocompromised patients (Cannon et al., 2010; Lancini et al., 2014). HCMV has the ability to establish a state of latency and persist indefinitely in the host despite the continuously induced antiviral immune responses (Dupont and Reeves, 2016; Paludan et al., 2011).

Apoptosis is one of the first lines of defense against viral infections. With a slow replication cycle, HCMV depends on the sustained cell viability (Paludan et al., 2011) and, in order to prevent the premature death of infected cells, the virus has evolved various strategies to block apoptotic signaling pathways and subvert the host antiviral response (Fliss and Brune, 2012; Goldmacher, 2005). HCMV encodes vMIA (also named pUL37x1) that plays an important role on the inhibition of apoptosis

III. Results

(Goldmacher et al., 1999; Ma et al., 2012). vMIA prevents the formation of the mitochondrial permeability transition pore, the release of cytochrome c and pro-apoptotic factors into the cytosol as well as the activation of executioner caspases (Fliss and Brune, 2012; Goldmacher, 2005). Although the mechanism involved is still somewhat controversial, it was shown that vMIA interferes with Bax and triggers the blockage of the mitochondrial outer membrane permeabilization (Ma et al., 2012; Poncet et al., 2004). Among other functions, vMIA also induces calcium (Ca^{2+}) efflux from the ER, regulates viral early gene expression and disrupts F-actin (Sharon-Friling et al., 2006).

vMIA has also been shown to inhibit the cellular antiviral response by dampening signaling downstream from the mitochondrial MAVS and triggering mitochondria fragmentation, a phenomenon proven to be essential for this signaling inhibition (Castanier et al., 2010; McCormick et al., 2003).

MAVS-dependent antiviral signaling is activated by the recognition of the viral genome by the soluble RLR, such as RIG-I and MDA-5. Upon viral stimulation, these proteins undergo a conformational change, leading to their dimerization and interaction with MAVS through their CARD domains (Moore and Ting, 2008). This leads to a signaling cascade that culminates with the induction of type I IFNs and ISGs that may function as direct antiviral effectors, preventing important steps in viral propagation. It has been suggested that vMIA inhibition of the MAVS-dependent signaling may be due to a reduction of the interaction between MAVS and the cytosolic DNA sensor STING, an ER protein that was reported to be associated with MAVS and to be important for type I IFN production after viral infection (Ishikawa et al., 2009; Sun et al., 2009). It has been suggested that, by inducing mitochondrial fragmentation, vMIA affects the association between this organelle and the ER, disturbs the MAVS-STING interaction and, consequently, dampens type I IFN signaling and ISGs production (Campello and Scorrano, 2010; Castanier et al., 2010).

Dixit et al (Dixit et al., 2010) have demonstrated that MAVS is also localized at peroxisomes and that peroxisomal and mitochondrial MAVS assume complementing functions within the antiviral response. The peroxisomal MAVS induces the rapid expression of ISGs, conferring short-term protection, while the mitochondrial MAVS activates an interferon-dependent signaling pathway with delayed kinetics that amplifies and stabilizes the antiviral response (Dixit et al., 2010).

Peroxisomes represent a class of ubiquitous and essential single-membrane bound subcellular organelles that fulfil important metabolic functions in, among others, lipid and ROS metabolism (Islinger et al., 2012b; Schrader and Fahimi, 2006). Like mitochondria, peroxisomes are dynamic and their protein composition, morphology and abundance is tightly regulated upon external stimuli to maintain cellular homeostasis (Ribeiro et al., 2012; Schrader and Fahimi, 2008). The discovery of the

presence of MAVS at peroxisomes has added a novel function to this organelle in cellular antiviral signaling, expanding their impact on health and disease.

Here, we investigated the possibility that HCMV would have developed a mechanism through which it could specifically interfere with the peroxisomal MAVS-dependent signaling pathway. Our results indeed demonstrate that vMIA is also localized at peroxisomes and dampens the peroxisomal MAVS-dependent production of ISGs. Furthermore, we demonstrate that vMIA induces peroxisomal fragmentation, a morphological change that, unlike for mitochondria, does not seem to be relevant for the antiviral signaling inhibition. We additionally demonstrate that vMIA interacts with MFF and this protein is crucial for vMIA effect on the inhibition of the peroxisomal MAVS-dependent antiviral signaling. Importantly, we also reveal that vMIA interacts with the peroxisomal MAVS and impedes the formation of MAVS oligomers, an essential step from the antiviral signaling response.

Results

Cytomegalovirus' protein vMIA localizes at peroxisomes and induces their fragmentation

The RLR adaptor protein MAVS is localized at mitochondria and peroxisomes (as well as at MAM), and these organelles act in concert to establish the cellular antiviral response (Dixit et al., 2010; Horner et al., 2011; Odendall et al., 2014). vMIA (Supplementary Data - Figure 22A) has been shown to induce mitochondrial fragmentation (Ma et al., 2012; McCormick et al., 2003) and modulate the mitochondrial MAVS-dependent signaling (Castanier et al., 2010). As peroxisomes and mitochondria share many of their membrane proteins, including the main components of their division machinery, we wondered whether vMIA would also localize at peroxisomes and interfere with the antiviral signaling pathway that is established at this organelle. To that end, HepG2 cells (human hepatocyte cell model) as well as HFF cells (human foreskin fibroblasts, a specific cell type that is commonly infected by HCMV) were transfected with myc-tagged vMIA and, after 24 hrs, subjected to immunolocalization analysis with antibodies against myc and the peroxisomal marker PEX14. In addition to displaying the expected localization pattern at fragmented mitochondria (Figure 11A and B and Supplementary Data - Figure 22D), we found vMIA to be also localized at peroxisomes, both in HepG2 (Figure 11A) and HFF cells (Figure 11B). An analysis of the Manders' co-localization coefficients indicates that 6.69% of the vMIA co-localizes with the peroxisomal marker in HepG2 cells and 26.12% in HFF cells.
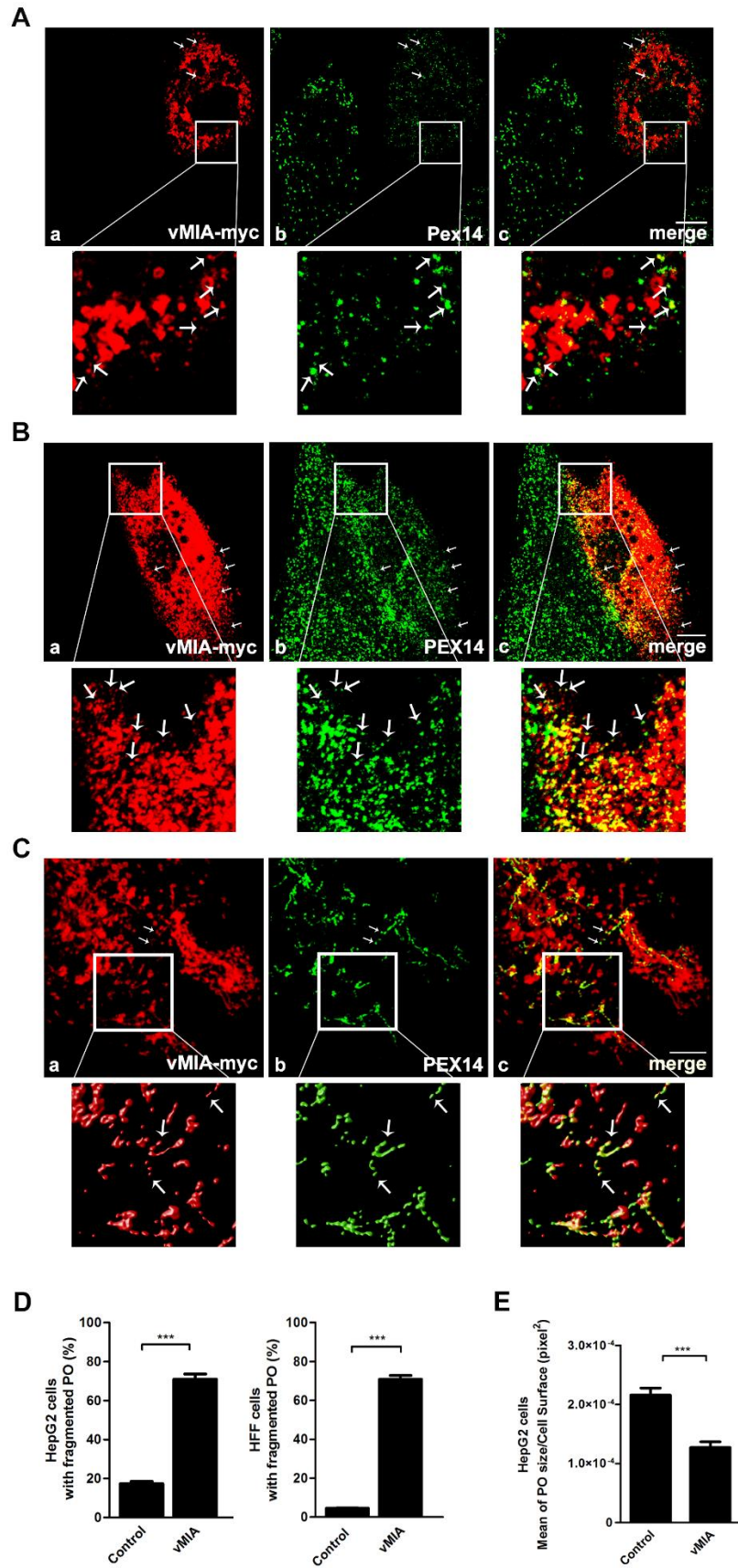
Figure 11. vMIA localizes at peroxisomes and causes their fragmentation. (A) (a-c) vMIA intracellular localization in HepG2 cells (a) vMIA-myc, (b) PEX14 and (c) merge image of a and b. (B) (a-c) vMIA intracellular

localization in HFF cells (a) vMIA-myc, (b) PEX14 and (c) merge image of a and b. (C) (a-c) vMIA intracellular localization in DLP1-patient cells. (a) vMIA-myc, (b) PEX14 and (c) merge image of a and b. The images presented in the zoom insets from panel C are the result of deconvolution and 3D rendering analysis. Confocal images from immunofluorescence staining. Bars represent 10 μm. Arrows represent co-localization loci. (D) Quantification analysis of peroxisome morphology in the presence and absence of vMIA in HepG2 and HFF cells. We considered cells containing "fragmented peroxisomes" as those whose peroxisomes were significantly smaller and in higher number when compared to the control cells. Data represents the means ± SEM of three independent experiments. Error bars represent SEM. ***$p < 0.001$ in a Student's t test. (E) Quantification analysis of peroxisomal area (pixel^2) in the presence or absence of vMIA in HepG2 cells, using the Spot Detector plug-in from Icy Bioimage Analysis Software. Data represents the means ± SEM of three independent experiments. Error bars represent SEM. ***$p < 0.001$ in a Student's t test.

In order to more clearly demonstrate the presence of vMIA at peroxisomes, we performed similar transfection and immunolocalization analysis in fibroblasts that present bigger and hypertubulated peroxisomes. These cells (which we here name DLP1-patient cells) were isolated from a patient with an heterozygous, dominant-negative mutation in the DLP1 gene (Waterham et al., 2007) and present a dramatic defect on peroxisomal and mitochondrial fission, exhibiting mainly hypertubulated organelles. As shown in Figure 11C (where the zoom insets present the results obtained with deconvolution and 3D rendering analyses), vMIA clearly localizes at the hypertubulated peroxisomes.

Interestingly, as shown in Figure 11A and 11B where one can compare a transfected and a non-transfected cell for each of the cell lines, vMIA overexpression induced a significant peroxisomal fragmentation: peroxisomes appear smaller and in higher number. In order to support this observation, we performed statistical analysis where six hundred cells (of each of the cell lines), from three independent experiments, were analyzed for each condition, taking into account the size/shape and number of their peroxisomes. We considered cells containing "fragmented peroxisomes" as those whose peroxisomes were significantly smaller and in higher number when compared to the control cells (differences in fluorescence intensities were taken into account for each cell and experiment). As shown in Figure 11D, 71% of the HepG2 cells expressing vMIA contained fragmented peroxisomes, while only 17% of control cells displayed this phenotype. Similarly, the results for HFF cells show an increase on the number of cells with fragmented peroxisomes from about 4% (in control cells) to 70% upon vMIA overexpression (Figure 11D). Using the Spot Detector plug-in from Icy Bioimage Analysis Software (de Chaumont et al., 2012), we confirmed that, upon vMIA overexpression in HepG2 cells, there was a decrease in the mean surface area of each peroxisome (Figure 11E). In all the cells exhibiting a peroxisomal fragmentation, a fragmentation of the mitochondrial network was also observed (Supplementary Data - Figure 22D).

In order to perform a biochemical analysis that would complement the results obtained with the immunofluorescence analyses and, as the current methodologies do not allow the preparation of pure peroxisomal fractions from cell cultures, we have performed differential centrifugation experiments

with lysates from HFF cells transfected with vMIA-myc and obtained a fraction that (although presenting some degree of contamination with light mitochondria and small vesicles such as lysosomes and endosomes) is highly enriched in peroxisomes (Figure 12A, PO). We found that vMIA is present at the enriched peroxisomal fractions (Figure 12A), confirming and complementing the results obtained with the immunofluorescence analyses. We have also performed a density gradient centrifugation (Figure 12B) with HepG2 cells and obtained similar results: the majority of vMIA co-migrates with the mitochondrial markers but is also present at the fraction where the peroxisomal markers are concentrated (Figure 12B, lane 4). As expected, and similarly to the fractionation experiment, there is some degree of contamination of this fraction with mitochondria. In fact, besides being a common drawback on the analysis of peroxisomal fractions with the currently available methodologies, this is enhanced by the presence of vMIA: as this protein induces mitochondrial fragmentation, there will be an increase on the presence of small mitochondria at the peroxisomal fractions. The density gradient results show also some level of co-migration of the peroxisomal and ER-markers. This is, however, irrelevant for the vMIA localization analysis as we, and others, have never observed the presence of this protein at this organelle.
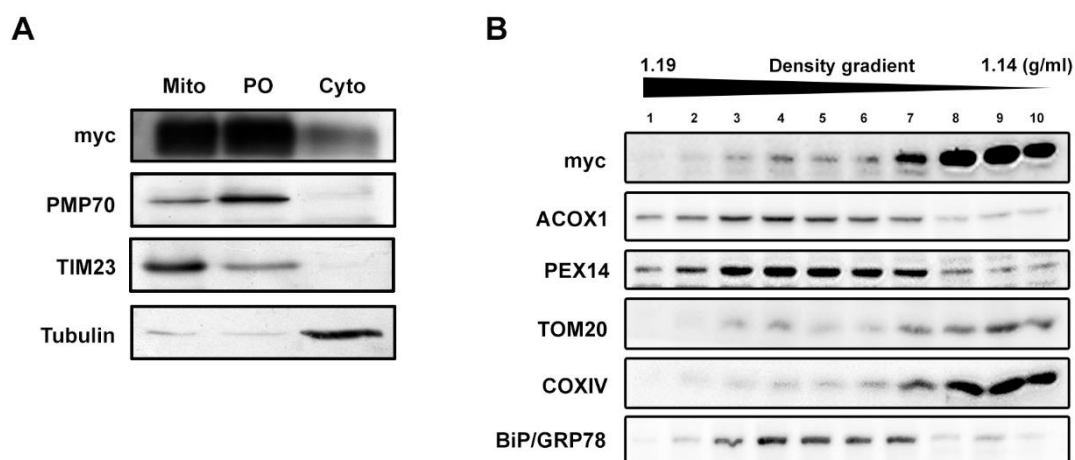
Figure 12. Biochemical analysis of vMIA intracellular localization. (A) Western blot analysis of the presence of vMIA in cytosolic (Cyto), mitochondrial (Mito) and peroxisomal-enriched (PO) fractions, upon differential centrifugation of HFF lysates. PMP70, TIM23 and tubulin were used as peroxisomal, mitochondrial and cytosolic markers, respectively. (B) Western blot analysis of the localization of vMIA after density gradient centrifugation of HepG2 lysates. ACOX1 and PEX14 are used as peroxisomal markers, TOM20 and COXIV are used as mitochondrial markers and BiP/GRP78 as ER marker.

In order to determine whether virally-produced vMIA is also present at peroxisomes, we analyzed the localization of this protein upon infection of HFF cells with HCMV. HFF cells where infected with the HCMV AD169 strain and, 8 hrs after infection, were subjected to immunofluorescence analysis with antibodies against vMIA and the peroxisomal marker catalase. As shown in Figure 13, the HCMV-

produced vMIA is not only localized at fragmented mitochondria but is also present at peroxisomes. We have once again calculated the Manders' co-localization coefficient and the results show that 11.65% of vMIA co-localizes with the peroxisomal marker. Interestingly, the infected cells (Figure 13 b-d) show some level of peroxisomal fragmentation (defined by a higher number of smaller peroxisomes) when compared to non-infected cells (Figure 13 a), similarly to what was observed upon vMIA overexpression. Overall, these results demonstrate that vMIA localizes at peroxisomes and regulates peroxisome morphology.
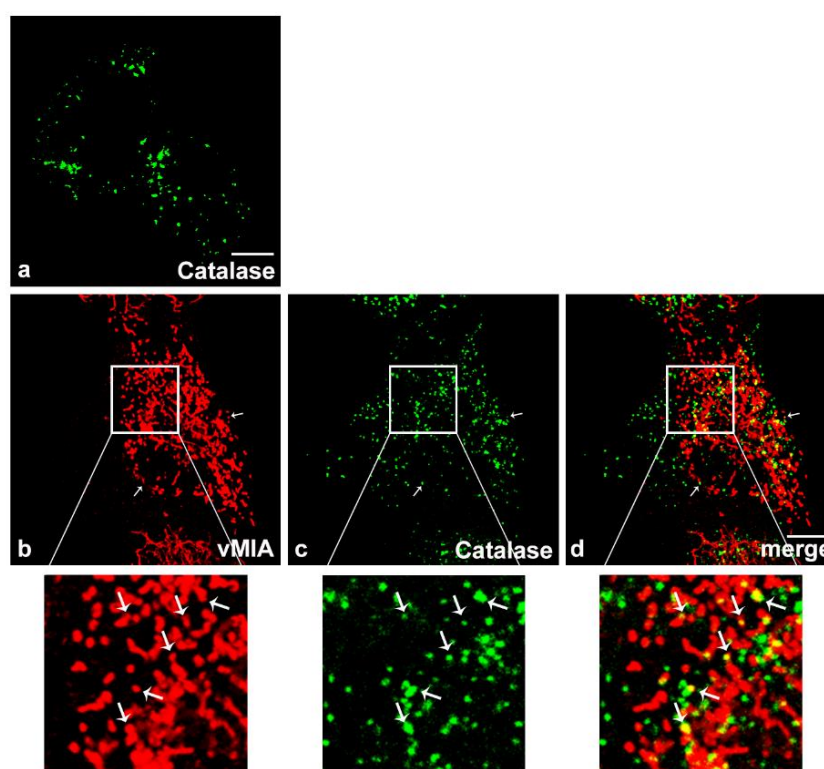
Figure 13. vMIA localization upon HCMV infection. (a) Representative image of peroxisomal morphology in uninfected HFF cells, stained with catalase. (b-d) HFF cells infected with HCMV, 8 hrs post-infection. (b) vMIA, (c) Catalase and (d) merge image of b and c. Arrows indicate co-localization loci. Bar represents 10 μm.

<u>vMIA travels to peroxisomes via interaction with PEX19</u>

The novel localization of vMIA at peroxisomes raises the question of how this viral protein is actually delivered to this organelle. Peroxisomal membrane proteins are mostly transported by interaction with the PEX19 cytosolic chaperone, which directs them to the organelle's membrane by interacting with PEX3 (Delille and Schrader, 2008; Halbach et al., 2006; Theodoulou et al., 2013). To test the hypothesis that HCMV could highjack the peroxisomal transport machinery in order to localize vMIA at this organelle, we analyzed a possible interaction between this protein and PEX19. To that end, we

co-transfected vMIA-myc and PEX19-YFP (for 24 hrs) in HepG2 cells and performed co-immunoprecipitation analyses. As shown in Figure 14A, vMIA interacts with PEX19 (with a 7-fold increase when comparing the bands from the immunoprecipitation -IP- and the control). Similar analyses were performed in HFF cells where vMIA-myc was overexpressed (for 24 hrs) and its co-immunoprecipitation with the endogenous PEX19 was analyzed. Figure 14B shows that, also in HFF, vMIA interacts with PEX19 (although with a lower 3-fold increase when comparing the IP and control bands). The interactions of peroxisomal membrane proteins with PEX19 are very transient and sometimes quite difficult to show, depending on the cell type. Hence, to complement and solidify these results, we have also demonstrated this interaction in HFF cells by co-immunoprecipitation upon overexpression of vMIA-myc and PEX19-YFP (for 24 hrs) (Figure 14C), obtaining a 5-fold increase when comparing the IP and control bands. Altogether these results support a model whereby PEX19 binds and chaperones this viral protein to the peroxisomal membranes.
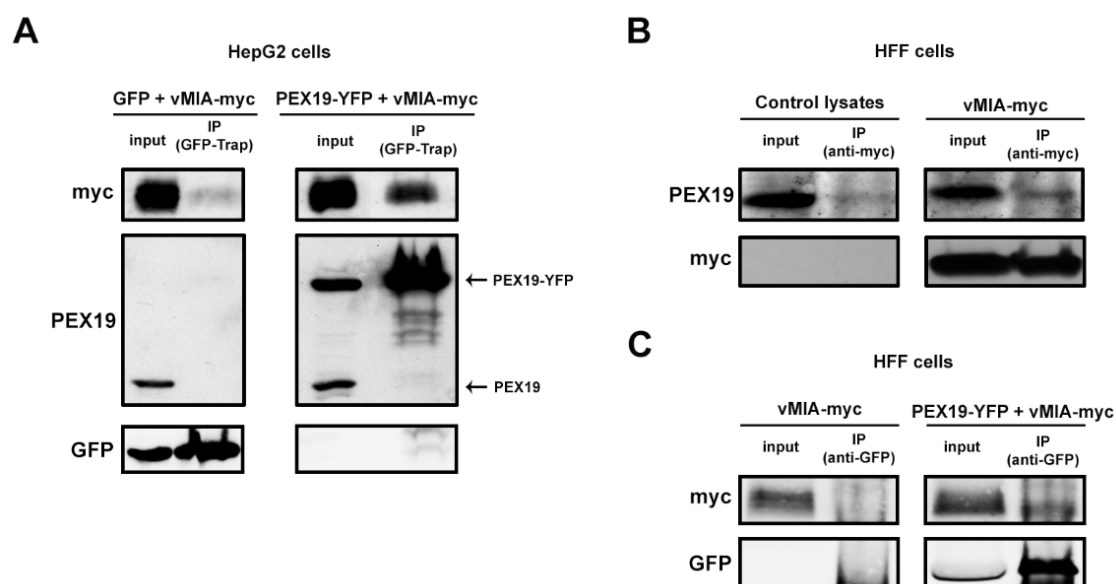
Figure 14. vMIA interacts with PEX19. (A) Co-immunoprecipitation analysis of the interaction between overexpressed PEX19-YFP and vMIA-myc in HepG2 cells. The pull-down was performed using GFP-Trap M kit. Negative control was performed by immunoprecipitating cells overexpressing GFP and vMIA-myc. Western blot was performed with antibodies against myc, PEX19 and GFP. Input represents total cell lysate and IP represents the immunoprecipitation. Arrows indicate endogenous PEX19 and the transfected PEX19-YFP. (B) Co-immunoprecipitation analysis of the interaction between overexpressed vMIA-myc and endogenous PEX19 in HFF cells. The pull-down was performed using an antibody against myc. Negative control was performed by immunoprecipitating non-transfected cells. Western blot was performed with antibodies against myc and PEX19. Input represents total cell lysate and IP represents the immunoprecipitation. (C) Co-immunoprecipitation analysis of the interaction between overexpressed PEX19-YFP and vMIA-myc in HFF cells. The pull-down was performed using an antibody against GFP. Negative control was performed by immunoprecipitating cells overexpressing vMIA-myc. Western blot was performed with antibodies against myc and GFP. Input represents total cell lysate and IP represents the immunoprecipitation.

<u>vMIA interacts with the peroxisomal MAVS and inhibits the peroxisomal-dependent antiviral signaling pathway</u>

vMIA has been suggested to impede signaling downstream from MAVS (Castanier et al., 2010). However, in these studies, neither the peroxisomal MAVS nor vMIA localization at peroxisomes were taken into account. To determine whether vMIA has any significant effect on the signaling downstream from the peroxisomal MAVS, we have expressed vMIA-myc in Mefs cells that contain MAVS solely at peroxisomes (Mefs MAVS-PEX cells, Figure 15A) (Dixit et al., 2010). In order to find out whether these cells would respond to vMIA overexpression in a similar way as HepG2 and HFF, we analyzed peroxisome fragmentation by immunolocalization. It is important to note that the peroxisomes in these cells are in general more elongated than in HepG2 or HFF cells. Figure 15A d-f shows examples of peroxisome morphology in un-transfected and vMIA-overexpressing Mefs MAVS-PEX cells. The analysis of the Manders' co-localization coefficient for these cells has shown that 8.60% of the vMIA co-localizes with the peroxisomal marker. Upon morphological and statistical analysis of the organelle's morphology under these two conditions (in a similar way as previously shown for HepG2 and HFF cells), the results show that vMIA also induces peroxisomal fragmentation in Mefs MAVS-PEX cells (Figure 15A and 15B). MAVS-dependent signaling events were stimulated in these cells by overexpressing a constitutively active version of RIG-I (GFP-RIG-I-CARD, (Yoneyama et al., 2004)). Six hours after GFP-RIG-I-CARD transfection, the expression of two ISGs (IRF1 and Viperin) was analyzed by Western blot (Figure 15C) and the production of their mRNA was quantified by RT-qPCR (Figure 15D). Both analyses demonstrated a clear increase on the production of IRF1 and Viperin upon GFP-RIG-I-CARD overexpression when compared with control un-stimulated Mefs MAVS-PEX cells. In the presence of vMIA, however, the production of IRF1 and Viperin remained close to the levels observed in unstimulated cells. Collectively, these results indicate that vMIA disrupts MAVS signaling transduction from peroxisomes.

In order to demonstrate that these results were not due to a lower GFP-RIG-I-CARD expression in the presence of vMIA, we have analyzed GFP-RIG-I-CARD expression levels in the presence and absence of the viral protein. Supplementary Data - Figure 23A shows that, when vMIA is present, there is no decrease (there is even an increase) in the expression of GFP-RIG-I-CARD (6 hrs post-transfection) when compared to control cells, where vMIA is absent. Similar results were obtained upon expression of a full version of RIG-I (GFP-RIG-I). We have also demonstrated that the presence of vMIA in the cells does not alter the production of GFP-RIG-I-CARD mRNA (Supplementary Data - Figure 23B). In order to specifically detect the transfected (human) GFP-RIG-I-CARD mRNA and exclude the (mouse) endogenous RIG-I, this analysis was performed with primers against the human RIG-I.

A

B

C

D
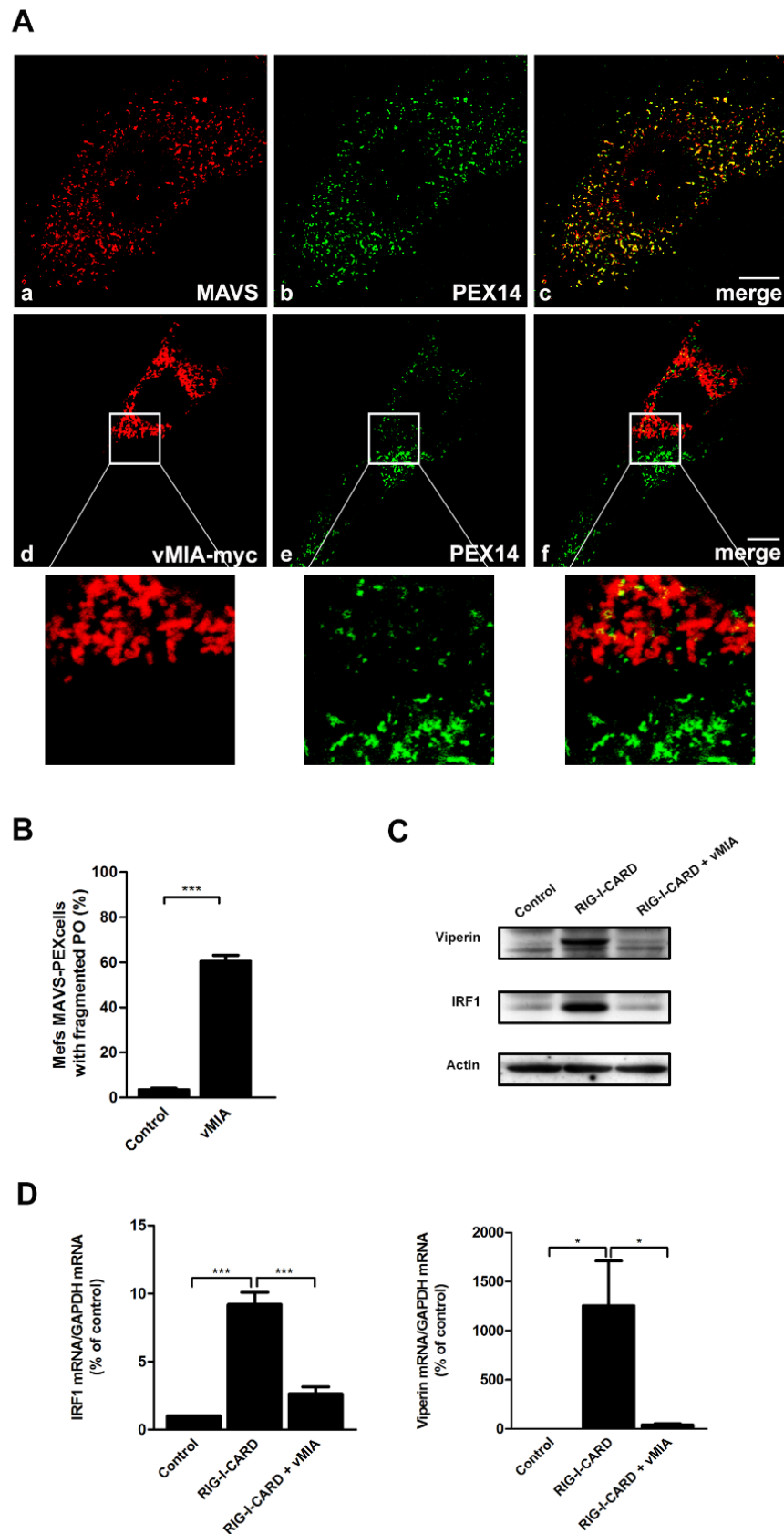
Figure 15. vMIA inhibits the peroxisomal-dependent antiviral signaling. (A) (a-c) MAVS intracellular localization in Mefs MAVS-PEX cells (a) MAVS, (b) PEX14 and (c) merge image of a and b. (d-f) localization of transfected vMIA in Mefs MAVS-PEX cells (d) vMIA-myc, (e) PEX14 and (f) merge image of d and e. Confocal images from immunofluorescence staining. Bar represents 10 μm. (B) Quantification analysis of peroxisome morphology in

the presence and absence of vMIA in Mefs MAVS-PEX cells. Data represents the means ± SEM of three independent experiments. Error bars represent SEM. ***p<0.001 in a Student's t test. (C) Western blot analysis of the production of IRF1 and Viperin in Mefs MAVS-PEX cells stimulated with GFP-RIG-I-CARD in the presence or absence of vMIA. Representative image of three independent experiments. Actin was used as a loading control. (D) RT-qPCR analysis of IRF1 and Viperin mRNA in Mefs MAVS-PEX cells stimulated with GFP-RIG-I-CARD in the presence or absence of vMIA. GAPDH was used as control. Data represents the means ± SEM of three independent experiments. Error bars represent SEM. *p<0.05 and ***p<0.001 in one-way ANOVA, with Bonferroni's post-test.

Up to now, no direct interaction between vMIA and MAVS has ever been demonstrated. In order to obtain more mechanistical details on the action of vMIA towards the peroxisomal MAVS-dependent signaling pathway, we analyzed whether vMIA would be able to specifically associate with the peroxisomal MAVS. To that end, Mefs MAVS-PEX cells were transfected with vMIA-myc and, after 24 hrs, co-immunoprecipitation analyses were performed with an antibody against MAVS. As clearly shown in Figure 16A, vMIA specifically interacts with the endogenous peroxisomal MAVS (with an 18-fold increase when comparing the bands from the immunoprecipitation -IP- and the control). To demonstrate that MAVS is not interacting with the myc-tag of vMIA-myc, we have performed co-immunoprecipitation analyses in Mefs MAVS-PEX cells transfected with a myc-tagged protein that does not interact with MAVS (myc-MIRO1, Figure 16B). Additionally, to demonstrate that vMIA-myc does not interact with the MAVS-antibody-coated beads, we performed co-immunoprecipitation analyses in Mefs MAVS-KO cells transfected with vMIA-myc (Figure 16C).
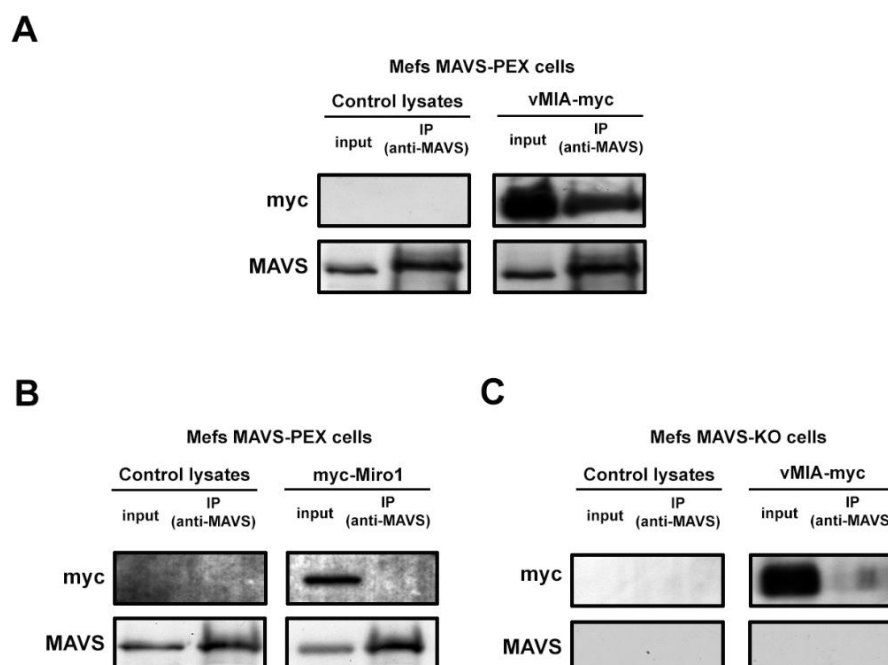
Figure 16. Interactions between peroxisomal MAVS and vMIA. (A) Co-immunoprecipitation analysis of the interaction between overexpressed vMIA-myc and endogenous MAVS in Mefs MAVS-PEX cells. Negative control was performed by immunoprecipitating non-transfected cells. The pull-down was performed using an antibody

against MAVS. Western blot was performed with antibodies against MAVS and myc. Input represents total cell lysate and IP represents the immunoprecipitation. (B) As negative control, the mitochondrial myc-tagged MIRO1 (myc-MIRO1) was transfected in Mefs MAVS-PEX cells. The pull-down was performed using an antibody against MAVS. Western Blot was performed with antibodies against MAVS and myc. Input represents total cell lysate and IP represents the immunoprecipitation. (C) As negative control, vMIA-myc was transfected in Mefs MAVS-KO cells. The pull-down was performed using an antibody against MAVS. Western Blot was performed with antibodies against MAVS and myc. Input represents total cell lysate and IP represents the immunoprecipitation.

<u>Peroxisomal fragmentation is not essential for the role of vMIA on the evasion of the immune response</u>

The localization of vMIA at peroxisomes and mitochondria has a strong effect on the organelles' morphology, causing their fragmentation (Figure 11, 15A and Supplementary Data - Figure 22D, (Ma et al., 2012)). Mitochondrial fragmentation was shown to be essential for the inhibition by vMIA of the mitochondrial MAVS-mediated signaling (Castanier et al., 2010). To determine if the ability of vMIA to induce peroxisome fragmentation similarly contributes to the disruption of peroxisomal MAVS signaling, we sought to prevent vMIA-induced peroxisome fragmentation. To that end, we interfered with the peroxisome morphology by silencing DLP1, the cytosolic GTPase that mediates peroxisomal fission. We reasoned that if peroxisomal fragmentation is important for vMIA to block MAVS signaling, inhibiting DLP1 functions should permit the expression of ISGs, even in the presence of vMIA. To test this prediction, we silenced the expression of DLP1 in Mefs MAVS-PEX cells which were afterwards transfected with vMIA-myc (Figure 17B). As shown in Figure 17A, the peroxisomes from the silenced cells are highly elongated or even hypertubulated. These cells were then transfected with GFP-RIG-I-CARD and, after 6 hrs, the amounts of IRF1 mRNA were analyzed by RT-qPCR. As shown in Figure 17C, upon DLP1 silencing and in the presence of vMIA, the values of IRF1 mRNAs are statistically similar to the ones obtained upon GFP-RIG-I-CARD stimulation in the presence of vMIA. These results demonstrate that, when peroxisomal division is impaired, vMIA is still able to exert its inhibiting effect. Peroxisomal fragmentation is, hence, not essential for the inhibition of the peroxisomal MAVS-dependent antiviral signaling by HCMV.
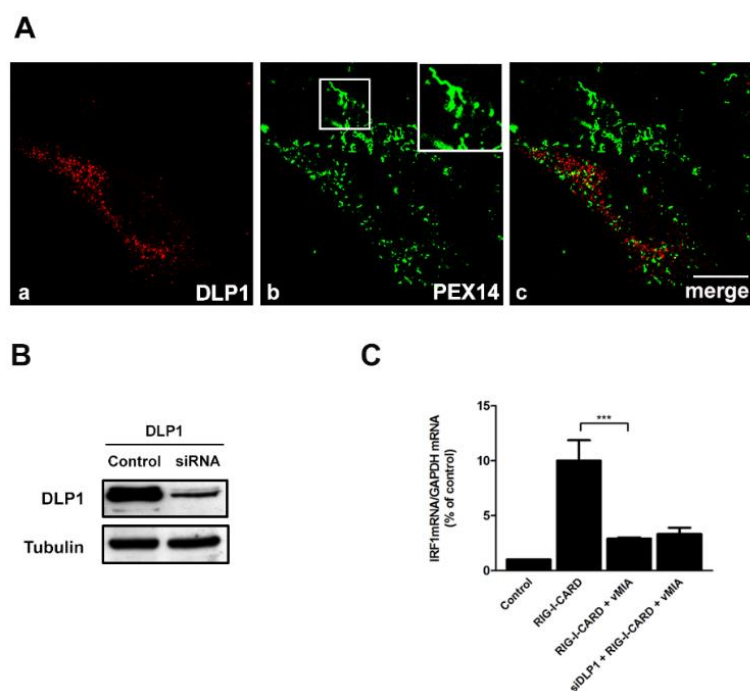
Figure 17. Peroxisomal fragmentation is not essential for vMIA's inhibition of the peroxisomal-dependent antiviral signaling. (A) (a-c) Peroxisome morphology in DLP1-silenced Mefs MAVS-PEX cells (a) DLP1, (b) PEX14 and (c) merge image of a and b. Confocal images from immunofluorescence staining. Bar represents 10 μm. (B) Western blot analysis of the silencing of DLP1 in Mefs MAVS-PEX cells. Representative image of three independent experiments. (C) RT-qPCR analysis of the expression of IRF1 mRNA in Mefs MAVS-PEX cells stimulated with GFP-RIG-I-CARD in the presence of vMIA-myc and upon silencing of DLP1. Non-silenced cells, as well as cells not expressing vMIA-myc were used as controls. GAPDH was measured as control. Data represents the means ± SEM of three independent experiments. Error bars represent SEM. ***$p < 0.001$ in one-way ANOVA, with Bonferroni's post-test.

<u>vMIA induction of peroxisomal fragmentation is independent of peroxisomal MAVS</u>

Our results seem to indicate that vMIA acts on peroxisomes via two distinct and independent mechanisms: one with the final goal of evading the antiviral immune response and one other involving organelle morphology changes with a yet unknown purpose. To further probe this distinction, we analyzed whether the presence of MAVS at peroxisomes would be essential for vMIA induction of peroxisomal fragmentation. To this end, we transfected Mefs MAVS-KO cells with vMIA-myc and, 24 hrs after, immunofluorescence was performed to analyze organelle's morphology by confocal microscopy. Cells were stained with antibodies against myc and PMP70. Statistical analyses were applied to quantify the alteration observed on the organelle's morphology. Surprisingly, as shown in Figure 18, even in the absence of MAVS, vMIA is able to induce a strong peroxisome fragmentation, solidifying the idea that this protein acts via two independent mechanisms.
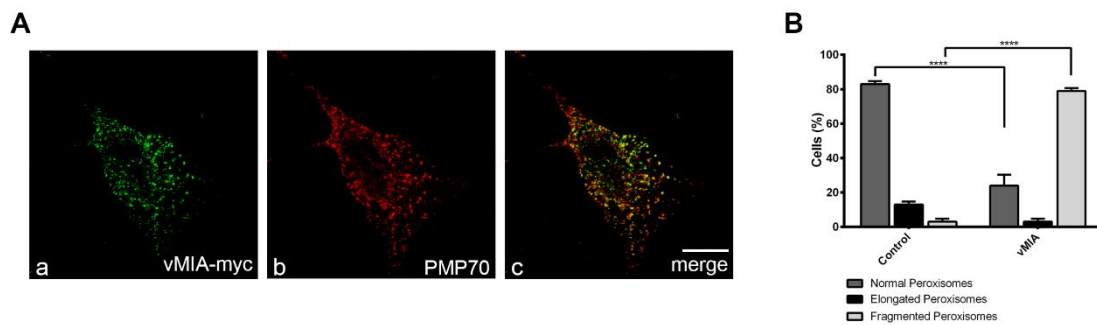
Figure 18. vMIA does not require MAVS to induce fragmentation of peroxisomes. (A) (a-c) Peroxisomes morphology in Mefs MAVS-KO cells in the presence of vMIA. (a) vMIA-myc, (b) PMP70, (c) merge image of a and b. Confocal images from immunofluorescence staining. Bar represents 10 µm. (B) Quantification analysis of peroxisome morphology in the presence and absence of vMIA in Mefs MAVS-KO cells. Data represents the means ± SEM of three independent experiments. Error bars represent SEM. ****$p<0.0001$ in a Student's t test.

MFF interacts with vMIA and is essential for its role on the inhibition of the peroxisome-dependent antiviral signaling

Besides the importance of DLP1 for the antiviral signaling, we have further analyzed the relevance of the other two major players on peroxisome membrane fission: MFF and FIS1, the tail-anchored membrane adaptors responsible for the recruitment of DLP1. Upon silencing the expression of MFF or FIS1 in Mefs MAVS-PEX cells, vMIA-myc was transfected and 24 hrs after the cells were stimulated with GFP-RIG-I-CARD. Six hours after stimulation, the mRNA expression of IRF1 was quantified by RT-qPCR. As show in Figure 18A, the absence of MFF strongly impaired the capability of vMIA to inhibit the expression of IRF1 (Figure 19A). However, in siFIS1 cells vMIA was still capable of inhibiting the peroxisomal antiviral signaling (Figure 19B). Surprisingly, these results indicate that MFF, but not FIS1, is essential for vMIA to dampen the peroxisomal-dependent antiviral signaling.

Since vMIA interacts with MAVS, we wondered whether MFF would also interact with vMIA or be part of this protein complex. In order to test this hypothesis, HepG2 cells were transfected with vMIA-myc and, 24 hrs after, a co-immunoprecipitation assay was performed with an antibody against the myc-tag. As shown in Figure 19D, vMIA interacts with endogenous MFF. To investigate the interaction between MAVS and MFF, HepG2 cells were transfected with GFP-MAVS-PEX plasmid and a co-immunoprecipitation was performed through pull-down of endogenous MFF. Figure 18E shows that, in fact, MFF interacts with the peroxisomal MAVS. These results suggest that vMIA, MFF and MAVS are present in a protein complex and that MFF is somehow mediating vMIA direct influence on the signaling cascade.
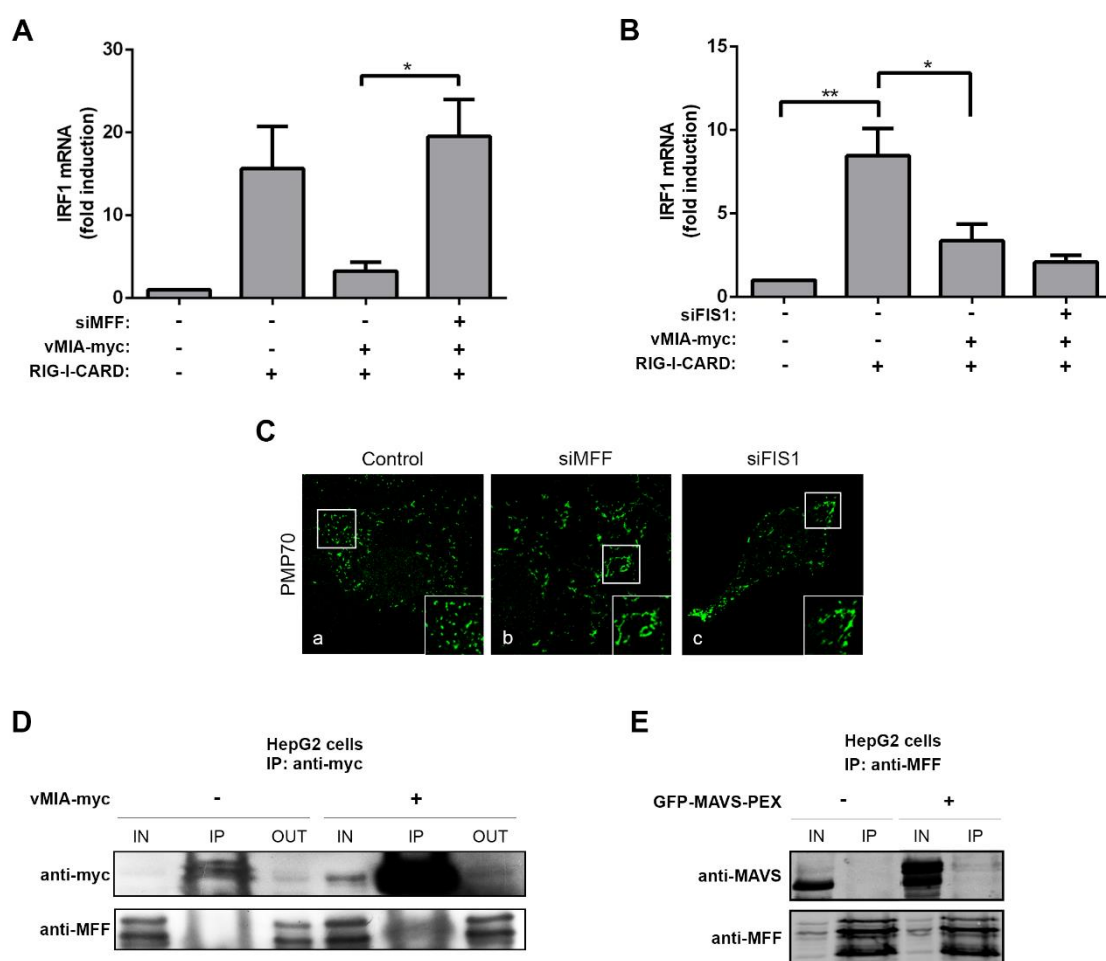
Figure 19. vMIA depends on the interaction with MFF to inhibit the peroxisomal-dependent antiviral response. (A) RT-qPCR analysis of the expression of IRF1 mRNA in Mefs MAVS-PEX cells stimulated with GFP-RIG-I-CARD in the presence of vMIA-myc and upon silencing of siMFF. (B) RT-qPCR analysis of the expression of IRF1 mRNA in Mefs MAVS-PEX cells stimulated with GFP-RIG-I-CARD in the presence of vMIA-myc and upon silencing of siFIS1. Non-silenced cells, as well as cells not expressing vMIA-myc were used as controls. GAPDH was measured as control. Data represents the means ± SEM of three independent experiments. Error bars represent SEM. *p < 0.05. **p<0.01 in one-way ANOVA, with Bonferroni's post-test. (C) (a-c) Peroxisomes morphology in Mefs MAVS-PEX cells after silencing of MFF or FIS1. (a) control, (b) siMFF (c) siFIS1, stained with PMP70, (Confocal images from immunofluorescence staining. Bar represents 10 μm. (D) Co-immunoprecipitation analysis of the interaction between overexpressed vMIA-myc and endogenous MFF in HepG2 cells. The pull-down was performed using an antibody against myc. Western blot was performed with antibodies against myc and MFF. (E) Co-immunoprecipitation analysis of the interaction between overexpressed GFP-MAVS-PEX and endogenous MFF in HepG2 cells. The pull-down was performed using an antibody against endogenous MFF. Western blot was performed with antibodies against MAVS and MFF. Negative control was performed by immunoprecipitating non-transfected cells. Input represents total cell lysate, IP represents the immunoprecipitation and OUT represents the fraction of protein that did not bind to beads.

<u>vMIA inhibits MAVS oligomerization and does not interfere with the interaction between MAVS and STING</u>

Castanier et al (Castanier et al., 2010) suggested that the mechanism of action of vMIA towards the mitochondrial MAVS signaling was dependent on the fragmentation of this organelle and consequent

reduction of its association with the ER, decreasing the level of interaction between MAVS and STING. Although we have demonstrated that peroxisomal fragmentation has no effect on vMIA's inhibition of the MAVS signaling, and no interaction has yet been shown between STING and peroxisomal MAVS, we decided to test the occurrence of this interaction in the absence and presence of vMIA. To that end, we co-transfected Mefs MAVS-PEX cells with FLAG-STING in the presence or absence of vMIA-myc and, 24 hrs after, performed co-immunoprecipitation analyses using an antibody against MAVS for the pull-down. As shown in Figure 20, STING clearly interacts with the peroxisomal MAVS in the absence of vMIA. Importantly, vMIA's presence (which, as shown before, causes massive peroxisome fragmentation) did not seem to decrease the interaction between these two proteins (although the band representing the interaction seems to be lighter in the presence of vMIA, this is due to a lower amount of FLAG-STING upon co-transfection with vMIA, as observed in the lighter input band). Once again, these results point out important differences between the mechanisms of action of vMIA towards peroxisomes and mitochondria.
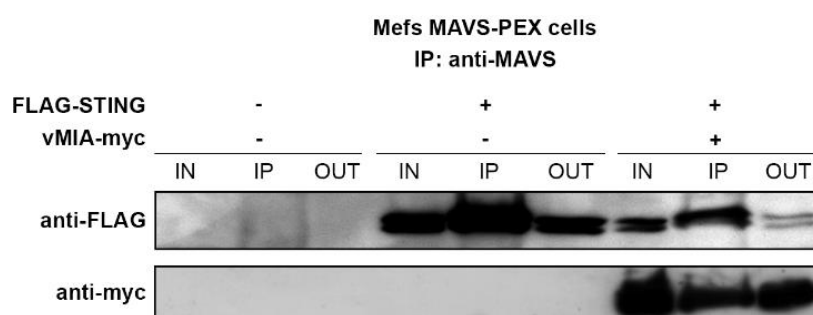
Figure 20. vMIA does not affect the interaction between peroxisomal MAVS and STING. (A) Co-immunoprecipitation analysis of the interaction between overexpressed FLAG-STING with endogenous peroxisomal MAVS in the presence or absence of overexpressed vMIA-myc in Mefs MAVS-PEX cells. This was accomplished using an antibody against endogenous MAVS. Western blot was performed with antibodies against FLAG and myc. Negative control was performed by immunoprecipitating non-transfected cells. Input represents total cell lysate, IP represents the immunoprecipitation and OUT represents the fraction of protein that did not bind to beads.

In order to further unravel the mechanism of inhibition of the peroxisomal MAVS-dependent antiviral signaling by vMIA, we analyzed the oligomerization of MAVS in the presence and absence of vMIA, upon infection with vesicular stomatitis virus (VSV) in 293T cells. Moreover, we also performed these analyses upon knock-down of MFF by siRNA. To that end, we implemented gradient assay experiments to isolate the oligomerized MAVS in different density fractions, after isolating peroxisomes by centrifugation series and treating with n-Dodecyl β-maltoside to disrupt the organelle membrane without affecting the proteins quaternary structure. Figure 21 shows a decrease in oligomerized MAVS in higher density fractions after stimulation with VSV in the presence of vMIA, clearly indicating that vMIA inhibits the oligomerization of MAVS. Additionally, in the absence of MFF the oligomerization of

MAVS is not inhibited by the presence of vMIA, corroborating our previous results showing that MFF is essential for vMIA to impair the peroxisomal MAVS-dependent antiviral signaling.
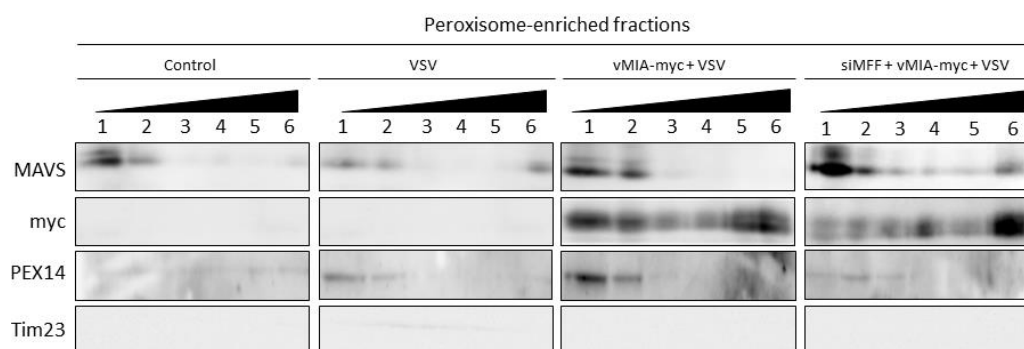
Figure 21. vMIA inhibits MAVS oligomerization at peroxisomes in a MFF-dependent manner. Gradient assays, from peroxisomal-enriched fraction obtained from 293T cells infected with VSV in the presence or absence of vMIA and MFF, and treated with n-dodecyl β-D-maltoside, were performed to separate MAVS oligomers based on their size. 1 – 6 represent the fractions isolated from the gradient assay, where 1 represents the fraction with lowest density and the 6 represents the fraction with highest density. Western blot was performed with antibodies against MAVS, myc and PEX14 and Tim23 as peroxisome and mitochondria markers, respectively.

Discussion

Viruses have developed many sophisticated mechanisms to evade the cellular antiviral response. HCMV encodes vMIA, a powerful inhibitor of apoptosis that has also been shown to play a role on the inhibition of the mitochondrial MAVS-dependent antiviral signaling (Castanier and Arnoult, 2011; Goldmacher, 2002). This protein has been described as localizing solely at mitochondria and all its reported metabolic functions were studied and justified based on its presence at this organelle (Castanier et al., 2010; Goldmacher, 2002; Poncet et al., 2004). Our results demonstrate for the first time that vMIA is also localized at peroxisomes, strongly affecting their morphology, and is able to interact with MAVS, impeding its oligomerization and specifically inhibiting the peroxisome-dependent antiviral signaling.

The localization of vMIA at peroxisomes was demonstrated by immunolocalization and confocal microscopy analyses, not only upon overexpression in hepatic cells (HepG2 cells), cells that are commonly infected by HCMV (HFF cells), DLP1-patient cells and Mefs MAVS-PEX cells, but also upon HCMV infection. Moreover, vMIA was also shown to be present in peroxisome-enriched fractions of HFF cells lysates and in the peroxisomal fractions of a density gradient of HepG2 cells.

Although the presence of viral proteins at peroxisomes is not unprecedented, most of the data available concerns the assembly of viral replication complexes of plant viruses (tombusvirus) at the

peroxisomal membranes (Jonczyk et al., 2007). We (section 3.1. from this thesis and (Ferreira et al., 2016)) and others have recently demonstrated that the hepatitis C virus protein complex NS3-4A travels to peroxisomes and cleaves the peroxisomal MAVS, inhibiting the peroxisome-dependent immune response (Bender et al., 2015; Horner et al., 2011; Magalhães et al., 2016). The HBx protein of hepatitis B virus has also been shown to localize at peroxisomes and increase the invasiveness of hepatocellular carcinoma cells (Han et al., 2014). The Npro from Pestivirus, that is able to bind and inactivate IRF3, was also found to partially localize at this organelle (Jefferson et al., 2014).

The role of peroxisomes on the establishment of the cellular antiviral response has been demonstrated by Dixit et al (2010), who have shown that peroxisomal and mitochondrial MAVS perform different but complementing functions within the antiviral response: while the peroxisomal MAVS induces a rapid and type I interferon-independent expression of defense factors providing short-term protection, the mitochondrial MAVS activates a type I interferon-dependent signaling pathway with delayed kinetics that amplifies and stabilizes the antiviral response. The same group has recently demonstrated that peroxisomes are the primary site of initiation of RLRs-induced type III interferon expression in a variety of human cell types (Odendall et al., 2014). One other recent report, however, somewhat contradicts these findings and show that, both peroxisomal and mitochondrial MAVS activation result in the production of type I and III interferons (Bender et al., 2015).

Besides its peroxisomal localization, we have also demonstrated that vMIA interacts with PEX19, a cytosolic chaperone that is responsible for the transport of most peroxisomal membrane proteins to this organelle (Delille and Schrader, 2008; Jones et al., 2004; Matsuzono et al., 2006; Yagita et al., 2013). Our results suggest that HCMV highjacks the peroxisomal proteins' targeting machinery to its own benefit, in order to transport vMIA to this organelle, upon exiting from the ER. Previous results have shown that PEX19 is also used to transport viral replication proteins to this organelle during tombovirus infection (Pathak et al., 2008), and its target by flaviviruses to enhance viral replication (You et al., 2015).

One of our most interesting results is the fact that the presence of vMIA at peroxisomes causes the organelle's fragmentation, a phenomenon that was not only observed upon the protein's overexpression but also during viral infection. However, intriguingly, this fragmentation was shown not to be crucial for vMIA's role on the inhibition of the peroxisomal-dependent antiviral signaling. vMIA had already been shown to induce mitochondrial fragmentation but this fragmentation was demonstrated to be essential for the inhibition of the mitochondrial-dependent signaling pathway (Castanier et al., 2010; McCormick et al., 2003). Peroxisomes and mitochondria share the main components of their division machinery (e.g. the tail-anchored membrane adaptors FIS1 and MFF that recruit the large dynamin-related GTPase DLP1), which appears to be an evolutionary conserved

strategy among organisms(Bonekamp et al., 2013; Itoyama et al., 2013; Kobayashi et al., 2007; Koch et al., 2005; Koirala et al., 2013; Losón et al., 2013; Otera et al., 2010; Schrader and Yoon, 2007; Zhang and Chan, 2007). The main reasoning for vMIA-induced mitochondrial fragmentation has, up to now, been based on its role as an anti-apoptotic protein. vMIA has been shown to interfere with Bax to prevent mitochondrial outer-membrane permeabilization (Ma et al., 2012; Poncet et al., 2004), as well as to mediate the release of ER Ca^{2+} stores into the cytosol, inducing mitochondrial fission (Sharon-Friling et al., 2006). However, no correlation between peroxisomes and apoptosis has ever been established.

Besides showing that peroxisomal fragmentation has no influence on vMIA-dependent signaling inhibition, we have, on the other hand, demonstrated that this organelle's morphological change occurs independently from the presence of MAVS. Moreover, we have also demonstrated that vMIA interacts with MFF at the peroxisomal membranes and that this protein is essential for its role on the inhibition of the antiviral immune response. Besides showing that vMIA inhibits peroxisomal MAVS oligomerization, we also disclose that MFF is also essential for this process. Our results clearly indicate that vMIA-induced peroxisomal fragmentation and its role on the inhibition of the peroxisomal antiviral signaling are two distinct phenomena.

Importantly, these observations constitute primary clues indicating that vMIA acts at peroxisomes and mitochondria via distinct mechanisms. Since mitochondrial fusion is required to enhance the interaction between MAVS and the ER STING, it has been suggested that the vMIA-induced mitochondrial fragmentation may cause the reduction of this association, dampening signaling downstream from MAVS (Campello and Scorrano, 2010; Castanier et al., 2010). However, as peroxisomes do not fuse (Bonekamp et al., 2012) and, even when elongated, assume a similar cellular distribution, it seems unlikely that peroxisomal fragmentation would decrease the association with the ER, substantiating the fact that vMIA-induced peroxisomal fragmentation is not the main mechanism responsible for the signaling inhibition in this organelle. Furthermore, besides demonstrating for the first time that STING interacts with the peroxisomal MAVS, our results clearly show that this interaction is not dampened in the presence of vMIA. Hence, our results support a model in which the mechanisms of vMIA-induced peroxisomal fragmentation and dampening of the peroxisomal-dependent antiviral signaling are different from the ones occurring in mitochondria. At peroxisomes, vMIA interacts with MAVS, impedes it oligomerization and impairs the downstream signaling cascade, independently of the organelle's morphology.

Our results not only substantiate the role of peroxisomes as a platform for viral evasion from the cellular antiviral response, but also present a novel mechanism by which HCMV is able to specifically evade the rapid and short-term peroxisomal MAVS-dependent antiviral signaling.

III. Results

Materials and Methods

<u>Antibodies and Plasmids</u>

Rabbit antibody directed to PEX14 (a kind gift from Dr. Crane, Griffith University, Brisbane, Australia) and mouse antibodies directed to catalase (Abcam, Cambridge, UK) and myc epitope (9E10, Santa Cruz Biotechnology, Dallas, Texas, USA) were used for morphological studies. Rabbit serum anti-vMIA, used to detect the protein in HCMV infected cells, was a kind gift from Dr. Mocarski from Stanford University (California, USA). Rabbit anti-MFF (kindly provided by Dr. A. van der Bliek, University of California, Los Angeles) and anti-FIS1 (Alexis Biochemicals, Grunberg, Germany) polyclonal antibodies were used for immunofluorescence and immunoblotting. Rabbit antibody directed to myc (71D10, Cell Signaling Technology, Beverly, Massachusetts, USA), FLAG epitope (Sigma-Aldrich, St. Louis, USA), mouse antibody directed against COXIV (Abcam, Cambridge, UK), mouse antibody directed against TOM20 (BD Bioscience, San Jose, California, USA), mouse antibody directed against BiP/GRP ((BD Bioscience, San Jose, California, USA), rabbit antibody directed against ACOX1 (a kind gift from Dr. Hashimoto, Shinshu University School of Medicine, Nagano, Japan), mouse antibody directed to TIM23 (BD Bioscience, San Jose, California, USA), mouse antibody directed to PMP70 (Sigma-Aldrich, St. Louis, Missouri, USA), mouse antibody directed to MAVS (E-3, Santa Cruz Biotechnology, Dallas, Texas, USA), mouse antibody directed to DLP1 (BD Bioscience, San Jose, California, USA), mouse antibody directed to PEX19 (Sigma-Aldrich, St. Louis, Missouri, USA) and rabbit antibody directed to RIG-I (H-300, Santa Cruz Biotechnology, Dallas, Texas, USA), were used for immunobloting. The anti-Viperin mouse MaP.VIP (a kind gift from Dr. Cresswell from Yale University, Connecticut, USA) and rabbit IRF1 (Santa Cruz Biotechnology, Dallas, Texas, USA) antibodies were used for immunobloting to measure the production of this two ISGs. Anti-actin mouse antibody (provided by Dr. Jockusch, Braunschweig University, Germany) and anti-α-tubulin mouse antibody (Sigma-Aldrich, St. Louis, Missouri, USA) were used for immunoblotting as loading controls. Species-specific anti-IgG antibodies conjugated to HRP (BioRad, Hercules, California, USA), IRDye 800CW and IRDye 680RD secondary antibodies (LI-COR Biotechonology, Cambridge, UK) or to the fluorophores TRITC (Jackson Immunoresearch, West Grove, Pennsylvania, USA) and Alexa 488 (Invitrogen, Waltham, Massachusetts, USA) were used.

The construct encoding vMIA-myc was a gift from Dr. Goldmacher (ImmunoGen Inc., Cambridge, Massachusetts, USA). The truncated version of RIG-I protein, GFP-RIG-I-CARD, containing the CARD domain (1 to 284 aa) and the full-length version of RIG-I protein, GFP-RIG-I, were kindly provided by Dr. Weber (Philipps-University Marburg, Germany). The construct encoding PEX19-YFP was kindly provided by Dr. Mayerhofer (University of Munich, Germany).

Cell Culture, transfections and RNA interference experiments

HepG2 (obtained from American Type Culture Collection, HB-8065), Human foreskin fibroblasts (HFF) (obtained from European Collection of Cell Cultures), Mefs MAVS-PEX cells (described in (Dixit et al., 2010)), 293T cell (kindly provided by Dr. Weber, University of Marburg, Germany) and DLP1-patient cell lines (kindly provided by Dr. Waterham, Academic Medical Center, Amsterdam, The Netherlands) (Waterham et al., 2007) (the parents consented for the use of these cells for scientific purposes) were cultured in Dulbecco's modified Eagle's medium supplemented with 100 U/mL penicillin, 100 mg/mL streptomycin and 10% fetal bovine serum (all from PAA Laboratories GmbH, Germany) and incubated at 37 $^{\circ}$C in atmosphere containing 5% CO_2. Cells were seeded on sterile glass coverslips and transfected 24 hrs after plating.

HepG2 and HFF cells were transfected with DNA constructs by incubation with TurboFect (Thermo Scientific, Waltham, Massachusetts, USA), by electroporation using the ECM 630 Electro Cell Manipulator (BTX Harvard Apparatus, Holliston, Massachusetts, USA) or using the Neon® Transfection System (Invitrogen, Carlsbad, CA) (1700V, Width:20, 1 pulse), according to the manufacturer's instructions. Mefs MAVS-PEX cells were transfected using Lipo3000 (Invitrogen, Waltham, Massachusetts, USA). The transfections were performed according to the manufacturer's instructions. HepG2 and 293T cells were also transfected using polyethylenimine (PEI 25 kDa, Polysciences INC, Eppelheim, Germany), in detail, plasmid DNA was mixed 1mg/mL stock solution of PEI, in a ratio of 1:8. The resulting DNA/PEI solution was diluted in serum free medium, incubated for 15 min at RT and subsequently used for transfection. 24 hrs after transfection, cells were trypsinized and collected by centrifugation at 500 x g. DLP1-patient cells and also HFF were microporated with DNA using the Neon® Transfection System (Invitrogen, Carlsbad, CA) (1700V, Width:20, 1 pulse), according to the manufacturer's instructions. Cells were harvested and fixed from 6 to 24 hrs after transfection.

To knock-down the expression of DLP1, MFF and FIS1 by RNA interference, a 21-nucleotide small interfering RNA (siRNA) duplexes (pre-designed siRNA from Ambion-Waltham, Massachusetts, USA, according to (Bonekamp et al., 2013)) were transfected in Mefs MAVS-PEX cells by incubation with Lipofectamine RNAiMax (Invitrogen, Waltham, Massachusetts, USA). siRNA oligonucleotides were obtained as pre-designed siRNAs from Ambion (Austin, TX) as follows: MFF (sense strand: 5'-CGCUGACCUGGAACAAGGAdTdT-3' for exon 2) (Gandre-Babbe and van der Bliek, 2008); DLP1 (sense strand: 5´-UCCGUGAUGAGUAUGCUUUdTdT-3´) (Koch et al., 2005). To knock down the expression of FIS1 (accession no. AF151893) by siRNA (sense strand, 5'-CGAGCUGGUGUCUGUGGAGdTdT-3') (Dharma- con, Lafayette, CO) was used.

III. Results

Viral infection and virus stock preparation

HFF cells were cultured on sterile glass coverslips and infected with 5 pfu/cell HCMV laboratory strain AD169. After 8 hrs post-infection, cells were washed with PBS and fixed with 4% paraformaldehyde.

The HCMV laboratory strain AD169 was obtained from Dr. John Sinclair (University of Cambridge, United Kingdom). To prepare virus stocks of AD169 virus HFF cells were infected at a multiplicity of infection (MOI) of 0.01. After virus adsorption for one hour, infected cells were cultured at 37 ºC and medium was collected every three days. Pre-cleared supernatants were centrifuged two hours at 12000 rpm at room temperature. Virus aliquots were stored at -80 ºC. Virus stock titers were determined by plaque assay. Briefly, HFF cells were cultured with 10-fold dilutions of virus suspension and allowed to absorb for 1h. Cells were then cultured with complete medium containing 10% carboxymethylcellulose (CMC) for 10-15 days. Cellular monolayers were fixed in 4% paraformaldehyde and stained with 0.1% toluidine blue. Quantification of the viral plaques was performed using a dissecting microscope.

293T were infected with VSV with a MOI of 3, diluted in serum and antibiotic free media. After removing the growth media, virus dilution was added to the plates. After incubating cells for 1 hr, at 37ºC, the same virus dilution volume of growth media containing 20% of FBS was added to the cells. Infections occurred for 8 hrs before cells being collected.

Immunofluorescence and microscopy analyses

Cells were processed for immunofluorescence as in (Valença et al., 2015). In short, cells grown on glass coverslips were fixed with 4% paraformaldehyde in PBS, pH 7.4, for 20 min, permeabilized with 0.2% Triton X-100 for 10 min, blocked with 1% BSA solution for 10 min and incubated with the indicated primary and secondary antibodies for 1 hr each. Finally cells were mounted in slides, using Mowiol 4-88 (AppliChem Inc. St. Louis, Missouri, USA) containing n-propylgallate (Sigma-Aldrich, St. Louis, Missouri, USA). Fixed samples were examined using an Olympus IX-81 inverted microscope (Olympus Optical Co. GmbH, Hamburg, Germany) equipped with the appropriate filter combinations and a 100x objective (Plan-Neofluar, 100x/1.35 oil objective). Confocal images were acquired using a Zeiss LSM 510 confocal microscope (Carl Zeiss, Oberkochen, Germany) using a Plan-Apochromat 63× and 100×/1.4 NA oil objectives, a 561 nm DPSS laser and the argon laser line 488 nm (BP 505-550 and 595-750 nm filters). All the confocal images presented in this manuscript represent a single plane, with the exception of the one where we present deconvolution analyses, Figure 1 C, were a z-stack was made. Images were processed using LSM 510 software (Carl Zeiss MicroImaging, Inc.). Digital images were

optimized for contrast and brightness using Adobe Photoshop (Adobe Systems, San Jose, CA, USA). The Manders' co-localization coefficient was applied to quantify the co-localization percentages between vMIA and the peroxisomes. After cropping the region of interest (ROI) from selected cells, channels were split, and quantifications were performed using the JACoP plugin (ImageJ, Bethesda, MD, USA) with a manually set threshold (Bolte and Cordelières, 2006).

Quantification analysis of the area of peroxisomes in HepG2 cells was performed using the Spot Detector plug-in (Olivo-Marin, 2002) from Icy Bioimage Analysis Software created by the Quantitative Image Analysis Unit at Institute Pasteur (Paris, France) (de Chaumont et al., 2012).

To generate high resolution images of the vMIA localization at the hypertubulated peroxisomes from DLP1-patient cells, deconvolution microscopy was performed. Fixed cells were examined by confocal microscopy. Using the 488 and 543 nm laser lines, z-stacks of transfected cells were generated (8x zoom) using the optimal number of slices suggested by the program. Oversaturation of signals was avoided by adjusting of respective photomultipliers. Image deconvolution and 3D rendering was performed using Huygens Professional Software (Scientific Volume Imaging, Hilversum, The Netherlands).

Cell fractionations

For the cellular fractionation, HFF expressing vMIA-myc were homogenized in homogenization buffer (5 mM MOPS, pH 7.4, 250 mM sucrose, 1 mM EDTA, protease inhibitor mixture) by passing gently through a 26.5-gauge syringe needle. The homogenate was cleared by centrifugation (500 x g for 5 min). Heavy mitochondria were subfractionated by centrifugation at 2500 x g for 10 min (Mito). The organelle pellet was then gently resuspended in homogenization buffer and the supernatant was centrifuged again at 25,000 x g to obtain the peroxisome-enriched fraction (PO). Pellet with the enriched PO fraction was gently resuspended in homogenization buffer and the supernatant was collected (Cyto). The organelle fractions were analyzed by SDS-PAGE and immunoblotting

For the density gradient, HepG2 cells expressing vMIA-myc were suspended in homogenization buffer (250 mM sucrose, 5 mM MOPS, 1 mM EDTA, 2 mM PMSF, 1 mM DTT, 1 mM ε-aminocaproic acid, pH 7.4) and homogenized by shearing through a syringe with a 27-gauge needle. Thereafter, cellular debris and nuclei were separated from the post-nuclear supernatant (PNS) by centrifugation at 600 x g, 10 min, 4 °C. The PNS was subsequently centrifuged at 2000 x g yielding the pellet of heavy mitochondria. The corresponding supernatant was subjected to another centrifugation at 20000 x g to produce the peroxisome-enriched light mitochondrial pellet. This pellet was resupended in homogenization buffer and placed onto a linear Nykodenz gradient with a density between 1.14 – 1.19

III. Results

g/mL. The gradients were centrifuged at a velocity of 100000 x g for 3 hrs and collected in 12 equal sized fractions. For further analysis the individual fractions were pelleted by centrifugation and suspended in an appropriate volume of homogenization buffer. Protein concentrations were determined by the Bradford method; only fractions containing significant amounts of protein were subjected to immunoblotting.

293T cellular fractionation was performed by homogenizing cells in homogenization buffer (see above) and passing gently through a 26.5-gauge syringe needle. The homogenate was cleared of nuclei and membranes by centrifugation (500 g for 5 min, at 4ºC), and of heavy mitochondria by centrifugation at 2000 g for 10 min. The supernatant was centrifuged again at 25,000g to obtain the peroxisome-enriched fraction. Pellet with the peroxisomal-enriched fraction was gently resuspended in homogenization buffer supplemented with 2% n-Dodecyl β-D-maltoside to disrupt the organelle membrane without affecting the proteins quaternary structure. The organelle fractions were then processed for the separation of MAVS prions by sucrose gradient.

MAVS prion separation through sucrose separation

The peroxisomal-enriched fraction was loaded in 30%-60% sucrose gradient. Samples were then centrifuged at 170 000g for 2 hrs at 4ºC. Starting from the top, several equal fractions were collected and processed for SDS-PAGE and analyzed by immunoblotting.

Immunoprecipitation analyses

To study the interaction of PEX19 and vMIA, HepG2 cells were co-transfected with PEX19-YFP and vMIA-myc by electroporation, using the ECM 630 Electro Cell Manipulator. For immunoprecipitation of PEX19-YFP the GFP-Trap_M kit (Chromotek, Planegg-Martinsried, Germany), consisting of a high quality GFP-binding protein coupled to a monovalent matrix of magnetic agarose beads, was used. Co-transfection of vMIA-myc and GFP-N1 was used as negative control. Twenty four hours post-transfection, the cell pellets were incubated with lysis buffer (10 mM Tris-HCl, pH 7.5, 150 mM NaCl, 0.5 mM EDTA, 0.5% NP-40 and a protease-inhibitor mix). The lysate was cleared by centrifugation (17,000 x g, 15 min) and diluted with dilution buffer (10 mM Tris-HCl, pH 7.5, 150 mM NaCl, 0.5 mM EDTA and a protease-inhibitor mix). Protein concentrations were determined by the Bradford assay (BioRad, Hercules, CA, USA). Ice-cold dilution buffer was used to equilibrate beads and then cell lysate was incubated for 2 hrs at 4 °C on a rotary mixer. Beads were washed 3 times with dilution buffer and then resuspended in 3x SDS-sample buffer and boiled for 10 min to elute bound proteins.

With the same purpose, HFF cells were transfected with vMIA-myc or with vMIA-myc and PEX19-YFP, using the Neon® Transfection System (Invitrogen, Carlsbad, CA) (1700V, Width:20, 1 pulse), according to the manufacturer's instructions . For immunoprecipitation of vMIA-myc the Protein G Magnetic beads kit (Millipore, Massachusetts, USA) was used. HFF cell lysate was used as negative control. After 24 hrs of transfection cell pellets were incubated with lysis buffer (10 mM Tris-HCl, pH 7.5, 150 mM NaCl, 0.5 mM EDTA, 0.5% NP-40 and a protease-inhibitor mix). Protein concentrations were determined by Bradford assay. The cell lysate was incubated with myc antibody for 2 hrs at 4 °C on a rotary mixer and then the beads were added to the mixture and rotated for 10 min at room temperature. The complex was washed 3 times with PBS containing 0.1% Tween 20 and then resuspended in 3x SDS-sample buffer and boiled for 10 min to elute bound proteins. For immunoprecipitation of vMIA-myc and PEX19-YFP the Dynabeads Protein G beads (Invitrogen, Waltham, Massachusetts, USA) were used. HFF cells transfected with vMIA-myc were used as negative control. Cells lysates were prepared as described above, as well as protein concentration. Then, cells lysates incubated with GFP antibody overnight at 4 °C on a rotary mixer. Beads were added to the mixture and rotated for 2 hrs at 4 °C on a rotary mixer. The complex was washed 3 times with PBS containing 0.1% Tween 20 and then resuspended in 3x SDS-sample buffer and boiled for 10 min to elute bound proteins. All the immunoprecipitated samples were separated by running in a 12,5% SDS-polyacrylamide gel.

To study the interaction of MAVS-vMIA and STING-MAVS in Mefs MAVS-PEX cells and and vMIA-MFF and MAVS-MFF in HepG2, Dynabeads Protein G Magnetic beads kit was used, following the manufacture's protocol. Untransfeted cells were also used as negative control for each immunoprecipitation.

Gel Electrophoresis and Immunoblotting

Cells were lysed with specific lysis buffer (25 mM Tris-HCl, pH 8.0, 50 mM sodium chloride, 0.5% sodium deoxycholate, 0.5% Triton X-100 and a protease-inhibitor mix). To improve protein extraction, samples were passed 20 times through a 26-gauge syringe needle and then incubated on a rotary mixer for 30 min at 4 °C. After clearing by centrifugation (17000 x g, 15 min), protein concentrations were determined using the Bradford assay. Protein samples were separated by SDS-PAGE on 10% or 12.5% polyacrylamide gels, transferred to nitrocellulose (PROTAN®, Whatman®, Dassel, Germany) using a wet or a semidry system (BioRad, Hercules, California, USA), and analyzed by immunoblotting. Immunoblots were processed using specific primary antibodies, and either HRP-conjugated secondary antibodies and enhanced chemiluminescence reagents (GE Healthcare, Waukesha, Wisconsin, USA)

or IRDye 800CW and IRDye 680RD secondary antibodies (LI-COR Biotechonology, Cambridge, UK). For quantification, immunoblots were scanned with a Bio-Rad GS-800 (BioRad, Hercules, California, USA) calibrated imaging densitometer or with Odyssey CLx (LI-COR Biotechonology, Cambridge, UK) and processed using the volume tools from Bio-Rad Laboratories Quantity One software (BioRad, Hercules, California, USA). The background intensity was calculated using the local background subtraction method.

<u>RNA extraction, cDNA synthesis and quantitative real-time polymerase chain reaction</u>

Total RNA was isolated from Mefs MAVS-PEX cells using TriFast reagent (Peqlab, VWR International GmbH, Erlangen, Germany). RNA concentration was determined using NanoDrop 1000 (Thermo Scientific, Waltham, Massachusetts, USA). 1-3 µg of total RNA and M-MuLV reverse transcriptase (New England Biolabs, Ipswich, Massachusetts, USA) was used to perform cDNA synthesis. Real-time polymerase chain reaction was performed with duplicates using iTaq™ Universal SYBR® Green Supermix (BioRad, Hercules, California, USA) and reactions were run on Applied Biosystems® 7500 Real-Time PCR System (Applied Biosystems, Waltham, Massachusetts, USA). Primer sequences were designed using Beacon Designer™ 7 (Premier Biosoft, Palo Alto, California, USA) for the IRF1, Viperin, PEX14, and GAPDH mouse genes, as well as for the RIG-I human gene. The oligonucleotides used for IRF1 were 5'-GGTCAGGACTTGGATATGGAA-3' and 5'-AGTGGTGCTATCTGGTATAATGT-3'; for Viperin the 5'-TGTGAGCATAGTGAGCAATGG-3' and 5'-TGTCGCAGGAGATAGCAAGA-3'; for PEX14 the 5'-GCCACCACATCAACCAACT-3' and 5'-GGGAAGGAGGGAACTGTC-3'; for mouse GAPDH the 5'-AGTATGTCGTGGAGTCTA-3' and 5'-CAATCTTGAGTGAGTTGTC-3'; and for human RIG-I the 5'-CTGGACCCTACCTACATC-3' and 5'- CCAACAGGAACTTGAGAA-3'. GAPDH was used as a reference gene. For gene expression analysis, 2 µL of 1:10 diluted cDNA was added to 10 µL of 2× iTaq SYBR Green Master Mix (BioRad, Hercules, California, USA) and the final concentration of each primer was 250 nM in 20 µL total volume. The thermocycling reaction was initiated by activation of iTaq DNA Polymerase by heating at 95 °C during 3 min, followed by 40 cycles of a 12 s denaturation step at 95°C and a 30 s annealing/elongation step at 60 °C. The fluorescence was measured after the extension step using the Applied Biosystems software (Applied Biosystems, Waltham, Massachusetts, USA). After the thermocycling reaction, the melting step was performed with slow heating, starting at 60 °C and with a rate of 1%, up to 95 °C, with continuous measurement of fluorescence. Data analysis was performed using the $2^{-\Delta\Delta CT}$ method.

<u>Statistical analyses</u>

Statistical analysis was performed in Graph Pad Prism 5 (GraphPad Software, Inc., La Jolla, California, USA). Quantitative data are presented as mean ± standard error mean (SEM). Differences among groups were analyzed by one-way ANOVA, followed by Bonferroni's multiple comparison test; comparisons between two groups were made by Student's t test. P values of ≤0.05 were considered as significant.

Supplementary Data
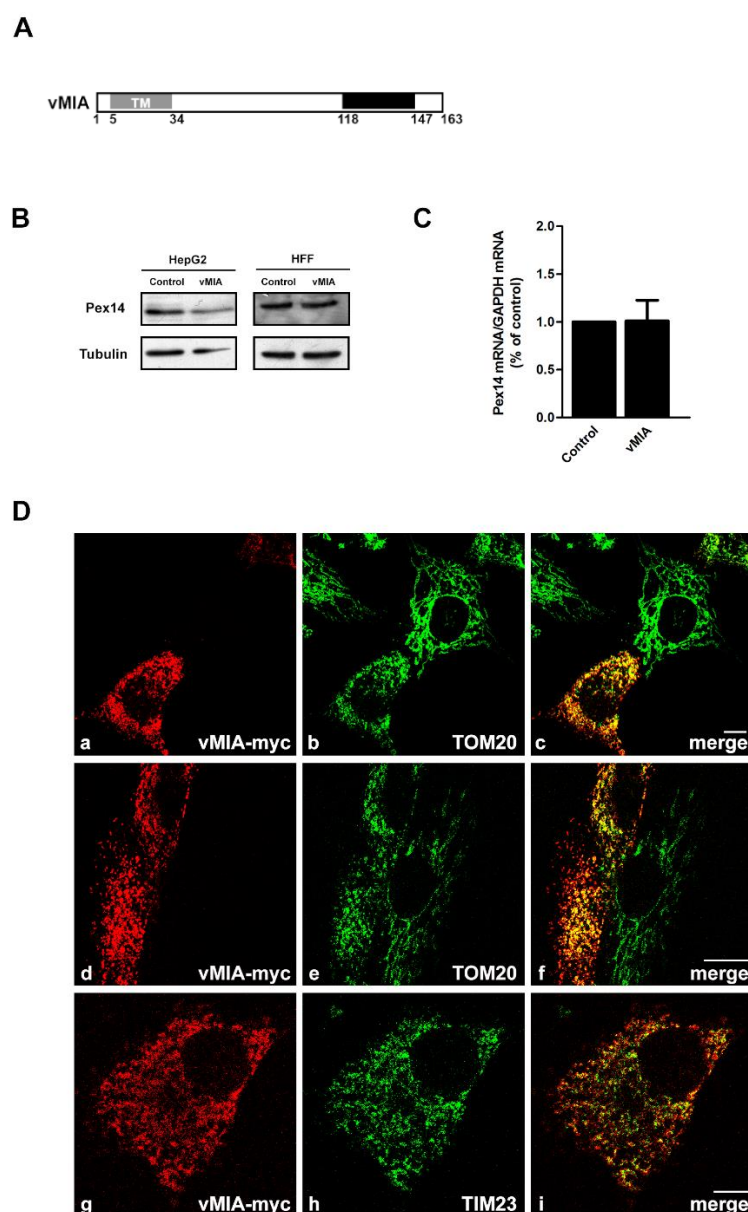
Figure 22. (A) Schematic representation of vMIA topology. vMIA is constituted by 163 amino acids. In the N-terminal it contains a transmembrane domain (TM), localized between the amino acids 5 – 34. The C-terminal functional domain (in black) is located between the amino acids 118-147. Adapted from (Goldmacher, 2002). (B)

III. Results

Western blot analysis of the PEX14 expression in the absence or presence of vMIA in HepG2 and HFF cells. Representative image of three independent experiments. Tubulin was used as a loading control. (C) RT-qPCR analysis of PEX14 mRNA production in the absence or presence of vMIA in Mefs MAVS-PEX cells. GAPDH was used as control. Data represents the means ± SEM of three independent experiments. Error bars represent SEM. (D) (a-c) vMIA intracellular localization in HepG2 cells (a) vMIA-myc, (b) TOM20 and (c) merge image of a and b. (d-f) vMIA intracellular localization in HFF cells (d) vMIA-myc, (e) TOM20 and (f) merge image of d and e. (g-i) vMIA intracellular localization in Mefs MAVS-PEX cells (g) vMIA-myc, (h) TIM23 and (i) merge image of g and h. Confocal images from immunofluorescence staining. Bars represent 10 μm.
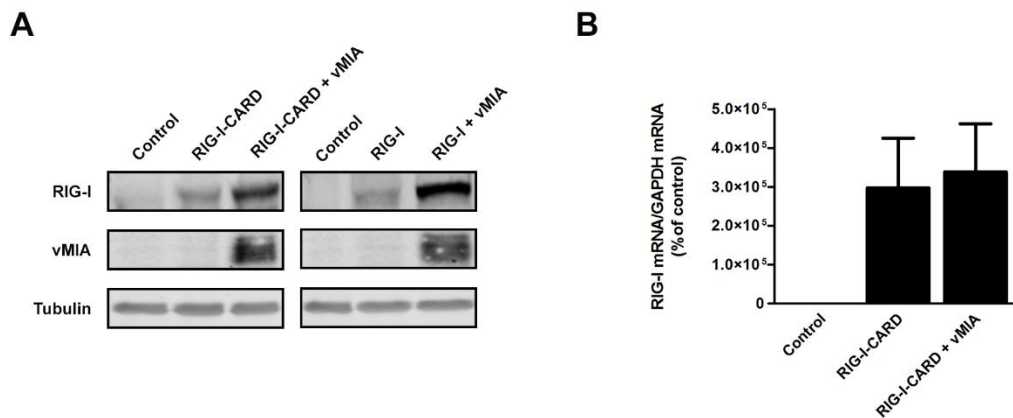
Figure 23. (A) Western blot analysis of the production of GFP-RIG-I-CARD and GFP-RIG-I in Mefs MAVS-PEX cells in the presence or absence of vMIA. Tubulin was used as a loading control. (B) RT-qPCR analysis of RIG-I mRNA in Mefs MAVS-PEX cells stimulated with GFP-RIG-I-CARD in the presence or absence of vMIA (performed with primers annealing with the human RIG-I, in order to solely analyze the transfected human GFP-RIG-I-CARD). GAPDH was used as control. Data represents the means ± SEM of three independent experiments. Error bars represent SEM.

3.3. New insights on the interplay between viruses and peroxisomes: a protein-protein interaction analysis

The results from this section will soon be submitted as:

Abstract

The urgent need to develop broad-spectrum antiviral therapeutics, in order to effectively combat the current and emerging viral hazards, has highlighted the significance of studying the interactions between viruses and their host cells. The growing evidence of peroxisomes relevance for the establishment of the cellular antiviral response has raised the importance for studies of the specific interplay between this organelle and different medically-significant viruses. Up to now, only few reports have highlighted interactions between human peroxisomal proteins and specific viral proteins. Here, we present a thorough study of the human virus-peroxisome interactome, based on experimentally-verified interactions contained in manually-curated protein-protein interactions databases. Our results have unveiled novel insights on protein-protein interactions between peroxisomes and viruses, as well as on the peroxisomal mechanisms that may be of relevance on this interplay. We demonstrated that a total of 16 different viral species interact with 25 different peroxisomal proteins. Importantly, most of the identified viruses establish multiple interactions with peroxisomal proteins. These viruses have distinct characteristics, infect different cells and have dissimilar life cycles, substantiating the importance of peroxisomes on the interplay between the host cells and several different viruses. A detailed analysis of the identified peroxisomal proteins suggests that lipid metabolism may be the most relevant function of this organelle associated with viral infections. These results may constitute a base for new studies on specific virus-host interactions, as well as for the unravelling of novel targets for broad-spectrum antiviral therapeutics.

Introduction

Viral infections pose a prominent and persistent threat to human health. Most of the existing antiviral therapeutics are prone to resistance due to the high frequency of viral mutations. Furthermore, these are mainly directed to specific viruses or strains and not applicable for emerging or engineered viral hazards. The required development of broad-spectrum antiviral therapeutics may imply the discovery of common mechanisms shared by different viruses, e.g. as part of their life cycle or the cellular antiviral response mechanisms (Debing et al., 2015).

Peroxisomes are ubiquitous and essential subcellular organelles that fulfil important metabolic functions in lipid and reactive oxygen species metabolism (Islinger et al., 2012b; Wanders, 2014).

III. Results

Peroxisome dynamics and morphology play an important role in cell pathology and defects in these machineries lead to significant implications in health and disease (Ribeiro et al., 2012). The recent and exciting discovery that peroxisomes act as signaling platforms in early antiviral defense (Dixit et al., 2010; Odendall et al., 2014) has not only revealed a novel function for this organelle, but also possibly uncovered one or more target mechanisms for the development of broad-spectrum antiviral strategies.

A few recent studies have reported on the interplay between human-infecting viruses and peroxisomes. The human cytomegalovirus has been shown to interfere with peroxisomes through its protein vMIA, which localizes at this organelle and inhibits the peroxisome-dependent antiviral signaling (section 3.2 from this thesis and (Magalhães et al., 2016)). A similar role was attributed to the hepatitis C virus' protein NS3-4A, which was shown to cleave the peroxisomal MAVS, an essential protein for the establishment of the antiviral response (section 3.1 from this thesis and (Ferreira et al., 2016). The HBx and Npro proteins of, respectively, hepatitis B virus and pestivirus, have similarly been reported to localize at this organelle (Han et al., 2014; Jefferson et al., 2014). The West Nile and Dengue viruses have also been shown to impair peroxisome biogenesis and interfere with the early antiviral signaling (You et al., 2015). The genomic RNA and Nef protein from the human immunodeficiency virus were also found to localize at peroxisomes, and this organelle was suggested to play an essential role on the NF-κB and IRFs activation against this virus (Cohen et al., 2000). The VP4 protein from rotavirus was shown to be localized at peroxisomes as a functional advantage for viral propagation (Mohan et al., 2002). The peroxisomal protein HSD17B4 was also found to interact with the NS1 protein from the influenza A and B viruses (Wolff et al., 1996).

In the last few years, several methods and technologies have emerged, allowing the identification and characterization of protein-protein interactions (PPIs) and contributing to the generation of large-scale PPIs data. The study of PPIs allows not only the understanding of the protein function in a complex context, but also the identification of new proteins and ultimately of possible targets for therapeutic intervention (Chautard et al., 2009; Ma-Lauer et al., 2012). Several studies have reported PPI-mediated mechanisms of communication between specific viruses and their host cells (Bosque et al., 2014; Dyer et al., 2008; Franzosa and Xia, 2011; König and Stertz, 2015) and a few of these have specifically reported PPIs between viruses and peroxisomes (Tanner et al., 2014; Zhou et al., 2015). However, to our knowledge, no study has ever been presented that includes a general analysis of the landscape and context of these interactions.

In order to contribute to a better understanding of the role of peroxisomes on the viral life cycles, establishment of the infection process, as well as on the cellular antiviral defense mechanisms, we present here a thorough study of the human virus-peroxisome interactome, based on experimentally-

verified interactions annotated in PPI databases. Our results provide a first global view on the virus-peroxisome PPIs, as well as novel insights on the peroxisomal mechanisms that may be of relevance on the interplay between viruses and this organelle. These results may constitute a base for new studies that may contribute to the development of virus-specific or broad-spectrum antiviral strategies.

Results and discussion

The human virus-peroxisome interactome: new insights on PPIs between peroxisomes and viruses

The analysis of the virus-host interactome has recently gained interest among the virology (Dyer et al., 2008) and immunology (Gardy et al., 2009) fields, by highlighting important interactions that may lead to the discovery of novel targets for antiviral therapy.

As peroxisomes have been recently revealed as platforms for the establishment of the cellular antiviral immune response, we aimed at specifically analyzing the interactions occurring between viral and human peroxisomal proteins.

In order to obtain a dataset with all known human peroxisomal proteins, we made use of UniProt, a database that contains information about protein sequence and annotations (Consortium, 2017; UniProt Consortium, 2015), from which we extracted a list of manually-annotated proteins (Supplementary Data - Table 3).

To retrieve all the interactions found on the International Molecular Exchange (IMEx) consortium databases (Orchard et al., 2012) (reunites all the manually curated databases that contain non-redundant and consistently annotated interactions) and obtain the interactors of the selected peroxisomal proteins, we used Cytoscape, an open-source software which allows the visualization and analysis of networks. After retrieving the interactors of the selected proteins, the network was filtered in order to show solely virus and human proteins (Figure 24). The nodes were differentiated using a two-color system (blue for human proteins and red for viral proteins). The topological features of the network were assessed using the NetworkAnalyzer tool (Assenov et al., 2008).

Figure 24. Human virus-peroxisome interaction network retrieved from IMEx consortium databases. The network was visualized and analyzed on the Cytoscape software. Nodes in red and blue represent viral and peroxisomal proteins, respectively. The size of the nodes corresponds to the betweenness centrality of each node.

The most common metrics in network analysis is the measurement of the degree of a node that corresponds to the number of interactions that it has with adjacent nodes, being the nodes with higher degree designated as hubs. Another interesting topological property of a network is the measurement of the number of all shortest paths that passes a given node and it is designated betweenness centrality (Ma'ayan, 2011; Roy, 2012). Other topological properties can be analyzed and conclusions should be taken correlating all the information, also taking into consideration the clustering analysis and the Gene Ontology annotations, which defines the function, location and biological processes associated (Ma'ayan, 2011).

In the network depicted on Figure 24, the peroxisomal proteins FAR1, MAVS, ALDH3A2, ACSL3, PEX14, ABCD3 and ABCD1 and the viral proteins 1C, M2 and E5A exhibit higher degree, being designated as

hub nodes. The viral proteins belong to human respiratory syncytial virus A, influenza A and Epstein-Bar virus, respectively.

There are currently several databases with viral genome sequences and virus-host interactions (Albà et al., 2001; Calderone et al., 2015; Hulo et al., 2011; Pickett et al., 2012; Rozenblatt-Rosen et al., 2012). However, for the study of viral-host interactions, VirusMentha proves to be user-friendly and allows a quick look over the interactions of a specific dataset of target proteins (Calderone et al., 2015). Using the list of peroxisomal proteins retrieved from UniProt, we performed a similar analysis by retrieving the interactors directly from the VirusMentha browser (Figure 25, differentiated using a two-color system (blue for human proteins and red for viral proteins), as before).

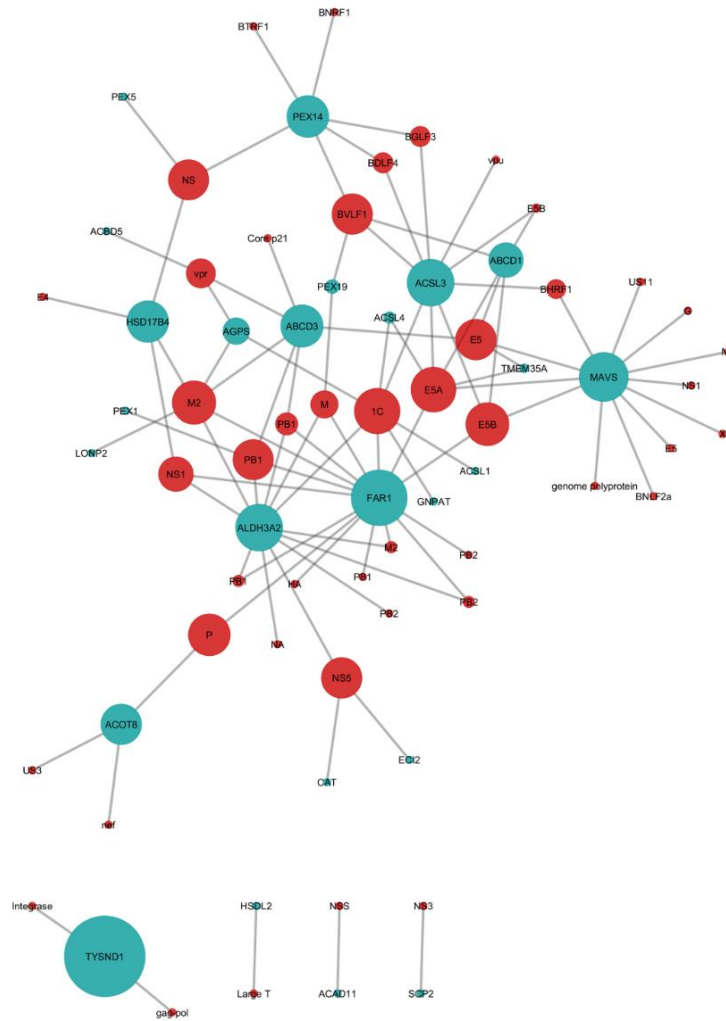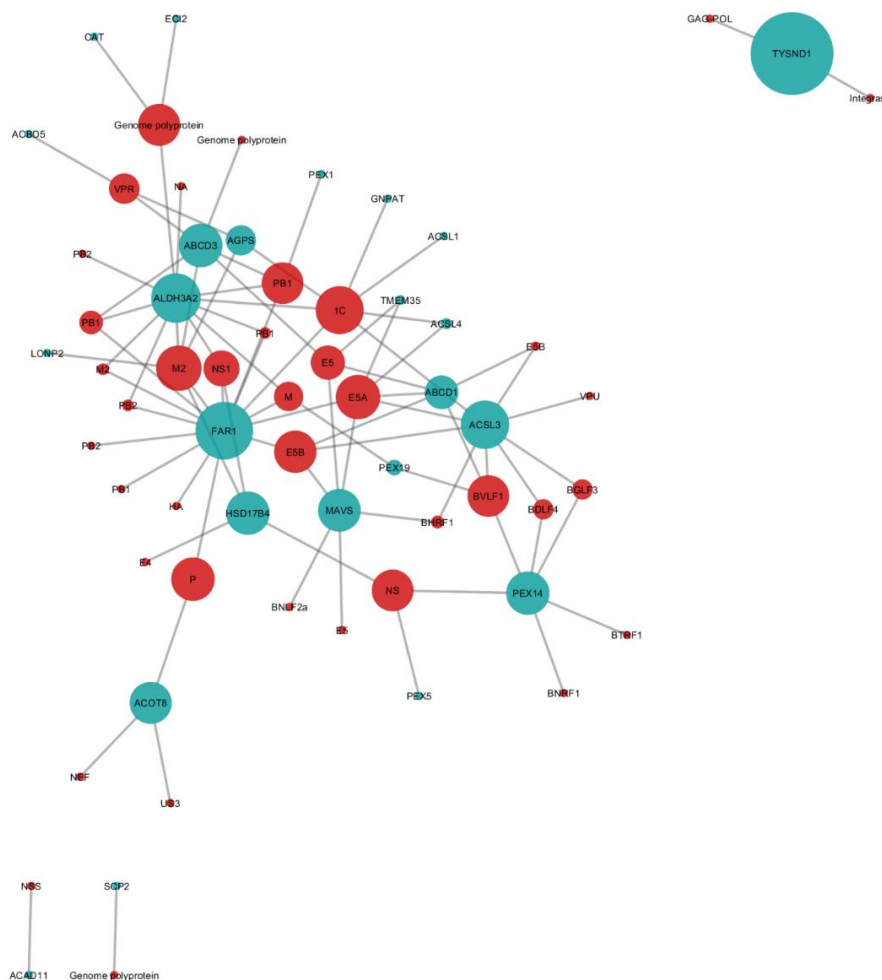**Figure 25. Human virus-peroxisome interaction network retrieved from VirusMentha.** The network was visualized and analyzed on the Cytoscape software. Nodes in red and blue represent viral and peroxisomal proteins, respectively. The size of the nodes corresponds to the betweenness centrality of each node.

III. Results

In contrast with the network obtained from merging the IMEx databases' networks, it was not necessary to filter out the network obtained from VirusMentha in order to only show viral-human proteins interactions, as the input proteins were human and this browser only shows the viral interactors for the input proteins. One drawback of VirusMentha is its inability to identify the individual proteins that result from the processing of viral polyproteins. Although, comparatively, the network retrieved from the VirusMentha is easier and less time-consuming to extract, but in order to objectively compare the applicability and reliability of both methods a more comprehensive virus-host PPI network would have to be analyzed.

Despite the differences of the methods to generate the networks, both identified the same peroxisomal and the viral proteins as the ones presenting higher degree, with minor differences in the total network.

As the main objective of this work was to obtain a comprehensive view of peroxisome-virus interactions in humans, we proceeded our analyses based on a network that resulted from the combination of IMEx partners- and VirusMentha-derived networks. This interactome the viral proteins were grouped using a colored scheme that specifies the viral species they belong to (Figure 26). It is important to point out that this interactome does not represent coordinated interactions that occur simultaneously or on a specific condition. After analyzing the network using the NetworkAnalyzer plugin we confirmed that the proteins which present higher degree were the same found in each individual network. To analyze the topological characteristics of the network, the size of the nodes was adjusted in order to translate the betweenness centrality of each node: the bigger the node, the higher betweenness centrality (Figure 26). Taking this into consideration, it is possible to observe that FAR1, MAVS, ALDH3A2 and ACLS3 are the peroxisomal nodes with higher betweenness centrality (Supplementary Data – Table 4). As some of these proteins are not exclusively peroxisomal, one has to consider that some of the interactions revealed by this interactome may not (or have yet be proven to) occur at or solely at peroxisomes. One of the exclusive peroxisomal proteins with more interactions in the network is FAR1, which is responsible for the reduction of fatty acids (preferentially 16 to 18 carbons) and presents 15 interactions (Table 1).

Table 1. Peroxisomal proteins found in the peroxisome-virus interactome with respective function and number of interacting viral proteins. * identifies the proteins non-exclusively peroxisomal. Functions were retrieved from Entrez Gene, a database created and maintained by the National Center for Biotechnology Information (NCBI). Abbrev.: IAV – influenza A virus, HPV – human papillomavirus; EBV – Epstein-Barr virus; HRSV - human respiratory syncytial virus; HIV - human immunodeficiency virus; HHV - human herpesvirus; MeV - measles virus; HCV – hepatitis C virus; DENV - Dengue virus; RV - rotavirus ; RVFV - Rift Valley fever virus ; HAdV - human adenovirus C; BKV - BK polyomavirus; HBV - hepatitis B virus; HMPV - human metapneumovirus;

Peroxisomal proteins	Main functions	Number of interacting viral proteins	Viruses	
			Number	Name
FAR1	reduction of fatty acids to fatty alcohols; synthesis of monoesters and ether lipids	15	5	IAV; HPV; HRSV; MeV
MAVS*	regulate expression of interferon-β and contributes to antiviral immunity	12	7	HBV; RV; HHV; HCV; IAV; HPV; EBV
ALDH3A2*	detoxification of aldehydes generated by alcohol metabolism and lipid peroxidation	12	2	IAV; HRSV; DENV
ACSL3*	convert free long-chain fatty acids into fatty acyl-CoA esters; lipid biosynthesis and fatty acid degradation	9	4	EBV; HPV; HRSV; HIV
ABCD3	peroxisomal import of fatty acids and/or fatty acyl-CoAs; peroxisome biogenesis	6	4	IAV; HCV; HIV; HPV
PEX14	peroxisomal import machinery	6	2	EBV; IAV
ABCD1	peroxisomal import of fatty acids and/or fatty acyl-CoAs; peroxisomal transport or catabolism of very long chain fatty acids	5	2	HPV; EBV
HSD17B4	involved in peroxisomal β-oxidation pathway of fatty acids	4	2	IAV; HAdV
AGPS	catalyzes the second step of ether lipid biosynthesis	3	3	IAV; HRSV; HIV
ACOT8	peroxisomal thioesterase that appears to be involved in the oxidation of fatty acids	3	3	HHV; HIV; MeV

III. Results

TYSND1	removes the PTS1 (from protein in the peroxisomal matrix) and PTS2 (from proteins produced in the cytosol) signals; facilitates the import of proteins into the peroxisome	2	1	HIV
ACSL4*	convert free long-chain fatty acids into fatty acyl-CoA esters	2	2	HPV; HRSV;
PEX19	cytosolic chaperone and import receptor for peroxisomal membrane proteins	2	2	IAV; EBV
TMEM35A	undefined	2	1	HPV
GNPAT	synthesis of ether phospholipids	1	1	HRSV
CAT	converts the reactive oxygen species hydrogen peroxide to water and oxygen	1	1	DENV
SCP2*	peroxisome-associated thiolase; oxidation of branched chain fatty acids; intracellular lipid transfer protein	1	1	HCV
ACSL1*	convert free long-chain fatty acids into fatty acyl-CoA esters, lipid biosynthesis; fatty acid degradation	1	1	HRSV
ACBD5	transport and distribution of long chain acyl-Coenzyme A	1	1	HIV
HSDL2	oxidoreductase activity	1	1	BKV
PEX1	diverse cellular activities; import of proteins into peroxisomes and peroxisome biogenesis	1	2	IAV; EBV
ECI2*	β-oxidation of unsaturated fatty acids	1	1	DENV
PEX5	peroxisomal protein import	1	1	IAV
ACAD11*	acyl-CoA dehydrogenase enzyme (preferentially 20 and 26 carbons)	1	1	RVFV
LONP2	maintains the overall peroxisome homeostasis; proteolytically degrades peroxisomal proteins damaged by oxidation	1	1	IAV

1C, E5A M2 and E5B are the viral proteins with higher betweenness centrality in this interactome (Supplementary Data – Table 4). From these 4 proteins, the ones with higher degree are the 1C (from human respiratory syncytial virus, associated to viral evasion to host defenses) with 7 interactions. E5A (from human papillomavirus, associated with viral morphogenesis) and the M2 (from influenza A virus, indispensable for viral coating) present 6 interactions. These results indicate that peroxisomes may be necessary for different phases of the viral life cycle depending on the virus.
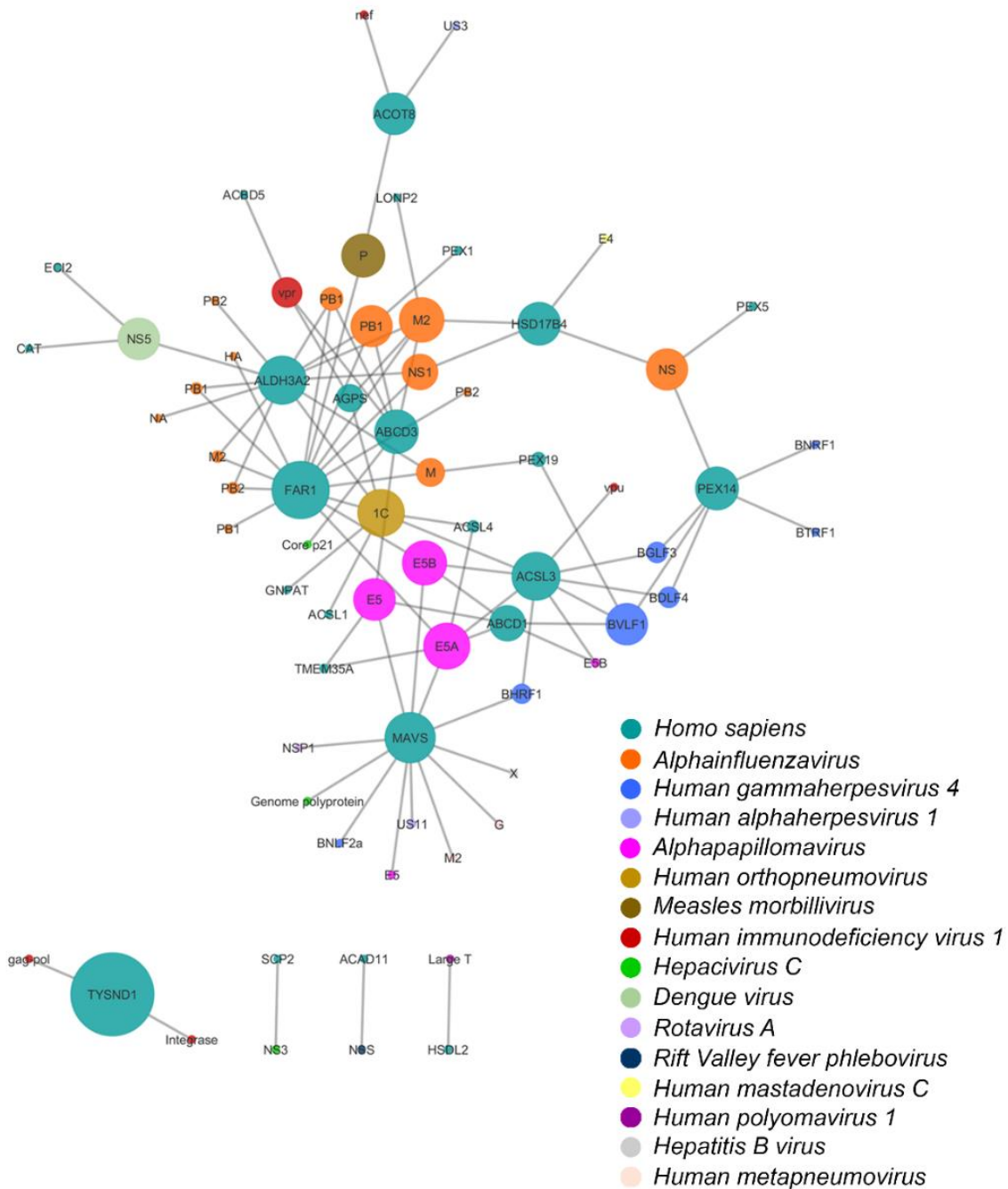
Figure 26. Global interaction network between human peroxisomal and viral proteins. The networks presented on Figure 24 and Figure 25 were combined on Cytoscape. Nodes that represent viral proteins were colored according with the species to which they belong.

III. Results

Although not much is known concerning the role of peroxisomes on human viruses' life cycle or on the establishment of a robust cellular antiviral immune response, the detailed analysis of this interactome revealed novel insights into the specific interactions between many peroxisomal proteins and many different virus species and families.

Different viruses, with distinct characteristics, interact with peroxisomes

Up to now only few reports highlighted specific interactions between human peroxisomal proteins and viral proteins. You at al. (You et al., 2015) reported the interaction between PEX19 and the capsid proteins of West Nile and Dengue viruses. The human immunodeficiency virus' protein Nef was found to interact with the peroxisomal hTE (ACOT8) (Cohen et al., 2000). The peroxisomal protein HSD17B4 was shown to interact with the NS1 proteins of influenza A and B viruses (Wolff et al., 1996). Our group has previously demonstrated that a protein from the human cytomegalovirus' vMIA is able to interact with PEX19, as well as with the peroxisomal MAVS (section 3.2. from this thesis and (Magalhães et al., 2016)). Our group and others have also shown that the protein NS3-4A from the hepatitis C virus interacts with the peroxisomal MAVS (section 3.1. from this thesis and (Bender et al., 2015; Ferreira et al., 2016)).

Here, we demonstrate that there are actually many more viruses that have been identified to somehow interact with peroxisomes, more specifically, 19 different viral species which belong to 13 different viral families (Table 2). The viruses here identified are quite distinct among them: 13 of the viral species are RNA viruses, 6 have dsDNA genomes and 2 are retroviruses. These viruses infect different cells and have dissimilar life cycles, suggesting once more that peroxisomes may be involved in distinct steps of virus particle formation, as well as on the establishment of the cellular defense against these viruses.

The influenza A virus, human papillomavirus, human respiratory syncytial virus, human immunodeficiency virus, Epstein-Barr virus, hepatitis C virus and Dengue virus are the ones which establish the highest number of interactions with peroxisomal proteins within this network. Importantly, most of these viruses interact with peroxisomes in more than one manner. In fact, analyzing the interactions that each viral species establish with peroxisomal proteins, one can notice that influenza A virus, Epstein-Barr virus, human papillomavirus and human immunodeficiency virus present different viral proteins that interact with peroxisomal proteins. It is also possible to notice that the human respiratory syncytial virus, measles virus and Dengue virus present one protein that interacts with several peroxisomal proteins (Table 2). Remarkably, the viral proteins that belong to the same viral species are distributed in groups around specific peroxisomal proteins (Figure 26). This

is visible with the influenza A virus proteins that surround the peroxisomal proteins ALDH3A2, FAR1, ABCD3 and HSD17B4. The Epstein-Barr virus proteins surround PEX14, ACSL3, and the human papillomavirus proteins frame ABDC1, ACSL3, FAR1 and MAVS. Although needing to be experimentally confirmed, these results suggest that these viruses may rely on these peroxisomal proteins to be able to proceed with infection or to control the host cell antiviral response.

Our results represent an interactome that was obtained from manually-curated databases. This network construction is influenced by the rate of curation of every interaction reported, lacking sometimes the most updated information. For example, the recently reported interactions between the human cytomegalovirus' vMIA with the peroxisomal PEX19 and MAVS (section 3.2. in this thesis and (Magalhães et al., 2016), as well as the interactions occurring between PEX19 and the capsid proteins of West Nile and Dengue viruses (You et al., 2015) are not yet included in these databases. Furthermore, the interaction between the hepatitis C virus NS3-4A and MAVS represented in the network had only been curated from a manuscript describing this interaction solely occurring in mitochondria (Li et al., 2005b). Although the manuscripts reporting these interactions specifically, at peroxisomes (Ferreira et al., 2016; Magalhães et al., 2016; You et al., 2015) are not yet curated, we have added them to this network.

Lipid metabolism seems to be the most relevant peroxisomal function associated with viral infections

Besides highlighting novel virus-peroxisome interactions, a deeper analysis of this interactome (Figure 26) allows the identifications of the enriched biological processes within the network. To that end, we used ClueGo and found that the peroxisomal proteins presented in this interactome are associated with the following biological processes: ether lipid biosynthetic process (p-value=6.3×10^{-7}), long-chain fatty acid metabolic process (p-value=9.7×10^{-10}), fatty acid catabolic process (p-value=3.2×10^{-17}) and peroxisome organization (p-value=1.4×10^{-20}), being the last two biological processes the most enriched in our network (Figure 27). These results suggest that many of the identified interactions between viruses and peroxisomes may somehow influence the organelle-dependent lipid metabolism as a benefit for the virus life cycle or the cellular control of viral infections.

III. Results

Table 2. Viral species found in the interactome and respective viral family, number of strains, type of genome, number of viral proteins found and number of interacting peroxisomal proteins. The color shade of each viral species correspond to the color attributed to each node in the Figure 26. * proteins non-exclusive to peroxisomes.

Viral Family	Viral species	Number of strains	Type of genome	Number of viral proteins	Peroxisomal proteins interations	
					Number	Protein name (uniprot ID)
Orthomyxoviridae	Alphainfluenzavirus	4	ssRNA (-)	14	10	PEX19 (P40855), PEX14 (O75381), FAR1 (Q8WVX9), ALDH3A2* (P51648), AGPS (O00116), ABCD3 (P28288), LONP2 (Q86WA8), PEX1 (O43933), PEX5 (P50542), HSD17B4 (P51659)
Herpesviridae	Human gammaherpesvirus 4	1	dsDNA	7	5	MAVS* (Q7Z434), ABCD1 (P33897), ACSL3* (O95573), PEX19 (P40855), PEX14 (O75381)
	Human alphaherpesvirus 1	1	dsDNA	2	2	MAVS* (Q7Z434), ACOT8 (O14734)
Papillomaviridae	Alphapapillomavirus	4	dsDNA	5	7	FAR1 (Q8WVX9), ABCD3 (P28288), ACSL4* (O60488), ACSL3* (O95573), ABCD1 (P33897), MAVS* (Q7Z434), TMEM35A (Q53FP2)
Paramyxoviridae	Human orthopneumovirus	1	ssRNA (-)	1	7	GNPAT (O15228), ACSL3* (O95573), ACSL4* (O60488), AGPS (O00116), ACSL1* (P33121), FAR1 (Q8WVX9), ALDH3A2* (P51648)
	Measles morbillivirus	1	ssRNA (-)	1	2	ACOT8 (O14734), FAR1 (Q8WVX9)
Retroviridae	Human immunodeficiency virus 1	4	retro-transcribing	5	6	ABCD3 (P28288), ACBD5 (Q5T8D3), AGPS (O00116), ACSL3* (O95573), ACOT8 (O14734), TYSND1 (Q2T9J0)
Flaviviridae	Hepacivirus C	3	ssRNA(+)	3	3	SCP2* (P22307), MAVS* (Q7Z434), ABCD3 (P28288)
	Dengue virus	1	ssRNA (+)	1	3	CAT (P04040), ECI2* (O75521), ALDH3A2* (P51648)
Reoviridae	Rotavirus A	1	dsRNA	1	1	MAVS* (Q7Z434)
Phenuiviridae	Rift Valley fever phlebovirus	1	ssRNA(-)	1	1	ACAD11* (Q709F0)
Adenoviridae	Human mastadenovirus C	1	dsDNA	1	1	HSD17B4 (P51659)
Polyomaviridae	Human polyomavirus 1	1	dsDNA	1	1	HSDL2 (Q6YN16)
Hepadnaviridae	Hepatitis B virus	1	retro-transcribing	1	1	MAVS* (Q7Z434)
Pneumoviridae	Human metapneumovirus	1	ssRNA (-)	2	1	MAVS* (Q7Z434)
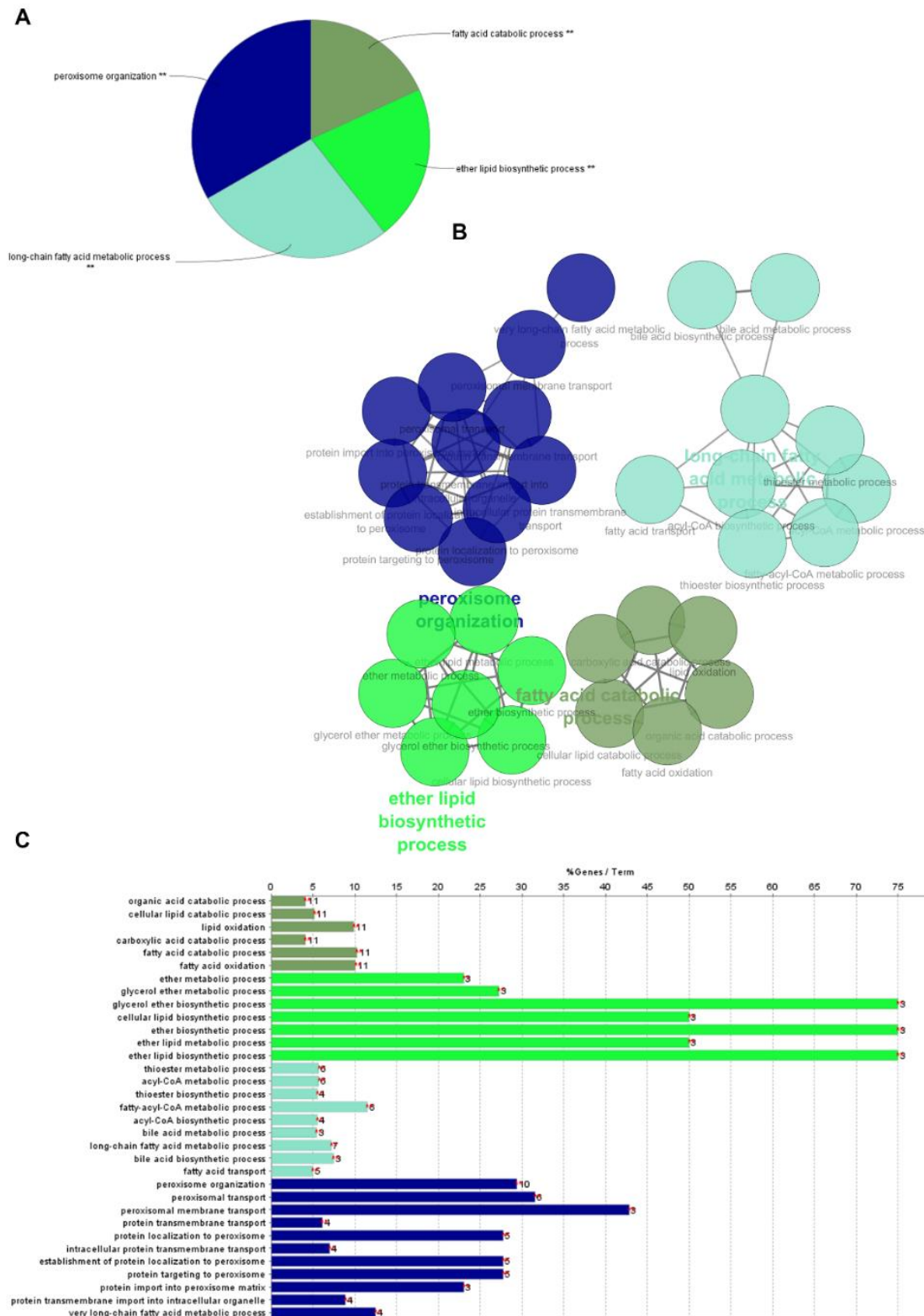
Figure 27. Biological processes enriched in the interaction network between peroxisomal and viral proteins in human. The functional enrichment analysis was performed using the ClueGo plug-in on Cytoscape. Bonferroni step-sown correction method was used and processes with p-value≤0.05 were selected. (A) Functional groups in ClueGO, (B) The biological role of the enriched human proteins and (C) Functional terms ClueGO Chart.

III. Results

Conclusions

Through a comprehensive analysis of the human virus-peroxisome interactome, we have unraveled novel insights on PPIs between peroxisomes and viruses, as well as on the peroxisomal mechanisms that may be of relevance for this interplay. A total of 19 different viral species are shown to interact with 30 different peroxisomal proteins and most of the identified viruses establish multiple interactions with peroxisomal proteins. These viruses present different features and distinct mechanisms of interaction with the host, substantiating the involvement of peroxisomes on different steps of the interplay between the host cells and several different viruses. The peroxisome-dependent lipid metabolism seems to be the most relevant function of this organelle associated with viral infections. These results will likely contribute to future studies involving the identification of novel peroxisome-based targets for antiviral therapy.

Materials and Methods

Data collection

A list of peroxisomal proteins was extracted from UniProt (Consortium, 2017; UniProt Consortium, 2015) (http://www.uniprot.org, accessed on February 12th, 2017) using the search terms: "peroxisome NOT ppar NOT "peroxisome proliferator activated receptor" AND organism:"Homo sapiens (Human) [9606]"", from which solely the manually-annotated entries were retrieved. A PPI network encompassing the 120 proteins identified was constructed using the Cytoscape software (version 3.4.0) (Su et al., 2014). IMEx partners (Orchard et al., 2012) — IntAct (Orchard et al., 2014), MINT (Licata et al., 2012; Orchard et al., 2014), UniProt (Consortium, 2017; UniProt Consortium, 2015), I2D-IMEx (Brown and Jurisica, 2005; Brown and Jurisica, 2007), bhf-ucl, MatrixDB (Launay et al., 2015), InnateDB-IMEx (Breuer et al., 2013) — were selected among the public databases panel of Cytoscape as PPI data sources. The use of the UniProtKB accessions allowed to manually combine the networks generated from each database.

The same list of proteins initially retrieved from UniProt was used to query the interactome browser VirusMentha (Calderone et al., 2013; Calderone et al., 2015) (http://virusmentha.uniroma2.it, accessed on February 12th, 2017). This browser allowed to extract details on virus-human PPIs in a tabular format, which contained the information on interactors identification (protein A and protein

B), gene and taxonomy, publication(s) that supported the interaction as well as a reliability score for each interaction.

Network visualization

Upon removal of self and duplicated edges (in this case, a table with the number of removed edges was added), the network obtained from public databases was manually filtered in order to solely contain proteins from viruses or humans. Subsequently, all the interactions were reviewed to eliminate all human-human interactions.

Cytoscape was also used to visualize the network extracted from VirusMentha. For this, it was necessary to manually identify in Cytoscape the fields corresponding to the source protein and the target protein, as well as the fields that characterized the interaction. As the output from VirusMentha shows solely interactions between the input proteins and viral proteins, it was not necessary to further filter the network to present only virus-human interactions.

Both networks (IMEx and VirusMentha) were also reviewed in order to remove the non-peroxisomal proteins VIM, AKAP11, ATAD1 and GBF1.

The two networks were merged to create a network that represented virtually the whole peroxisome proteins-viral proteins interactions. In this network, the nodes from the same virus species were identified with the same color. The identification of single proteins that result from the processing of a viral polyprotein (which is not directly established in VirusMentha) was performed upon merging the two networks, through a comparative analysis of the publications associated with in respective interactions.

Network integration and analysis

Networks were analyzed using the Cytoscape tool NetworkAnalyzer (version 2.7) (Assenov et al., 2008), in which we modified the size of the nodes in order to correspond to the betweenness centrality. The style of each network was also modified to easily differentiate viral from human proteins.

The Cytoscape plugin ClueGO (version 2.3.2) (Bindea et al., 2009) was used to unravel the biological meaning of the interactome. ClueGO functional enrichment analysis was applied to the network and the significance of the biological processes was calculated. This was corrected using the Bonferroni step-down correction method and only the pathways with p-value≤0.05 were showed.

III. Results

Supplementary Data

Table 3. Human peroxisomal proteins retrieved from UniProt on February 12th, 2017.

Entry	Entry name	Gene names
P50542	PEX5_HUMAN	PEX5 PXR1
O43933	PEX1_HUMAN	PEX1
Q13608	PEX6_HUMAN	PEX6 PXAAA1
P28328	PEX2_HUMAN	PEX2 PAF1 PMP3 PMP35 PXMP3 RNF72
O00623	PEX12_HUMAN	PEX12 PAF3
O60683	PEX10_HUMAN	PEX10 RNF69
Q7Z412	PEX26_HUMAN	PEX26
P40855	PEX19_HUMAN	PEX19 HK33 PXF OK/SW-cl.22
O00429	DNM1L_HUMAN	DNM1L DLP1 DRP1
Q8IYB4	PEX5R_HUMAN	PEX5L PEX5R PXR2
P33897	ABCD1_HUMAN	ABCD1 ALD
O75381	PEX14_HUMAN	PEX14
Q9Y5Y5	PEX16_HUMAN	PEX16
P56589	PEX3_HUMAN	PEX3
P21549	SPYA_HUMAN	AGXT AGT1 SPAT
P00441	SODC_HUMAN	SOD1
Q92968	PEX13_HUMAN	PEX13
O96011	PX11B_HUMAN	PEX11B
O14734	ACOT8_HUMAN	ACOT8 ACTEIII PTE1 PTE2
Q15067	ACOX1_HUMAN	ACOX1 ACOX
O00628	PEX7_HUMAN	PEX7 PTS2R
Q7Z434	MAVS_HUMAN	MAVS IPS1 KIAA1271 VISA
P22307	NLTP_HUMAN	SCP2
Q969V5	MUL1_HUMAN	MUL1 C1orf166 GIDE MAPL MULAN RNF218
P51659	DHB4_HUMAN	HSD17B4 EDH17B4 SDR8C1
O94972	TRI37_HUMAN	TRIM37 KIAA0898 MUL POB1
Q5T8D3	ACBD5_HUMAN	ACBD5 KIAA1996
P33121	ACSL1_HUMAN	ACSL1 FACL1 FACL2 LACS LACS1 LACS2
Q99424	ACOX2_HUMAN	ACOX2
O15254	ACOX3_HUMAN	ACOX3 BRCOX PRCOX
O95573	ACSL3_HUMAN	ACSL3 ACS3 FACL3 LACS3
Q8N9L9	ACOT4_HUMAN	ACOT4 PTE2B PTEIB
Q9UBJ2	ABCD2_HUMAN	ABCD2 ALD1 ALDL1 ALDR ALDRP
P28288	ABCD3_HUMAN	ABCD3 PMP70 PXMP1
Q709F0	ACD11_HUMAN	ACAD11
Q9UKU0	ACSL6_HUMAN	ACSL6 ACS2 FACL6 KIAA0837 LACS5
O14678	ABCD4_HUMAN	ABCD4 PXMP1L
Q9NUZ1	ACOXL_HUMAN	ACOXL

90

O60488	ACSL4_HUMAN	ACSL4 ACS4 FACL4 LACS4
O00116	ADAS_HUMAN	AGPS AAG5
Q9UHK6	AMACR_HUMAN	AMACR
Q9UKA4	AKA11_HUMAN	AKAP11 AKAP220 KIAA0629
P19801	AOC1_HUMAN	AOC1 ABP1 DAO1
P51648	AL3A2_HUMAN	ALDH3A2 ALDH10 FALDH
Q8NBU5	ATAD1_HUMAN	ATAD1 FNP001
Q14032	BAAT_HUMAN	BAAT
Q9NXR7	BRE_HUMAN	BRE BRCC45
P43155	CACP_HUMAN	CRAT CAT1
P04040	CATA_HUMAN	CAT
Q9BTZ2	DHRS4_HUMAN	DHRS4 SDR25C2 UNQ851/PRO1800
Q9NUI1	DECR2_HUMAN	DECR2 PDCR SDR17C1
O95822	DCMC_HUMAN	MLYCD
Q92538	GBF1_HUMAN	GBF1 KIAA0248
P35914	HMGCL_HUMAN	HMGCL
P14735	IDE_HUMAN	IDE
P34913	HYES_HUMAN	EPHX2
Q6YN16	HSDL2_HUMAN	HSDL2 C9orf99 SDR13C1
Q8IV20	LACC1_HUMAN	LACC1 C13orf31 FAMIN
O75521	ECI2_HUMAN	ECI2 DRS1 HCA88 PECI
Q08426	ECHP_HUMAN	EHHADH ECHD
Q13011	ECH1_HUMAN	ECH1
Q8WVX9	FACR1_HUMAN	FAR1 MLSTD2 UNQ2423/PRO4981
Q96K12	FACR2_HUMAN	FAR2 MLSTD1
Q8NAU1	FNDC5_HUMAN	FNDC5 FRCP2
Q9Y3D6	FIS1_HUMAN	FIS1 TTC11 CGI-135
O15228	GNPAT_HUMAN	GNPAT DAPAT DHAPAT
Q9NYQ3	HAOX2_HUMAN	HAO2 HAOX2 GIG16
Q9Y2Q3	GSTK1_HUMAN	GSTK1 HDCMD47P
Q9UJ83	HACL1_HUMAN	HACL1 HPCL HPCL2 PHYH2 HSPC279
Q9UJM8	HAOX1_HUMAN	HAO1 GOX1 HAOX1
Q13907	IDI1_HUMAN	IDI1
Q9BXS1	IDI2_HUMAN	IDI2
O75874	IDHC_HUMAN	IDH1 PICD
P48735	IDHP_HUMAN	IDH2
Q96CN7	ISOC1_HUMAN	ISOC1 CGI-111
Q86WA8	LONP2_HUMAN	LONP2 LONP
Q969Z3	MARC2_HUMAN	MARC2 MOSC2
Q9Y4F3	MARF1_HUMAN	KIAA0430 LKAP MARF1
Q9GZY8	MFF_HUMAN	MFF C2orf33 AD030 AD033 GL004
Q2QL34	MP17L_HUMAN	MPV17L
P39210	MPV17_HUMAN	MPV17
P35228	NOS2_HUMAN	NOS2 NOS2A

III. Results

A8MXV4	NUD19_HUMAN	NUDT19
P0C024	NUDT7_HUMAN	NUDT7
Q9UKG9	OCTC_HUMAN	CROT COT
Q9BQG2	NUD12_HUMAN	NUDT12
Q99489	OXDD_HUMAN	DDO
P14920	OXDA_HUMAN	DAO DAMOX
O14832	PAHX_HUMAN	PHYH PAHX
Q8TE04	PANK1_HUMAN	PANK1 PANK
Q9BY49	PECR_HUMAN	PECR SDR29C1 PRO1004
Q6QHF9	PAOX_HUMAN	PAOX PAO UNQ1923/PRO4398
O43808	PM34_HUMAN	SLC25A17 PMP34
Q15126	PMVK_HUMAN	PMVK PMKI
Q9NP80	PLPL8_HUMAN	PNPLA8 IPLA22 IPLA2G BM-043
P30044	PRDX5_HUMAN	PRDX5 ACR1 SBBI10
Q9Y6I8	PXMP4_HUMAN	PXMP4 PMP24
Q8N4Q0	PTGR3_HUMAN	ZADH2 PTGR3
O75192	PX11A_HUMAN	PEX11A PEX11
Q9NR77	PXMP2_HUMAN	PXMP2 PMP22
Q8NFP0	PXT1_HUMAN	PXT1 STEPP
Q92930	RAB8B_HUMAN	RAB8B
O14975	S27A2_HUMAN	SLC27A2 ACSVL1 FACVL1 FATP2 VLACS
Q9NR31	SAR1A_HUMAN	SAR1A SAR1 SARA SARA1
Q96JE7	SC16B_HUMAN	SEC16B KIAA1928 LZTR2 RGPR SEC16S
Q9H4I8	SEHL2_HUMAN	SERHL2 SERHL
Q9P0Z9	SOX_HUMAN	PIPOX LPIPOX PSO
O43581	SYT7_HUMAN	SYT7 PCANAP7
Q86WV6	STING_HUMAN	TMEM173 ERIS MITA STING
Q5T011	SZT2_HUMAN	SZT2 C1orf84 KIAA0467
P09110	THIK_HUMAN	ACAA1 ACAA PTHIO
Q86UB9	TM135_HUMAN	TMEM135
Q53FP2	TM35A_HUMAN	TMEM35A TMEM35
P29401	TKT_HUMAN	TKT
Q2T9J0	TYSD1_HUMAN	TYSND1
A6NGE7	URAD_HUMAN	URAD PRHOXNB
P52758	UK114_HUMAN	HRSP12 PSP
P08670	VIME_HUMAN	VIM
P47989	XDH_HUMAN	XDH XDHA
Q6FIF0	ZFAN6_HUMAN	ZFAND6 AWP1 ZA20D3 HT032

Table 4. Proteins with higher degree on Figure 26 network. Rows in red and blue represent viral and peroxisomal proteins, respectively. * identifies the proteins non-exclusively peroxisomal.

Protein name	Uniprot ID	Taxonomy ID	Degree	BetweennessCentrality
FAR1	Q8WVX9	9606	15	0.42089452
MAVS*	Q7Z434	9606	12	0.25967505
ALDH3A2*	P51648	9606	12	0.21243801
ACSL3*	O95573	9606	9	0.20915693
1C	P04544	11259	7	0.18051225
E5A	P06460	10600	6	0.16539721
M2	B4URE8	382835	6	0.13196571
ABCD3	P28288	9606	6	0.10596282
PEX14	O75381	9606	6	0.09396271
ABCD1	P33897	9606	5	0.04419556

IV. General Discussion and Future Perspectives

Peroxisomes are ubiquitous, multifunctional and highly dynamic organelles, essential for cell survival and tissue homeostasis, and have been associated to severe metabolic disorders, as well as ageing, cancer, neurodegeneration, infection and inflammation (Aubourg and Wanders, 2013; Islinger et al., 2018).

Upon viral infection, cells mount an antiviral defense in response to viral genome sensing. RLRs detect viral RNA in the cytosol, which results in the activation of their adaptor protein MAVS, both at peroxisomes and mitochondria (Dixit et al., 2010; Seth et al., 2005). Consequently, MAVS activation induces a signaling cascade that culminates with the expression of IFNs and ISGs that counteract viral infection and spreading (Dixit and Kagan, 2013; Yoneyama et al., 2015).

The main goal of this thesis was to understand and elucidate the importance of peroxisomes during viral infections and, most importantly, their role in the cellular antiviral defense. Until the beginning of this work, only few reports have addressed this important peroxisomal function. As introduced in section 1.2.1., Dixit et al. showed for the first time in 2010 that MAVS is also present at peroxisomes, in addition to mitochondria, and further separated the signaling pathway from each organelle to study their kinetics. They reported that, upon viral infection, peroxisomal and mitochondrial MAVS act in a complementing manner: peroxisomal MAVS induces a rapid but short response, whereas mitochondria is responsible for a delayed but long-lasting antiviral response. Additionally, they reported that peroxisomes are responsible for the RLR-induced type III IFNs, which complement the type I IFNs induced by mitochondria-dependent RLR signaling (Odendall et al., 2014). However, another group has more recently challenged these results and reported that activation of MAVS at each organelle induces the expression of both type I and type III IFNs, in similar levels. Moreover, they suggest that the absence of peroxisomes does not affect the capacity of cells to mount an effective antiviral response (Bender et al., 2015). These contradictory results may be due to distinct experimental setups, cell lines and methodologies used, but should certainly be clarified in the near future.

Nevertheless, the results obtained in the context of this thesis, have certainly contributed to highlight the role of peroxisomes as platforms for the establishment of an effective cellular antiviral defense. We have studied two distinct RNA and DNA viruses, HCV and HCMV, respectively. RNA viruses are well studied inducers of RLR-dependent immune responses, since viral RNA is directly sensed by RIG-I and/or MDA-5, and consequently activate MAVS, at both peroxisomes and mitochondria (Dixit and Kagan, 2013; Loo and Gale, 2011; Yoneyama et al., 2015). Additionally, we have also selected a DNA virus since, although controversial, previous reports have shown that RLRs may have a function in DNA-sensing immune responses (Ablasser et al., 2009; Chiu et al., 2009; Choi et al., 2009; Marques et

al., 2018; Melchjorsen et al., 2010) and that DNA viruses encode viral proteins which specifically target the RLR pathway (Castanier et al., 2010; Inn et al., 2011; Jin Choi et al., 2018; Zhao et al., 2012).

In section 3.1., we report that HCV NS3-4A, a known inhibitor of the RLR signaling at mitochondria (see section 1.5.2.), is also capable of inhibiting the peroxisomal-dependent RLR response. We show that NS3-4A localizes at peroxisomes, cleaving the peroxisomal MAVS at the Cys-508, and consequentially decreasing the expression of ISGs (Figure 28). Although peroxisomal and mitochondrial-dependent RLR signaling has been reported to have different kinetics, we showed that NS3-4A cleaves both peroxisomal and mitochondrial MAVS with a similar rate. We further demonstrate that NS3-4A is able to localize at peroxisomes even in the absence of MAVS (section 3.1.). It is well known that HCV life cycle is highly dependent on the host cell lipid metabolism, taking advantage of LD and ER. Furthermore, NS3-4A, besides inhibiting the host antiviral response, is also essential for the formation of the replication complex and the assembly of virions (Morikawa et al., 2011; Targett-Adams et al., 2010). Thus, it is tempting to hypothesize whether the location of HCV NS3-4A at peroxisomes has other proposes that go beyond the impairment of RLR signaling (Figure 28). To address this question, peroxisomal metabolic functions should be evaluated in the presence and absence of NS3-4A and throughout the course of HCV infection.
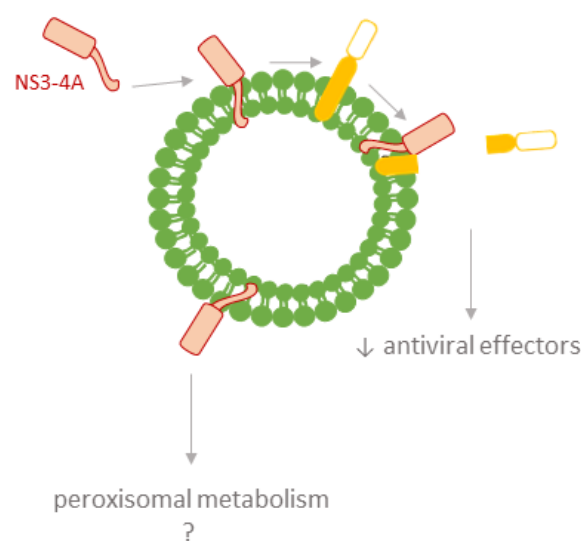
Figure 28. Proposed model of HCV NS3-4A interaction with peroxisomes. NS3-4A binds to peroxisomes membrane via NS4A transmembrane domain. When at peroxisomes, NS3-4A interacts with MAVS cleaving its Cys-508 which releases the cytosolic tail required for the activation of the peroxisomal-dependent RLR signaling and consequential downregulation of antiviral effectors expression. The interaction of NS3-4A with peroxisomes is independent of MAVS and may occur to control peroxisomal metabolism.

In section 3.2., we demonstrate that HCMV specifically highjacks the peroxisomal protein transport machinery in order to transport vMIA to the organelle's membrane. vMIA interacts with PEX19 to travel to the peroxisomal membrane where it interacts with MAVS and impairs the antiviral response.

We furthermore show that the inhibition of peroxisomal MAVS-dependent signaling by vMIA is dependent of MFF (Figure 29). As indicated in section 1.1.1., MFF is the adaptor protein of DLP1 that is recruited to peroxisomes constriction sites, together with FIS1, allowing the fission of peroxisomal membrane by DLP1. Additionally, we demonstrate that vMIA and peroxisomal MAVS interact with MFF and, hence, suggest that MFF mediates the interaction between vMIA and MAVS at peroxisomes (Figure 29). However, the reason behind this role of MFF in mediating this interaction remains unclear.
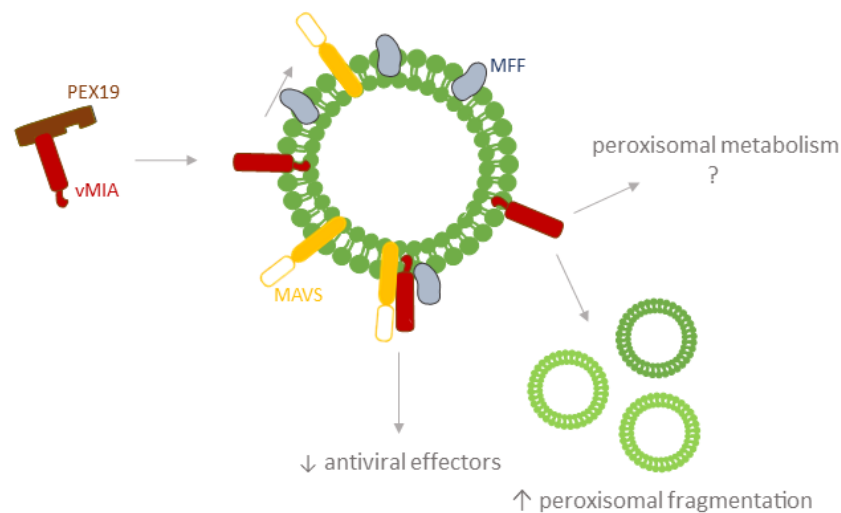
Figure 29. Proposed model of vMIA interaction with peroxisomes. HCMV vMIA hijacks PEX19, to travel to peroxisomes and be inserted in the peroxisomal membrane. Here, it interacts with MFF which is required for vMIA to interact and inhibit the peroxisomal MAVS-dependent antiviral signaling. Moreover, vMIA localization at peroxisomes induces peroxisomal fragmentation, which is independent of MAVS and suggests that vMIA may target to peroxisomes to modulate peroxisomal functions.

Importantly, we demonstrate that vMIA impairs (in a MFF-dependent manner) the oligomerization of MAVS at peroxisomes, which is essential for the activation of the signaling cascade required for the expression of antiviral effectors.

While targeting peroxisomes to inhibit the RLR signaling, vMIA also induces peroxisomal fragmentation. Previously work of Castanier et al. proposed that vMIA, in order to dampen the mitochondria-dependent RLR signaling, induces mitochondrial fragmentation (Castanier et al., 2010). Moreover, it has been shown that the activation of the RLR pathway induces elongation of the mitochondrial network and alterations on mitochondrial dynamics modulate signaling downstream from MAVS (Castanier et al., 2010; Onoguchi et al., 2010). Although we have observed the same induction of fragmentation at peroxisomes, we show that this is not essential for vMIA to impair the peroxisomal MAVS-downstream signaling. These discrepancies imply that peroxisomes and mitochondria dynamics affect RLR signaling differently and corroborate that both organelles may play different functions in the RLR antiviral signaling.

IV. General Discussion and Future Perspectives

In addition, we also describe that vMIA does not require the presence of MAVS at peroxisomes to induce their fragmentation. This result enforces that induction of peroxisomal fragmentation and impairment of RLR signaling at peroxisomes are two distinct and independent functions of vMIA. We hence speculate whether vMIA modulates peroxisomal morphology with the propose of controlling peroxisomal functions in order to enhance viral replication and dissemination (Figure 29). To further unravel this theory, the quantification of peroxisomal enzymes and/or products of peroxisomal metabolism after transfection of vMIA and during HCMV infection should be performed. A detailed mutagenesis analysis of the domains of vMIA that are responsible for the peroxisome's morphology change and/or the inhibition of the peroxisome-dependent antiviral response may also help unravelling the real mechanisms by which the virus interacts with this organelle for its own benefit.

vMIA is also known for its anti-apoptotic function, and it was proposed to inactivate the pro-apoptotic protein BAX, leading to the blockage of the mitochondrial outer membrane permeabilization. The Bcl-2 family member BAK, a pro-apoptotic protein, was reported to re-localize at peroxisomes, in certain conditions, controlling the permeabilization of peroxisomal membrane (Hosoi et al., 2017). We have also observed (unpublished data) the presence of some of the anti-apoptotic proteins from the Bcl-2 family at the peroxisomal membrane. With this, we raise the question whether vMIA could have some anti-apoptotic role at peroxisomes, although no connection as yet been established between this organelle and apoptosis

The results obtained for HCV and HCMV clearly reinforce the importance of peroxisomes as platforms of the RLR immune signaling for both RNA and DNA viruses. Moreover, these are the first reports to show that viral proteins target peroxisomes to inhibit the MAVS-dependent antiviral response.

As far as we known, until now there is no studies reporting that RLRs sense and are required for the antiviral defense against HCMV. Nevertheless, during HCMV infection, due to viral protein synthesis, there is the accumulation of dsRNA, that induces antiviral innate immune responses (Marshall et al., 2009). It was shown that HCMV induces RIG-I degradation (Scott, 2009) and HCMV-encoded US9 glycoprotein targets MAVS, inhibiting IFN-β expression in later stages of infection (Jin Choi et al., 2018). With the work presented in section 3.2., we demonstration another example of a different mechanism that HCMV has developed to inhibit the specific peroxisomal-mediated RLR response, which is different from the mechanism reported for the inhibition of mitochondria-dependent RLR signaling (Castanier et al., 2010).

The focus on the role of peroxisomes in innate immunity increased after the discovery of their function within the RLR antiviral pathway (Dixit et al., 2010). However, additional functions in innate immunity, other than antiviral defense, have been disclosed. Peroxisomes were first associated to phagocytosis,

in rat peritoneal macrophages (Eguchi et al., 1979). In drosophila's cells and murine macrophages, peroxisomes were also reported to be essential for microbe engulfment. Peroxisomal-mediated lipid metabolism and ROS signaling seem to be essential for macrophagic resolution of infection, and their impairment lead to weakened responses to microbes and decreased of organisms survival to infection (Di Cara et al., 2017). Nonetheless, peroxisomes were seen also to have an autoregulatory function in macrophages, rendering protection against uncontrolled activation (Vijayan et al., 2017). Peroxisomes were also shown to be essential for the innate immune responses at the central nervous system (Bottelbergs et al., 2012; Verheijden et al., 2015). Altogether, these data represent evidence of peroxisomes' importance to innate immunity and inflammation and show that peroxisome functions exceed the antiviral defense.

Although this thesis mainly focuses on HCV and HCMV, we performed a bioinformatics analysis and constructed the interactome of human viruses with peroxisomal proteins (section 3.3). This study surprisingly showed that several viruses, with distinct characteristics and dissimilar life cycles, interact with different peroxisomal proteins. A detailed analysis demonstrated that, from the several known peroxisomal functions, the most enriched in the network is definitely lipid metabolism. These results intensely highlight the importance of the interplay between peroxisomes and viruses and can redirect future research to explore the role of this organelle in the life cycle of the identified viruses and in the antiviral defense against them.

V. Final Remarks

Concluding Remarks

With the work presented in this thesis we unravel the mechanisms by which HCV NS3-4A and HCMV vMIA target peroxisomes to impair the peroxisome-dependent RLR antiviral signaling. Additionally, we show that the targeting of peroxisomes by these proteins may have other purposes beyond the impairment of the cellular antiviral defense

Moreover, our proteomic analysis highlights the fact that many other viral proteins, encoded by very distinct viruses, interact with many different peroxisomal proteins, mainly associated to peroxisomal lipid metabolism.

Altogether, these results empathize the importance of peroxisomes as platforms for the RLR-mediated antiviral defense and demonstrate that peroxisomes may be exploited by viruses to enhance viral infection and spreading.

Finally, the follow-up of this work may certainly lead to the discovery of novel peroxisome-derived mechanisms, which can ultimately be used as targets for antiviral therapeutics.

Publications Resulting from this work

Ferreira, A. R., Magalhães, A. C., Camões, F., Gouveia, A., Vieira, M., Kagan, J. C. and Ribeiro, D. (2016). Hepatitis C virus NS3-4A inhibits the peroxisomal MAVS-dependent antiviral signaling response. J. Cell. Mol. Med. 20, 750–757.

Magalhães, A. C.*, **Ferreira, A. R.***, Gomes, S., Vieira, M., Gouveia, A., Islinger, M., Nascimento, R., Schrader, M., Kagan, J. C., and Ribeiro D. (2016). Peroxisomes are platforms for cytomegalovirus' evasion from the cellular immune response. Sci. Rep. 6, 26028.

Ferreira, A. R.*, Gouveia, A.*, Marques M., Valença, I., Kagan, J. C. and Ribeiro, D. Human Cytomegalovirus' vMIA controls peroxisome morphology and dampens antiviral signaling via MAVS and MFF. – soon to be submitted to Molecular Cell

Ferreira, A. R., Valença, I., Marques M., Felgueiras J., and Ribeiro, D. New insights on the interplay between viruses and peroxisomes: a protein-protein interaction analysis. – soon to be submitted to Journal of Molecular Sciences

*Shared co-authorship

VI.   References

Ablasser, A., Bauernfeind, F., Hartmann, G., Latz, E., Fitzgerald, K. A. and Hornung, V. (2009). RIG-I-dependent sensing of poly(dA:dT) through the induction of an RNA polymerase III–transcribed RNA intermediate. *Nat. Immunol.* **10**, 1065–1072.

Adachi, O., Kawai, T., Takeda, K., Matsumoto, M., Tsutsui, H., Sakagami, M., Nakanishi, K. and Akira, S. (1998). Targeted disruption of the MyD88 gene results in loss of IL-1- and IL-18-mediated function. *Immunity* **9**, 143–50.

Albà, M. M., Lee, D., Pearl, F. M. G., Shepherd, A. J., Martin, N., Orengo, C. A. and Kellam, P. (2001). VIDA: a virus database system for the organization of animal virus genome open reading frames. *Nucleic Acids Res.* **29**, 133–136.

Alwine, J. C. (2012). The Human Cytomegalovirus Assembly Compartment: A Masterpiece of Viral Manipulation of Cellular Processes That Facilitates Assembly and Egress. *PLoS Pathog.* **8**, 1–4.

Appel, N., Schaller, T., Penin, F. and Bartenschlager, R. (2006). From structure to function: new insights into hepatitis C virus RNA replication. *J. Biol. Chem.* **281**, 9833–9836.

Aranovich, A., Hua, R., Rutenberg, A. D. and Kim, P. K. (2014). PEX16 contributes to peroxisome maintenance by constantly trafficking PEX3 via the ER. *J. Cell Sci.* **127**, 3675–86.

Artini, M., Nisini, R., Missale, G., Costanzo, A., Accapezzato, D., Balsano, C., Barnaba, V. and Levrero, M. (1995). Infection of Circulating and Liver Infiltrating T Cells by Hepatitis C Virus of Different Subtypes. *Viral Immunol.* **8**, 63–73.

Assenov, Y., Ramirez, F., Schelhorn, S.-E., Lengauer, T. and Albrecht, M. (2008). Computing topological parameters of biological networks. *Bioinformatics* **24**, 282–284.

Bartenschlager, R., Penin, F., Lohmann, V. and André, P. (2011). Assembly of infectious hepatitis C virus particles. *Trends Microbiol.* **19**, 95–103.

Bartosch, B. and Cosset, F.-L. (2006). Cell entry of hepatitis C virus. *Virology* **348**, 1–12.

Beachboard, D. C. and Horner, S. M. (2016). Innate immune evasion strategies of DNA and RNA viruses. *Curr. Opin. Microbiol.* **32**, 113–119.

Bender, S., Reuter, A., Eberle, F., Einhorn, E., Binder, M. and Bartenschlager, R. (2015). Activation of Type I and III Interferon Response by Mitochondrial and Peroxisomal MAVS and Inhibition by Hepatitis C Virus. *PLOS Pathog.* **11**, e1005264.

Berg, R. K., Melchjorsen, J., Rintahaka, J., Diget, E., Søby, S., Horan, K. a, Gorelick, R. J., Matikainen, S., Larsen, C. S., Ostergaard, L., et al. (2012). Genomic HIV RNA induces innate immune responses through RIG-I-dependent sensing of secondary-structured RNA. *PLoS One* **7**, e29291.

VI. References

Bindea, G., Mlecnik, B., Hackl, H., Charoentong, P., Tosolini, M., Kirilovsky, A., Fridman, W.-H., Pages, F., Trajanoski, Z. and Galon, J. (2009). ClueGO: a Cytoscape plug-in to decipher functionally grouped gene ontology and pathway annotation networks. *Bioinformatics* **25**, 1091–1093.

Biolatti, M., Gugliesi, F., Dell'Oste, V. and Landolfo, S. (2018). Modulation of the innate immune response by human cytomegalovirus. *Infect. Genet. Evol.* **64**, 105–114.

Bolte, S. and Cordelières, F. P. (2006). A guided tour into subcellular colocalization analysis in light microscopy. *J. Microsc.* **224**, 213–32.

Bonekamp, N. A., Sampaio, P., de Abreu, F. V., Lüers, G. H. and Schrader, M. (2012). Transient complex interactions of mammalian peroxisomes without exchange of matrix or membrane marker proteins. *Traffic* **13**, 960–78.

Bonekamp, N. a, Grille, S., Cardoso, M. J., Almeida, M., Aroso, M., Gomes, S., Magalhaes, A. C., Ribeiro, D., Islinger, M. and Schrader, M. (2013). Self-interaction of human Pex11pβ during peroxisomal growth and division. *PLoS One* **8**, e53424.

Bosque, G., Folch-Fortuny, A., Picó, J., Ferrer, A. and Elena, S. F. (2014). Topology analysis and visualization of Potyvirus protein-protein interaction network. *BMC Syst. Biol.* **8**, 129.

Boulant, S., Douglas, M. W., Moody, L., Budkowska, A., Targett-Adams, P. and McLauchlan, J. (2008). Hepatitis C virus core protein induces lipid droplet redistribution in a microtubule- and dynein-dependent manner. *Traffic* **9**, 1268–82.

Braverman, N. E., D'Agostino, M. D. and Maclean, G. E. (2013). Peroxisome biogenesis disorders: Biological, clinical and pathophysiological perspectives. *Dev. Disabil. Res. Rev.* **17**, 187–196.

Breiman, A., Vitour, D., Vilasco, M., Ottone, C., Molina, S., Pichard, L., Fournier, C., Delgrange, D., Charneau, P., Duverlie, G., et al. (2006). A hepatitis C virus (HCV) NS3/4A protease-dependent strategy for the identification and purification of HCV-infected cells. *J. Gen. Virol.* **87**, 3587–3598.

Breuer, K., Foroushani, A. K., Laird, M. R., Chen, C., Sribnaia, A., Lo, R., Winsor, G. L., Hancock, R. E. W., Brinkman, F. S. L. and Lynn, D. J. (2013). InnateDB: systems biology of innate immunity and beyond-recent updates and continuing curation. *Nucleic Acids Res.* **41**, D1228-33.

Brown, K. R. and Jurisica, I. (2005). Online Predicted Human Interaction Database. *Bioinformatics* **21**, 2076–2082.

Brown, K. R. and Jurisica, I. (2007). Unequal evolutionary conservation of human protein

interactions in interologous networks. *Genome Biol.* **8**, R95.

Calderone, A., Castagnoli, L. and Cesareni, G. (2013). mentha: a resource for browsing integrated protein-interaction networks. *Nat. Methods* **10**, 690–691.

Calderone, A., Licata, L. and Cesareni, G. (2015). VirusMentha: a new resource for virus-host protein interactions. *Nucleic Acids Res.* **43**, D588–D592.

Camões, F., Bonekamp, N. A., Delille, H. K. and Schrader, M. (2009). Organelle dynamics and dysfunction: A closer link between peroxisomes and mitochondria. *J. Inherit. Metab. Dis.* **32**, 163–80.

Campello, S. and Scorrano, L. (2010). Mitochondrial shape changes: orchestrating cell pathophysiology. *EMBO Rep.* **11**, 678–84.

Cannon, M. J., Schmid, D. S. and Hyde, T. B. (2010). Review of cytomegalovirus seroprevalence and demographic characteristics associated with infection. *Rev. Med. Virol.* **20**, 202–213.

Cao, X., Ding, Q., Lu, J., Tao, W., Huang, B., Zhao, Y., Niu, J., Liu, Y.-J. and Zhong, J. (2014). MDA5 Plays a Critical Role in Interferon Response during Hepatitis C Virus Infection. *J. Hepatol.* **62**, 771–778.

Castanier, C. and Arnoult, D. (2011). Mitochondrial localization of viral proteins as a means to subvert host defense. *Biochim. Biophys. Acta - Mol. Cell Res.* **1813**, 575–583.

Castanier, C., Garcin, D., Vazquez, A., Arnoult, D., Ablasser, A., Bauernfeind, F., Hartmann, G., Latz, E., Fitzgerald, K., Hornung, V., et al. (2010). Mitochondrial dynamics regulate the RIG-I-like receptor antiviral pathway. *EMBO Rep.* **11**, 133–138.

Castro, I. G., Richards, D. M., Metz, J., Costello, J. L., Passmore, J. B., Schrader, T. A., Gouveia, A., Ribeiro, D., Schrader, M. and Michael Schrader, C. (2018). A role for Mitochondrial Rho GTPase 1 (MIRO1) in motility and membrane dynamics of peroxisomes. *Traffic* **19**, 229–242.

Catanese, M. T., Uryu, K., Kopp, M., Edwards, T. J., Andrus, L., Rice, W. J., Silvestry, M., Kuhn, R. J. and Rice, C. M. (2013). Ultrastructural analysis of hepatitis C virus particles. *Proc. Natl. Acad. Sci. U. S. A.* **110**, 9505–10.

Chambers, J., Angulo, A., Amaratunga, D., Guo, H., Jiang, Y., Wan, J. S., Bittner, A., Frueh, K., Jackson, M. R., Peterson, P. a, et al. (1999). DNA Microarrays of the Complex Human Cytomegalovirus Genome: Profiling Kinetic Class with Drug Sensitivity of Viral Gene Expression. *J Virol* **73**, 5757–66.

Chan, Y. K. and Gack, M. U. (2015). RIG-I-like receptor regulation in virus infection and immunity.

VI. References

Curr. Opin. Virol. **12**, 7–14.

Chautard, E., Thierry-Mieg, N. and Ricard-Blum, S. (2009). Interaction networks: from protein functions to drug discovery. A review. *Pathol. Biol. (Paris).* **57**, 324–33.

Chen, S. L. and Morgan, T. R. (2006). The natural history of hepatitis C virus (HCV) infection. *Int. J. Med. Sci.* **3**, 47–52.

Chen, H., Sun, H., You, F., Sun, W., Zhou, X., Chen, L., Yang, J., Wang, Y., Tang, H., Guan, Y., et al. (2011). Activation of STAT6 by STING Is Critical for Antiviral Innate Immunity. *Cell* **147**, 436–446.

Chen, Y., Chen, J., Wang, H., Shi, J., Wu, K., Liu, S., Liu, Y. and Wu, J. (2013). HCV-induced miR-21 contributes to evasion of host immune system by targeting MyD88 and IRAK1. *PLoS Pathog.* **9**, e1003248.

Chevaliez, S. and Pawlotsky, J. (2006). HCV Genome and Life Cycle. In *Hepatitis C Viruses: Genomes and Molecular Biology* (ed. Tan, S.), pp. 5–47. Norfolk (UK): Horizon Bioscience.

Childs, K. S., Randall, R. E., Goodbourn, S. and Mossman, K. L. (2013). LGP2 Plays a Critical Role in Sensitizing mda-5 to Activation by Double-Stranded RNA. *PLoS One* **8**, e64202.

Chiu, Y.-H., MacMillian, J. B. and Chen, Z. J. (2009). RNA Polymerase III Detects Cytosolic DNA and Induces Type I Interferons through the RIG-I Pathway. *Cell* **138**, 576–591.

Choi, M. K., Wang, Z., Ban, T., Yanai, H., Lu, Y., Koshiba, R., Nakaima, Y., Hangai, S., Savitsky, D., Nakasato, M., et al. (2009). A selective contribution of the RIG-I-like receptor pathway to type I interferon responses activated by cytosolic DNA. *Proc. Natl. Acad. Sci. U. S. A.* **106**, 17870–17875.

Choi, Y. B., Choi, Y. and Harhaj, E. W. (2018). Peroxisomes support human herpesvirus 8 latency by stabilizing the viral oncogenic protein vFLIP via the MAVS-TRAF complex. *PLoS Pathog.* **14**, e1007058.

Chow, J., Franz, K. M. and Kagan, J. C. (2015). PRRs are watching you: Localization of innate sensing and signaling regulators. *Virology* **479**–**480**, 104–109.

Christensen, M. H. and Paludan, S. R. (2017). Viral evasion of DNA-stimulated innate immune responses. *Cell. Mol. Immunol.* **14**, 4–13.

Cipolla, C. M. and Lodhi, I. J. (2017). Peroxisomal Dysfunction in Age-Related Diseases. *Trends Endocrinol. Metab.* **28**, 297–308.

Civril, F., Bennett, M., Moldt, M., Deimling, T., Witte, G., Schiesser, S., Carell, T. and Hopfner, K.-P. (2011). The RIG-I ATPase domain structure reveals insights into ATP-dependent antiviral

signalling. *EMBO Rep.* **12**, 1127–34.

Cohen, G. B., Rangan, V. S., Chen, B. K., Smith, S. and Baltimore, D. (2000). The human thioesterase II protein binds to a site on HIV-1 Nef critical for CD4 down-regulation. *J. Biol. Chem.* **275**, 23097–23105.

Cohen, S., Valm, A. M. and Lippincott-Schwartz, J. (2018). Interacting organelles. *Curr. Opin. Cell Biol.* **53**, 84–91.

Consortium, T. U. (2017). UniProt: the universal protein knowledgebase. *Nucleic Acids Res.* **45**,.

Costello, J. L. and Schrader, M. (2018). Unloosing the Gordian knot of peroxisome formation. *Curr. Opin. Cell Biol.* **50**, 50–56.

Costello, J. L., Castro, I. G., Camões, F., Schrader, T. A., Mcneall, D., Yang, J., Giannopoulou, E.-A., Gomes, S., Pogenberg, V., Bonekamp, N. A., et al. (2017a). Predicting the targeting of tail-anchored proteins to subcellular compartments in mammalian cells. *J. Cell Sci.* **130**, 1675–1687.

Costello, J. L., Castro, I. G., Hacker, C., Schrader, T. A., Metz, J., Zeuschner, D., Azadi, A. S., Godinho, L. F., Costina, V., Findeisen, P., et al. (2017b). ACBD5 and VAPB mediate membrane associations between peroxisomes and the ER. *J. Cell Biol.* **216**, 331–342.

Costello, J. L., Castro, I. G., Schrader, T. A., Islinger, M. and Schrader, M. (2017c). Peroxisomal ACBD4 interacts with VAPB and promotes ER-peroxisome associations. *Cell Cycle* **16**, 1039–1045.

Coyaud, E., Ranadheera, C., Cheng, D., Gonçalves, J., Dyakov, B. J. A., Laurent, E. M. N., St-Germain, J., Pelletier, L., Gingras, A.-C., Brumell, J. H., et al. (2018). Global Interactomics Uncovers Extensive Organellar Targeting by Zika Virus. *Mol. Cell. Proteomics* **17**, 2242–2255.

Crovatto, M., Pozzato, G., Zorat, F., Pussini, E., Nascimben, F., Baracetti, S., Grando, M. G., Mazzaro, C., Reitano, M., Modolo, M. L., et al. (2000). Peripheral blood neutrophils from hepatitis C virus-infected patients are replication sites of the virus. *Haematologica* **85**, 356–61.

Dahabieh, M. S., Di Pietro, E., Jangal, M., Goncalves, C., Witcher, M., Braverman, N. E. and del Rincón, S. V. (2018). Peroxisomes and cancer: The role of a metabolic specialist in a disease of aberrant metabolism. *Biochim. Biophys. Acta - Rev. Cancer* **1870**, 103–121.

Dan Dunn, J., Alvarez, L. A., Zhang, X. and Soldati, T. (2015). Reactive oxygen species and mitochondria: A nexus of cellular homeostasis. *Redox Biol.* **6**, 472–485.

de Chaumont, F., Dallongeville, S., Chenouard, N., Hervé, N., Pop, S., Provoost, T., Meas-Yedid, V., Pankajakshan, P., Lecomte, T., Le Montagner, Y., et al. (2012). Icy: an open bioimage

VI. References

informatics platform for extended reproducible research. *Nat. Methods* **9**, 690–696.

Debing, Y., Neyts, J. and Delang, L. (2015). The future of antivirals. *Curr. Opin. Infect. Dis.* **28**, 596–602.

Delille, H. K. and Schrader, M. (2008). Targeting of hFis1 to Peroxisomes Is Mediated by Pex19p. *J. Biol. Chem.* **283**, 31107–31115.

Delille, H. K., Agricola, B., Guimaraes, S. C., Borta, H., Lüers, G. H., Fransen, M. and Schrader, M. (2010). Pex11pbeta-mediated growth and division of mammalian peroxisomes follows a maturation pathway. *J. Cell Sci.* **123**, 2750–62.

Deosaran, E., Larsen, K. B., Hua, R., Sargent, G., Wang, Y., Kim, S., Lamark, T., Jauregui, M., Law, K., Lippincott-Schwartz, J., et al. (2013). NBR1 acts as an autophagy receptor for peroxisomes. *J. Cell Sci.* **126**, 939–52.

Di Cara, F., Sheshachalam, A., Braverman, N. E., Rachubinski, R. A. and Simmonds, A. J. (2017). Peroxisome-Mediated Metabolism Is Required for Immune Response to Microbial Infection. *Immunity* **47**, 93–106.e7.

Dias, A. F., Francisco, T., Rodrigues, T. A., Grou, C. P. and Azevedo, J. E. (2016). The first minutes in the life of a peroxisomal matrix protein. *Biochim. Biophys. Acta - Mol. Cell Res.* **1863**, 814–820.

Ding, Q., Cao, X., Lu, J., Huang, B., Liu, Y.-J., Kato, N., Shu, H.-B. and Zhong, J. (2013). Hepatitis C virus NS4B blocks the interaction of STING and TBK1 to evade host innate immunity. *J. Hepatol.* **59**, 52–8.

Dixit, E. and Kagan, J. C. (2013). Intracellular Pathogen Detection by RIG-I-Like Receptors. In *Advances in immunology*, pp. 99–125. Elsevier Inc.

Dixit, E., Boulant, S., Zhang, Y., Lee, A. S. Y., Odendall, C., Shum, B., Hacohen, N., Chen, Z. J., Whelan, S. P., Fransen, M., et al. (2010). Peroxisomes are signaling platforms for antiviral innate immunity. *Cell* **141**, 668–81.

Dorninger, F., Forss-Petter, S. and Berger, J. (2017). From peroxisomal disorders to common neurodegenerative diseases - the role of ether phospholipids in the nervous system. *FEBS Lett.* **591**, 2761–2788.

Dupont, L. and Reeves, M. B. (2016). Cytomegalovirus latency and reactivation: recent insights into an age old problem. *Rev Med Virol* **26**, 75–89.

Dyer, M. D., Murali, T. M. and Sobral, B. W. (2008). The Landscape of Human Proteins Interacting with Viruses and Other Pathogens. *Plos Pathog.* **4**, e32.

Egger, D., Wölk, B., Gosert, R., Bianchi, L., Blum, H. E., Moradpour, D., Bienz, K. and Bianchi, L. (2002). Expression of hepatitis C virus proteins induces distinct membrane alterations including a candidate viral replication complex. *J. Virol.* **76**, 5974–84.

Fagarasanu, A., Mast, F. D., Knoblach, B. and Rachubinski, R. A. (2010). Molecular mechanisms of organelle inheritance: lessons from peroxisomes in yeast. *Nat. Rev. Mol. Cell Biol.* **11**, 644–654.

Fahimi, H. D., Baumgart, E. and Völkl, A. (1993). Ultrastructural aspects of the biogenesis of peroxisomes in rat liver. *Biochimie* **75**, 201–208.

Fang, Y., Morrell, J. C., Jones, J. M. and Gould, S. J. (2004). PEX3 functions as a PEX19 docking factor in the import of class I peroxisomal membrane proteins. *J. Cell Biol.* **164**, 863–75.

Ferreira, A. R., Magalhães, A. C., Camões, F., Gouveia, A., Vieira, M., Kagan, J. C. and Ribeiro, D. (2016). Hepatitis C virus NS3-4A inhibits the peroxisomal MAVS-dependent antiviral signalling response. *J. Cell. Mol. Med.* **20**, 750–757.

Fliss, P. M. and Brune, W. (2012). Prevention of cellular suicide by cytomegaloviruses. *Viruses* **4**, 1928–49.

Foy, E., Li, K., Wang, C., Sumpter, R., Ikeda, M., Lemon, S. M. and Gale, M. (2003). Regulation of interferon regulatory factor-3 by the hepatitis C virus serine protease. *Science* **300**, 1145–8.

Francisco, T., Rodrigues, T. A., Dias, A. F., Barros-Barbosa, A., Bicho, D. and Azevedo, J. E. (2017). Protein transport into peroxisomes: Knowns and unknowns. *BioEssays* **39**, 1700047.

Fransen, M., Wylin, T., Brees, C., Mannaerts, G. P. and Van Veldhoven, P. P. (2001). Human pex19p binds peroxisomal integral membrane proteins at regions distinct from their sorting sequences. *Mol. Cell. Biol.* **21**, 4413–24.

Fransen, M., Nordgren, M., Wang, B. and Apanasets, O. (2012). Role of peroxisomes in ROS/RNS-metabolism: Implications for human disease. *Biochim. Biophys. Acta - Mol. Basis Dis.* **1822**, 1363–1373.

Franz, K. M., Neidermyer, W. J., Tan, Y.-J., Whelan, S. P. J. and Kagan, J. C. (2018). STING-dependent translation inhibition restricts RNA virus replication. *Proc. Natl. Acad. Sci.* 201716937.

Franzosa, E. A. and Xia, Y. (2011). Structural principles within the human-virus protein-protein interaction network. *Proc. Natl. Acad. Sci. U. S. A.* **108**, 10538–10543.

Fredericksen, B. L., Keller, B. C., Fornek, J., Katze, M. G. and Gale, M. (2008). Establishment and Maintenance of the Innate Antiviral Response to West Nile Virus Involves both RIG-I and MDA5

Signaling through IPS-1. *J. Virol.* **82**, 609–616.

Fujiki, Y., Rachubinski, R. A., Lazarow, P. B., Fujiki, Y., Ogasawara, Y., Yamamoto, A., Tagaya, M. and Tani, K. (1984). Synthesis of a major integral membrane polypeptide of rat liver peroxisomes on free polysomes. *Proc. Natl. Acad. Sci. U. S. A.* **81**, 7127–31.

Gack, M. U., Shin, Y. C., Joo, C.-H., Urano, T., Liang, C., Sun, L., Takeuchi, O., Akira, S., Chen, Z., Inoue, S., et al. (2007). TRIM25 RING-finger E3 ubiquitin ligase is essential for RIG-I-mediated antiviral activity. *Nature* **446**, 916–920.

Gandre-Babbe, S. and van der Bliek, A. M. (2008). The novel tail-anchored membrane protein Mff controls mitochondrial and peroxisomal fission in mammalian cells. *Mol. Biol. Cell* **19**, 2402–12.

Garaigorta, U. and Chisari, F. V (2009). Hepatitis C virus blocks interferon effector function by inducing protein kinase R phosphorylation. *Cell Host Microbe* **6**, 513–22.

Gardy, J. L., Lynn, D. J., Brinkman, F. S. L. and Hancock, R. E. W. (2009). Enabling a systems biology approach to immunology: focus on innate immunity. *Trends Immunol.* **30**, 249–262.

Geuze, H. J., Murk, J. L., Stroobants, A. K., Griffith, J. M., Kleijmeer, M. J., Koster, A. J., Verkleij, A. J., Distel, B. and Tabak, H. F. (2003). Involvement of the Endoplasmic Reticulum in Peroxisome Formation. *Mol. Biol. Cell* **14**, 2900–2907.

Ghaedi, K., Tamura, S., Okumoto, K., Matsuzono, Y. and Fujiki, Y. (2000). The peroxin pex3p initiates membrane assembly in peroxisome biogenesis. *Mol. Biol. Cell* **11**, 2085–102.

Gill, K., Ghazinian, H., Manch, R. and Gish, R. (2016). Hepatitis C virus as a systemic disease: reaching beyond the liver. *Hepatol. Int.* **10**, 415–423.

Gitlin, L., Barchet, W., Gilfillan, S., Cella, M., Beutler, B., Flavell, R. A., Diamond, M. S. and Colonna, M. (2006). Essential role of mda-5 in type I IFN responses to polyriboinosinic:polyribocytidylic acid and encephalomyocarditis picornavirus. *Proc. Natl. Acad. Sci. U. S. A.* **103**, 8459–8464.

Gokhale, N. S., Vazquez, C. and Horner, S. M. (2014). Hepatitis C Virus. Strategies to Evade Antiviral Responses. *Future Virol.* **9**, 1061–1075.

Goldmacher, V. S. (2002). vMIA, a viral inhibitor of apoptosis targeting mitochondria. *Biochimie* **84**, 177–185.

Goldmacher, V. S. (2005). Cell death suppression by cytomegaloviruses. *Apoptosis* **10**, 251–265.

Goldmacher, V. S., Bartle, L. M., Skaletskaya, A., Dionne, C. A., Kedersha, N. L., Vater, C. A., Han, J. W., Lutz, R. J., Watanabe, S., Cahir McFarland, E. D., et al. (1999). A cytomegalovirus-encoded mitochondria-localized inhibitor of apoptosis structurally unrelated to Bcl-2. *Proc. Natl. Acad.*

Sci. U. S. A. **96**, 12536–41.

Gosert, R., Egger, D., Lohmann, V., Bartenschlager, R., Blum, H. E., Bienz, K. and Moradpour, D. (2003). Identification of the Hepatitis C Virus RNA Replication Complex in Huh-7 Cells Harboring Subgenomic Replicons. *J. Virol.* **77**, 5487–5492.

Gould, S. J., Keller, G. A., Hosken, N., Wilkinson, J. and Subramani, S. (1989). A conserved tripeptide sorts proteins to peroxisomes. *J. Cell Biol.* **108**, 1657–64.

Guo, L., Fang, H., Collins, J., Fan, X., Dial, S., Wong, A., Mehta, K., Blann, E., Shi, L., Tong, W., et al. (2006). Differential gene expression in mouse primary hepatocytes exposed to the peroxisome proliferator-activated receptor α agonists. *BMC Bioinformatics* **7**, S18.

Guo, T., Gregg, C., Boukh-Viner, T., Kyryakov, P., Goldberg, A., Bourque, S., Banu, F., Haile, S., Milijevic, S., San, K. H. Y., et al. (2007). A signal from inside the peroxisome initiates its division by promoting the remodeling of the peroxisomal membrane. *J. Cell Biol.* **177**, 289–303.

Gurvitz, A. and Rottensteiner, H. (2006). The biochemistry of oleate induction: Transcriptional upregulation and peroxisome proliferation. *Biochim. Biophys. Acta - Mol. Cell Res.* **1763**, 1392–1402.

Halbach, A., Landgraf, C., Lorenzen, S., Rosenkranz, K., Volkmer-Engert, R., Erdmann, R. and Rottensteiner, H. (2006). Targeting of the tail-anchored peroxisomal membrane proteins PEX26 and PEX15 occurs through C-terminal PEX19-binding sites. *J. Cell Sci.* **119**, 2508–17.

Han, J. M., Kang, J. A., Han, M. H., Chung, K. H., Lee, C. R., Song, W. K., Jun, Y. and Park, S. G. (2014). Peroxisome-localized hepatitis Bx protein increases the invasion property of hepatocellular carcinoma cells. *Arch. Virol.* **159**, 2549–2557.

Hara-Kuge, S. and Fujiki, Y. (2008). The peroxin Pex14p is involved in LC3-dependent degradation of mammalian peroxisomes. *Exp. Cell Res.* **314**, 3531–41.

He, Y., Weng, L., Li, R., Li, L., Toyoda, T. and Zhong, J. (2012). The N-terminal helix α(0) of hepatitis C virus NS3 protein dictates the subcellular localization and stability of NS3/NS4A complex. *Virology* **422**, 214–23.

Hei, L. and Zhong, J. (2017). Laboratory of genetics and physiology 2 (LGP2) plays an essential role in hepatitis C virus infection-induced interferon responses. *Hepatology* **65**, 1478–1491.

Hess, R., Staübli, W. and Riess, W. (1965). Nature of the hepatomegalic effect produced by ethyl-chlorophenoxy-isobutyrate in the rat. *Nature* **208**, 856–858.

Hettema, E. H., Erdmann, R., van der Klei, I. and Veenhuis, M. (2014). Evolving models for

peroxisome biogenesis. *Curr. Opin. Cell Biol.* **29**, 25–30.

Hijikata, M., Mizushima, H., Tanji, Y., Komoda, Y., Hirowatari, Y., Akagi, T., Kato, N., Kimura, K. and Shimotohno, K. (1993). Proteolytic processing and membrane association of putative nonstructural proteins of hepatitis C virus. *Proc. Natl. Acad. Sci. U. S. A.* **90**, 10773–10777.

Hoepfner, D., Schildknegt, D., Braakman, I., Philippsen, P. and Tabak, H. F. (2005). Contribution of the Endoplasmic Reticulum to Peroxisome Formation. *Cell* **122**, 85–95.

Hoffman, B. and Liu, Q. (2011). Hepatitis C viral protein translation: mechanisms and implications in developing antivirals. *Liver Int.* **31**, 1449–67.

Holm, C. K., Jensen, S. B., Jakobsen, M. R., Cheshenko, N., Horan, K. A., Moeller, H. B., Gonzalez-Dosal, R., Rasmussen, S. B., Christensen, M. H., Yarovinsky, T. O., et al. (2013). Virus-cell fusion as a trigger of innate immunity dependent on the adaptor STING. *Nat. Immunol.* **13**, 737–743.

Holm, C. K., Rahbek, S. H., Gad, H. H., Bak, R. O., Jakobsen, M. R., Jiang, Z., Hansen, A. L., Jensen, S. K., Sun, C., Thomsen, M. K., et al. (2016). Influenza A virus targets a cGAS-independent STING pathway that controls enveloped RNA viruses. *Nat. Commun.* **7**, 10680.

Horner, S. M., Liu, H. M., Park, H. S., Briley, J. and Gale, M. (2011). Mitochondrial-associated endoplasmic reticulum membranes (MAM) form innate immune synapses and are targeted by hepatitis C virus. *Proc. Natl. Acad. Sci. U. S. A.* **108**, 14590–5.

Hornung, V., Ellegast, J., Kim, S., Brzozka, K., Jung, A., Kato, H., Poeck, H., Akira, S., Conzelmann, K.-K., Schlee, M., et al. (2006). 5'-Triphosphate RNA Is the Ligand for RIG-I. *Science (80-.).* **314**, 994–997.

Hou, F., Sun, L., Zheng, H., Skaug, B., Jiang, Q.-X. and Chen, Z. J. (2011). MAVS forms functional prion-like aggregates to activate and propagate antiviral innate immune response. *Cell* **146**, 448–61.

Hua, R., Gidda, S. K., Aranovich, A., Mullen, R. T. and Kim, P. K. (2015). Multiple Domains in PEX16 Mediate Its Trafficking and Recruitment of Peroxisomal Proteins to the ER. *Traffic* **16**, 832–852.

Hulo, C., de Castro, E., Masson, P., Bougueleret, L., Bairoch, A., Xenarios, I. and Le Mercier, P. (2011). ViralZone: a knowledge resource to understand virus diversity. *Nucleic Acids Res.* **39**, D576-82.

Hunt, M. C., Siponen, M. I. and Alexson, S. E. H. (2012). The emerging role of acyl-CoA thioesterases and acyltransferases in regulating peroxisomal lipid metabolism. *Biochim. Biophys. Acta - Mol.*

Basis Dis. **1822**, 1397–1410.

Huybrechts, S. J., Van Veldhoven, P. P., Brees, C., Mannaerts, G. P., Los, G. V. and Fransen, M. (2009). Peroxisome Dynamics in Cultured Mammalian Cells. *Traffic* **10**, 1722–1733.

Inn, K.-S. K.-S., Lee, S.-H. S.-H., Rathbun, J. Y., Wong, L.-Y. L.-Y., Toth, Z., Machida, K., Ou, J.-H. J. J.-H. J. and Jung, J. U. (2011). Inhibition of RIG-I-Mediated Signaling by Kaposi's Sarcoma-Associated Herpesvirus-Encoded Deubiquitinase ORF64. *J. Virol.* **85**, 10899–10904.

Isaacson, M. K. and Compton, T. (2009). Human Cytomegalovirus Glycoprotein B Is Required for Virus Entry and Cell-to-Cell Spread but Not for Virion Attachment, Assembly, or Egress. *J Virol.* **83**, 3891–3903.

Ishii, K., Tanaka, Y., Yap, C.-C., Aizaki, H., Matsuura, Y. and Miyamura, T. (1999). Expression of hepatitis C virus NS5B protein: Characterization of its RNA polymerase activity and RNA binding. *Hepatology* **29**, 1227–1235.

Ishikawa, H. and Barber, G. N. (2008). STING is an endoplasmic reticulum adaptor that facilitates innate immune signalling. *Nature* **455**, 674–678.

Ishikawa, H., Ma, Z. and Barber, G. N. (2009). STING regulates intracellular DNA-mediated, type I interferon-dependent innate immunity. *Nature* **461**, 788–792.

Islinger, M., Abdolzade-Bavil, A., Liebler, S., Weber, G. and Völkl, A. (2012a). Assessing Heterogeneity of Peroxisomes: Isolation of Two Subpopulations from Rat Liver. In *Liver Proteomics*, pp. 83–96. Totowa, NJ: Humana Press.

Islinger, M., Grille, S., Fahimi, H. D. and Schrader, M. (2012b). The peroxisome: an update on mysteries. *Histochem. Cell Biol.* **137**, 547–74.

Itabe, H. (2010). Intracellular lipid droplet-associated proteins: unique members and their biological functions. Foreword. *Biol. Pharm. Bull.* **33**, 341.

Itoyama, A., Michiyuki, S., Honsho, M., Yamamoto, T., Moser, A., Yoshida, Y. and Fujiki, Y. (2013). Mff functions with Pex11pβ and DLP1 in peroxisomal fission. *Biol. Open* **2**, 998–1006.

Janeway, C. A. (1989). Approaching the Asymptote? Evolution and Revolution in Immunology. *Cold Spring Harb. Symp. Quant. Biol.* **54**, 1–13.

Janeway, C. A. and Medzhitov, R. (2002). Innate immune recognition. *Annu. Rev. Immunol.* **20**, 197–216.

Jarvis, M. A. and Nelson, J. A. (2002). Mechanisms of human cytomegalovirus persistence and latency. *Front Biosci* **7**, d1575-1582.

VI. References

Jefferson, M., Whelband, M., Mohorianu, I. and Powell, P. P. (2014). The pestivirus N terminal protease Npro redistributes to mitochondria and peroxisomes suggesting new sites for regulation of IRF3 by Npro. *PLoS One* **9**, e88838.

Jiang, X., Kinch, L. N., Brautigam, C. a., Chen, X., Du, F., Grishin, N. V. and Chen, Z. J. (2012). Ubiquitin-induced oligomerization of the RNA sensors RIG-I and MDA5 activates antiviral innate immune response. *Immunity* **36**, 959–73.

Jin, L., Waterman, P. M., Jonscher, K. R., Short, C. M., Reisdorph, N. A. and Cambier, J. C. (2008). MPYS, a novel membrane tetraspanner, is associated with major histocompatibility complex class II and mediates transduction of apoptotic signals. *Mol. Cell. Biol.* **28**, 5014–26.

Jin Choi, H., Park, A., Kang, S., Lee, E., Lee, T. A., Ra, E. A., Lee, J., Lee, S. and Park, B. (2018). Human cytomegalovirus-encoded US9 targets MAVS and STING signaling to evade type I interferon immune responses. *Nat. Commun.* **9**, 125.

Jonczyk, M., Pathak, K. B., Sharma, M. and Nagy, P. D. (2007). Exploiting alternative subcellular location for replication: tombusvirus replication switches to the endoplasmic reticulum in the absence of peroxisomes. *Virology* **362**, 320–30.

Jones, J. M., Morrell, J. C. and Gould, S. J. (2001). Multiple distinct targeting signals in integral peroxisomal membrane proteins. *J. Cell Biol.* **153**, 1141–50.

Jones, J. M., Morrell, J. C. and Gould, S. J. (2004). PEX19 is a predominantly cytosolic chaperone and import receptor for class 1 peroxisomal membrane proteins. *J. Cell Biol.* **164**, 57–67.

Joshi, S., Agrawal, G. and Subramani, S. (2012). Phosphorylation-dependent Pex11p and Fis1p interaction regulates peroxisome division. *Mol. Biol. Cell* **23**, 1307–1315.

Kalejta, R. F. (2008). Tegument proteins of human cytomegalovirus. *Microbiol. Mol. Biol. Rev.* **72**, 249–65, table of contents.

Kang, D.-C., Gopalkrishnan, R. V, Wu, Q., Jankowsky, E., Pyle, A. M., Fisher, P. B. and Pardee, A. B. (2002). mda-5: An interferon-inducible putative RNA helicase with double-stranded RNA-dependent ATPase activity and melanoma growth-suppressive properties. *Proc. Natl. Acad. Sci. U. S. A.* **99**, 637–642.

Kato, H., Takeuchi, O., Sato, S., Yoneyama, M., Yamamoto, M., Matsui, K., Uematsu, S., Jung, A., Kawai, T., Ishii, K. J., et al. (2006). Differential roles of MDA5 and RIG-I helicases in the recognition of RNA viruses. *Nature* **441**, 101–105.

Kawai, T. and Akira, S. (2010). The role of pattern-recognition receptors in innate immunity: update

on Toll-like receptors. *Nat. Publ. Gr.* **11**, 373–84.

Kawai, T. and Akira, S. (2011). Toll-like Receptors and Their Crosstalk with Other Innate Receptors in Infection and Immunity. *Immunity* **34**, 637–650.

Kawai, T., Takahashi, K., Sato, S., Coban, C., Kumar, H., Kato, H., Ishii, K. J., Takeuchi, O. and Akira, S. (2005). IPS-1, an adaptor triggering RIG-I- and Mda5-mediated type I interferon induction. *Nat. Immunol.* **6**, 981–988.

Kim, C. W. and Chang, K.-M. (2013). Hepatitis C virus: virology and life cycle. *Clin. Mol. Hepatol.* 17–25.

Kim, P. K., Mullen, R. T., Schumann, U. and Lippincott-Schwartz, J. (2006). The origin and maintenance of mammalian peroxisomes involves a de novo PEX16-dependent pathway from the ER. *J. Cell Biol.* **173**, 521–32.

Kim, P. K., Hailey, D. W., Mullen, R. T. and Lippincott-Schwartz, J. (2008). Ubiquitin signals autophagic degradation of cytosolic proteins and peroxisomes. *Proc. Natl. Acad. Sci. U. S. A.* **105**, 20567–20574.

Klouwer, F. C. C., Berendse, K., Ferdinandusse, S., Wanders, R. J. A., Engelen, M. and Poll-The, B. T. (2015). Zellweger spectrum disorders: clinical overview and management approach. *Orphanet J. Rare Dis.* **10**, 151.

Knoblach, B. and Rachubinski, R. A. (2010). Phosphorylation-dependent activation of peroxisome proliferator protein PEX11 controls peroxisome abundance. *J. Biol. Chem.* **285**, 6670–80.

Kobayashi, S., Tanaka, A. and Fujiki, Y. (2007). Fis1, DLP1, and Pex11p coordinately regulate peroxisome morphogenesis. *Exp. Cell Res.* **313**, 1675–1686.

Koch, J. and Brocard, C. (2012). PEX11 proteins attract Mff and human Fis1 to coordinate peroxisomal fission. *J. Cell Sci.* **125**, 3813–3826.

Koch, J. O., Lohmann, V., Herian, U. and Bartenschlager, R. (1996). In vitro studies on the activation of the hepatitis C virus NS3 proteinase by the NS4A cofactor. *Virology* **221**, 54–66.

Koch, A., Thiemann, M., Grabenbauer, M., Yoon, Y., McNiven, M. a and Schrader, M. (2003). Dynamin-like protein 1 is involved in peroxisomal fission. *J. Biol. Chem.* **278**, 8597–605.

Koch, A., Yoon, Y., Bonekamp, N. A., Mcniven, M. A. and Schrader, M. (2005). A Role for Fis1 in Both Mitochondrial and Peroxisomal Fission in Mammalian Cells □. *Mol. Biol. Cell* **16**, 5077–5086.

Koch, J., Pranjic, K., Huber, A., Ellinger, A., Hartig, A., Kragler, F. and Brocard, C. (2010). PEX11

family members are membrane elongation factors that coordinate peroxisome proliferation and maintenance. *J. Cell Sci.* **123**, 3389–3400.

Koirala, S., Guo, Q., Kalia, R., Bui, H. T., Eckert, D. M., Frost, A. and Shaw, J. M. (2013). Interchangeable adaptors regulate mitochondrial dynamin assembly for membrane scission. *Proc. Natl. Acad. Sci. U. S. A.* **110**, E1342-51.

König, R. and Stertz, S. (2015). Recent strategies and progress in identifying host factors involved in virus replication. *Curr. Opin. Microbiol.* **26**, 79–88.

Kowalinski, E., Lunardi, T., McCarthy, A. a, Louber, J., Brunel, J., Grigorov, B., Gerlier, D. and Cusack, S. (2011). Structural basis for the activation of innate immune pattern-recognition receptor RIG-I by viral RNA. *Cell* **147**, 423–35.

Lancini, D., Faddy, H. M., Flower, R. and Hogan, C. (2014). Cytomegalovirus disease in immunocompetent adults. *Med. J. Aust.* **201**, 578–580.

Launay, G., Salza, R., Multedo, D., Thierry-Mieg, N. and Ricard-Blum, S. (2015). MatrixDB, the extracellular matrix interaction database: updated content, a new navigator and expanded functionalities. *Nucleic Acids Res.* **43**, D321–D327.

Lavie, M. and Dubuisson, J. (2017). Interplay between hepatitis C virus and lipid metabolism during virus entry and assembly. *Biochimie* **141**, 62–69.

Lawrence, J. W., Li, Y., Chen, S., DeLuca, J. G., Berger, J. P., Umbenhauer, D. R., Moller, D. E. and Zhou, G. (2001). Differential gene regulation in human versus rodent hepatocytes by peroxisome proliferator-activated receptor (PPAR) α. PPARα fails to induce peroxisome proliferation-associated genes in human cells independently of the level of receptor expression. *J. Biol. Chem.* **276**, 31521–7.

Lazarow, P. B. (2011). Viruses exploiting peroxisomes. *Curr. Opin. Microbiol.* **14**, 458–69.

Lazarow, P. B. and De Duve, C. (1976). A fatty acyl-CoA oxidizing system in rat liver peroxisomes; enhancement by clofibrate, a hypolipidemic drug. *Proc. Natl. Acad. Sci. U. S. A.* **73**, 2043–6.

Lazarow, P. B. and Fujiki, Y. (1985). Biogenesis of peroxisomes. *Annu. Rev. Cell Biol.* **1**, 489–530.

Leung, D. W. and Amarasinghe, G. K. (2012). Structural insights into RNA recognition and activation of RIG-I-like receptors. *Curr. Opin. Struct. Biol.* **22**, 297–303.

Leung, D. W., Basler, C. F. and Amarasinghe, G. K. (2012). Molecular mechanisms of viral inhibitors of RIG-I-like receptors. *Trends Microbiol.* **20**, 139–46.

Li, K., Foy, E., Ferreon, J. C., Nakamura, M., Ferreon, A. C. M., Ikeda, M., Ray, S. C., Gale, M. and

Lemon, S. M. (2005a). Immune evasion by hepatitis C virus NS3/4A protease-mediated cleavage of the Toll-like receptor 3 adaptor protein TRIF. *Proc. Natl. Acad. Sci. U. S. A.* **102**, 2992–7.

Li, X.-D., Sun, L., Seth, R. B., Pineda, G. and Chen, Z. J. (2005b). Hepatitis C virus protease NS3/4A cleaves mitochondrial antiviral signaling protein off the mitochondria to evade innate immunity. *Proc. Natl. Acad. Sci. U. S. A.* **102**, 17717–22.

Licata, L., Briganti, L., Peluso, D., Perfetto, L., Iannuccelli, M., Galeota, E., Sacco, F., Palma, A., Nardozza, A. P., Santonico, E., et al. (2012). MINT, the molecular interaction database: 2012 update. *Nucleic Acids Res.* **40**, D857–D861.

Lin, C. (2006). HCV NS3-4A Serine Protease. In *Hepatitis C Viruses: Genomes and Molecular Biology.* (ed. Tan, S.-L.), pp. 163–206. Norfolk (UK): Horizon Bioscience.

Litwin, J. A. and Bilińska, B. (1995). Morphological heterogeneity of peroxisomes in cultured mouse Leydig cells. *Folia Histochem. Cytobiol.* **33**, 255–8.

Liu, S. T. H., Sharon-Friling, R., Ivanova, P., Milne, S. B., Myers, D. S., Rabinowitz, J. D., Alex Brown, H. and Shenk, T. (2011). Synaptic vesicle-like lipidome of human cytomegalovirus virions reveals a role for SNARE machinery in virion egress. *Proc. Natl. Acad. Sci. U. S. A.* **108**, 12869–12874.

Liu, S., Chen, J., Cai, X., Wu, J., Chen, X., Wu, Y.-T., Sun, L. and Chen, Z. J. (2013). MAVS recruits multiple ubiquitin E3 ligases to activate antiviral signaling cascades. *Elife* **2**,.

Lodhi, I. J. and Semenkovich, C. F. (2014). Peroxisomes: A Nexus for Lipid Metabolism and Cellular Signaling. *Cell Metab.* **19**, 380–92.

Lohmann, V., Körner, F., Herian, U. and Bartenschlager, R. (1997). Biochemical properties of hepatitis C virus NS5B RNA-dependent RNA polymerase and identification of amino acid sequence motifs essential for enzymatic activity. *J. Virol.* **71**, 8416–28.

Loo, Y.-M. and Gale, M. (2011). Immune Signaling by RIG-I-like Receptors. *Immunity* **34**, 680–692.

Loo, Y.-M., Fornek, J., Crochet, N., Bajwa, G., Perwitasari, O., Martinez-Sobrido, L., Akira, S., Gill, M. A., Katze, M. G. and Gale, M. (2008). Distinct RIG-I and MDA5 Signaling by RNA Viruses in Innate Immunity. *J. Virol.* **82**, 335–345.

Losón, O. C., Song, Z., Chen, H. and Chan, D. C. (2013). Fis1, Mff, MiD49, and MiD51 mediate Drp1 recruitment in mitochondrial fission. *Mol. Biol. Cell* **24**, 659–67.

Luo, D., Kohlway, A., Vela, A. and Pyle, A. M. (2012). Visualizing the determinants of viral RNA

recognition by innate immune sensor RIG-I. *Structure* **20**, 1983–1988.

Lupfer, C. and Kanneganti, T.-D. (2013). The expanding role of NLRs in antiviral immunity. *Immunol. Rev.* **255**, 13–24.

Ma-Lauer, Y., Lei, J., Hilgenfeld, R. and von Brunn, A. (2012). Virus–host interactomes — antiviral drug discovery. *Curr. Opin. Virol.* **2**, 614–621.

Ma'ayan, A. (2011). Introduction to network analysis in systems biology. *Sci. Signal.* **4**, tr5.

Ma, J., Edlich, F., Bermejo, G. a, Norris, K. L., Youle, R. J. and Tjandra, N. (2012). Structural mechanism of Bax inhibition by cytomegalovirus protein vMIA. *Proc. Natl. Acad. Sci. U. S. A.* **109**, 20901–6.

Magalhães, A. C., Ferreira, A. R., Gomes, S., Vieira, M., Gouveia, A., Valença, I., Islinger, M., Nascimento, R., Schrader, M., Kagan, J. C., et al. (2016). Peroxisomes are platforms for cytomegalovirus' evasion from the cellular immune response. *Sci. Rep.* **6**, 26028.

Malur, M., Gale, M. and Krug, R. M. (2012). LGP2 downregulates interferon production during infection with seasonal human influenza A viruses that activate interferon regulatory factor 3. *J. Virol.* **86**, 10733–8.

Manns, M. P., Buti, M., Gane, E., Pawlotsky, J.-M., Razavi, H., Terrault, N. and Younossi, Z. (2017). Hepatitis C virus infection. *Nat. Rev. Dis. Prim.* **3**, 17006.

Mao, K., Liu, X., Feng, Y. and Klionsky, D. J. (2014). The progression of peroxisomal degradation through autophagy requires peroxisomal division. *Autophagy* **10**, 652–61.

Marques, M., Ferreira, A. and Ribeiro, D. (2018). The Interplay between Human Cytomegalovirus and Pathogen Recognition Receptor Signaling. *Viruses* **10**, 514.

Marshall, P. A., Dyer, J. M., Quick, M. E. and Goodman, J. M. (1996). Redox-sensitive homodimerization of Pex11p: a proposed mechanism to regulate peroxisomal division. *J. Cell Biol.* **135**, 123–37.

Marshall, E. E., Bierle, C. J., Brune, W. and Geballe, A. P. (2009). Essential Role for either TRS1 or IRS1 in Human Cytomegalovirus Replication. *J. Virol.* **83**, 4112–4120.

Matsuzaki, T. and Fujiki, Y. (2008). The peroxisomal membrane protein import receptor Pex3p is directly transported to peroxisomes by a novel Pex19p- and Pex16p-dependent pathway. *J. Cell Biol.* **183**, 1275–86.

Matsuzono, Y., Matsuzaki, T. and Fujiki, Y. (2006). Functional domain mapping of peroxin Pex19p: interaction with Pex3p is essential for function and translocation. *J. Cell Sci.* **119**, 3539–50.

Mawatari, S., Uto, H., Ido, A., Nakashima, K., Suzuki, T., Kanmura, S., Kumagai, K., Oda, K., Tabu, K., Tamai, T., et al. (2013). Hepatitis C Virus NS3/4A Protease Inhibits Complement Activation by Cleaving Complement Component 4. *PLoS One* **8**, e82094.

Mayerhofer, P. U. (2016). Targeting and insertion of peroxisomal membrane proteins: ER trafficking versus direct delivery to peroxisomes. *Biochim. Biophys. Acta - Mol. Cell Res.* **1863**, 870–880.

McCartney, S. A., Thackray, L. B., Gitlin, L., Gilfillan, S., Virgin IV, H. W. and Colonna, M. (2008). MDA-5 Recognition of a Murine Norovirus. *PLOS Pathog.* **4**, e1000108.

McCormick, A. L., Smith, V. L., Chow, D. and Mocarski, E. S. (2003). Disruption of Mitochondrial Networks by the Human Cytomegalovirus UL37 Gene Product Viral Mitochondrion-Localized Inhibitor of Apoptosis. *J. Virolo* **77**, 631–641.

Medzhitov, R., Preston-Hurlburt, P., Kopp, E., Stadlen, A., Chen, C., Ghosh, S. and Janeway, C. A. (1998). MyD88 is an adaptor protein in the hToll/IL-1 receptor family signaling pathways. *Mol. Cell* **2**, 253–8.

Melchjorsen, J., Rintahaka, J., Søby, S., Horan, K. a, Poltajainen, A., Østergaard, L., Paludan, S. R. and Matikainen, S. (2010). Early Innate Recognition of Herpes Simplex Virus in Human Primary Macrophages Is Mediated via the MDA5/MAVS-Dependent and MDA5/MAVS/RNA Polymerase III-Independent Pathways. *J. Virol.* **84**, 11350–8.

Meylan, E., Curran, J., Hofmann, K., Moradpour, D., Binder, M., Bartenschlager, R. and Tschopp, J. (2005). Cardif is an adaptor protein in the RIG-I antiviral pathway and is targeted by hepatitis C virus. *Nature* **437**, 1167–72.

Miao, Z., Xie, Z., Miao, J., Ran, J., Feng, Y., Xia, X. and Kuhn, J. H. (2017). Regulated Entry of Hepatitis C Virus into Hepatocytes. *Viruses* **9**, 100.

Mocarski, E. S., Shenk, T. and Pass, R. F. (2007). Cytomegaloviruses. In *Fields' Virology* (ed. Knipe, D. M.) and Howley, P. M.), pp. 2702–2772.

Mohan, K. V. K., Som, I. and Atreya, C. D. (2002). Identification of a type 1 peroxisomal targeting signal in a viral protein and demonstration of its targeting to the organelle. *J. Virol.* **76**, 2543–2547.

Möller, G., Leenders, F., van Grunsven, E. G., Dolez, V., Qualmann, B., Kessels, M. M., Markus, M., Krazeisen, A., Husen, B., Wanders, R. J., et al. (1999). Characterization of the HSD17B4 gene: D-specific multifunctional protein 2/17beta-hydroxysteroid dehydrogenase IV. *J. Steroid Biochem. Mol. Biol.* **69**, 441–6.

VI. References

Moore, C. B. and Ting, J. P. Y. Y. (2008). Regulation of Mitochondrial Antiviral Signaling Pathways. *Immunity* **28**, 735–739.

Moradpour, D. and Penin, F. (2013). Hepatitis C virus: From structure to Function. In *Hepatitis C Virus: From Molecular Virology to Antiviral Therapy* (ed. Bartenschlager, R.), pp. 113–142. Springer-Verlag Berlin Heidelberg.

Moradpour, D., Penin, F. and Rice, C. M. (2007). Replication of hepatitis C virus. *Nat. Rev. Microbiol.* **5**, 453–63.

Morikawa, K., Lange, C. M., Gouttenoire, J., Meylan, E., Brass, V., Penin, F. and Moradpour, D. (2011). Nonstructural protein 3-4A: the Swiss army knife of hepatitis C virus. *J. Viral Hepat.* **18**, 305–15.

Motley, A. M. and Hettema, E. H. (2007). Yeast peroxisomes multiply by growth and division. *J. Cell Biol.* **178**, 399–410.

Mukhopadhyay, S., Kuhn, R. J. and Rossmann, M. G. (2005). A structural perspective of the flavivirus life cycle. *Nat. Rev. Microbiol.* **3**, 13–22.

Muntau, A. C., Roscher, A. A., Kunau, W.-H. and Dodt, G. (2003). The interaction between human PEX3 and PEX19 characterized by fluorescence resonance energy transfer (FRET) analysis. *Eur. J. Cell Biol.* **82**, 333–342.

Nathan, C. and Shiloh, M. U. (2000). Reactive oxygen and nitrogen intermediates in the relationship between mammalian hosts and microbial pathogens. *Proc. Natl. Acad. Sci. U. S. A.* **97**, 8841–8.

Nazarko, T. Y. (2017). Pexophagy is responsible for 65% of cases of peroxisome biogenesis disorders. *Autophagy* **13**, 991–994.

Neuhaus, A., Eggeling, C. and Schliebs, W. (2016). Why do peroxisomes associate with the cytoskeleton? *Biochim. Biophys. Acta - Mol. Cell Res.* **1863**, 1019–1026.

Niepmann, M., Lohmann, V., Niepmann, M. and Lohmann, V. (2013). Hepatitis C Virus RNA Translation. In *Hepatitis C Virus: From Molecular Virology to Antiviral Therapy* (ed. Bartenschlager, R.), pp. 143–166. Berlin, Heidelberg: Springer Berlin Heidelberg.

Noriega, V., Redmann, V., Gardner, T. and Tortorella, D. (2012). Diverse immune evasion strategies by human cytomegalovirus. *Immunol. Res.* **54**, 140–151.

Novikoff, P. M. and Novikoff, A. B. (1972). Peroxisomes in absorptive cells of mammalian small intestine. *J. Cell Biol.* **53**, 532–60.

Odendall, C. and Kagan, J. C. (2013). Peroxisomes and the Antiviral Responses of Mammalian Cells.

In *Peroxisomes and their Role in Cellular Signalling* (ed. del Río, L. A.), pp. 67–75. Dordrecht: Springer Netherlands.

Odendall, C., Dixit, E., Stavru, F., Bierne, H., Franz, K. M., Durbin, A. F., Boulant, S., Gehrke, L., Cossart, P. and Kagan, J. C. (2014). Diverse intracellular pathogens activate type III interferon expression from peroxisomes. *Nat. Immunol.* **15**, 717–726.

Ogawa-Goto, K., Tanaka, K., Gibson, W., Moriishi, E., Miura, Y., Kurata, T., Irie, S. and Sata, T. (2003). Microtubule Network Facilitates Nuclear Targeting of Human Cytomegalovirus Capsid. *J Virol* **77**, 8541–8547.

Okumoto, K., Ono, T., Toyama, R., Shimomura, A., Nagata, A. and Fujiki, Y. (2018). New splicing variants of mitochondrial Rho GTPase-1 (Miro1) transport peroxisomes. *J. Cell Biol.* **217**, 619–633.

Olivo-Marin, J. C. (2002). Extraction of spots in biological images using multiscale products. *Pattern Recognit.* **35**, 1989–1996.

Opaliński, Ł., Kiel, J. A. K. W., Williams, C., Veenhuis, M. and van der Klei, I. J. (2011). Membrane curvature during peroxisome fission requires Pex11. *EMBO J.* **30**, 5–16.

Orchard, S., Kerrien, S., Abbani, S., Aranda, B., Bhate, J., Bidwell, S., Bridge, A., Briganti, L., Brinkman, F. S. L., Brinkman, F., et al. (2012). Protein interaction data curation: the International Molecular Exchange (IMEx) consortium. *Nat. Methods* **9**, 345–50.

Orchard, S., Ammari, M., Aranda, B., Breuza, L., Briganti, L., Broackes-Carter, F., Campbell, N. H., Chavali, G., Chen, C., del-Toro, N., et al. (2014). The MIntAct project--IntAct as a common curation platform for 11 molecular interaction databases. *Nucleic Acids Res.* **42**, D358-63.

Oshiumi, H., Matsumoto, M., Hatakeyama, S. and Seya, T. (2009). Riplet/RNF135, a RING finger protein, ubiquitinates RIG-I to promote interferon-beta induction during the early phase of viral infection. *J. Biol. Chem.* **284**, 807–17.

Osumi, T. and Hashimoto, T. (1980). Purification and properties of mitochondrial and peroxisomal 3-hydroxyacyl-CoA dehydrogenase from rat liver. *Arch. Biochem. Biophys.* **203**, 372–383.

Otera, H. and Mihara, K. (2011). Discovery of the membrane receptor for mitochondrial fission GTPase Drp1. *Small GTPases* **2**, 167–172.

Otera, H., Wang, C., Cleland, M. M., Setoguchi, K., Yokota, S., Youle, R. J. and Mihara, K. (2010). Mff is an essential factor for mitochondrial recruitment of Drp1 during mitochondrial fission in mammalian cells. *J. Cell Biol.* **191**, 1141–1158.

VI. References

Otto, G. a and Puglisi, J. D. (2004). The pathway of HCV IRES-mediated translation initiation. *Cell* **119**, 369–80.

Paludan, S. R. and Bowie, A. G. (2013). Immune Sensing of DNA. *Immunity* **38**, 870–880.

Paludan, S. R., Bowie, A. G., Horan, K. a and Fitzgerald, K. a (2011). Recognition of herpesviruses by the innate immune system. *Nat. Rev. Immunol.* **11**, 143–54.

Parisien, J., Lenoir, J. J., Mandhana, R., Rodriguez, K. R., Qian, K., Bruns, A. M. and Horvath, C. M. (2018). RNA sensor LGP2 inhibits TRAF ubiquitin ligase to negatively regulate innate immune signaling. *EMBO Rep.* **19**, e45176.

Pathak, K. B., Sasvari, Z. and Nagy, P. D. (2008). The host Pex19p plays a role in peroxisomal localization of tombusvirus replication proteins. *Virology* **379**, 294–305.

Petrovic, D., Stamataki, Z., Dempsey, E., Golden-Mason, L., Freeley, M., Doherty, D., Prichard, D., Keogh, C., Conroy, J., Mitchell, S., et al. (2011). Hepatitis C virus targets the T cell secretory machinery as a mechanism of immune evasion. *Hepatology* **53**, 1846–53.

Pichlmair, A., Schulz, O., Tan, C. P., Naslund, T. I., Liljestrom, P., Weber, F. and Reis e Sousa, C. (2006). RIG-I-Mediated Antiviral Responses to Single-Stranded RNA Bearing 5'-Phosphates. *Science (80-.).* **314**, 997–1001.

Pickett, B. E., Sadat, E. L., Zhang, Y., Noronha, J. M., Squires, R. B., Hunt, V., Liu, M., Kumar, S., Zaremba, S., Gu, Z., et al. (2012). ViPR: an open bioinformatics database and analysis resource for virology research. *Nucleic Acids Res.* **40**, D593-8.

Pinto, M. P., Grou, C. P., Fransen, M., Sá-Miranda, C. and Azevedo, J. E. (2009). The cytosolic domain of PEX3, a protein involved in the biogenesis of peroxisomes, binds membrane lipids. *Biochim. Biophys. Acta - Mol. Cell Res.* **1793**, 1669–1675.

Poirier, Y., Antonenkov, V. D., Glumoff, T. and Hiltunen, J. K. (2006). Peroxisomal beta-oxidation - a metabolic pathway with multiple functions. *Biochim. Biophys. Acta* **1763**, 1413–26.

Poncet, D., Larochette, N., Pauleau, A.-L., Boya, P., Jalil, A.-A., Cartron, P.-F., Vallette, F., Schnebelen, C., Bartle, L. M., Skaletskaya, A., et al. (2004). An anti-apoptotic viral protein that recruits Bax to mitochondria. *J. Biol. Chem.* **279**, 22605–14.

Popescu, C.-I., Rouillé, Y. and Dubuisson, J. (2011). Hepatitis C virus assembly imaging. *Viruses* **3**, 2238–54.

Pu, J., Ha, C. W., Zhang, S., Jung, J. P., Huh, W.-K. and Liu, P. (2011). Interactomic study on interaction between lipid droplets and mitochondria. *Protein Cell* **2**, 487–96.

Rachubinski, R. A. (1984). Acyl-Coa oxidase and hydratase-dehydrogenase, two enzymes of the peroxisomal beta-oxidation system, are synthesized on free polysomes of clofibrate-treated rat liver. *J. Cell Biol.* **99**, 2241–2246.

Raychaudhuri, S. and Prinz, W. A. (2008). Nonvesicular phospholipid transfer between peroxisomes and the endoplasmic reticulum. *Proc. Natl. Acad. Sci. U. S. A.* **105**, 15785–15790.

Reeves, M. and Sinclair, J. (2008). Aspects of human cytomegalovirus latency and reactivation. *Curr. Top. Microbiol. Immunol.* **325**, 297–313.

Ribeiro, D., Castro, I., Fahimi, H. D. and Schrader, M. (2012). Peroxisome morphology in pathology. *Histol. Histopathol.* **27**, 661–76.

Roth-Cross, J. K., Bender, S. J. and Weiss, S. R. (2008). Murine Coronavirus Mouse Hepatitis Virus Is Recognized by MDA5 and Induces Type I Interferon in Brain Macrophages/Microglia. *J. Virol.* **82**, 9829–9838.

Roy, S. (2012). Systems biology beyond degree, hubs and scale-free networks: the case for multiple metrics in complex networks. *Syst. Synth. Biol.* **6**, 31–4.

Rozenblatt-Rosen, O., Deo, R. C., Padi, M., Adelmant, G., Calderwood, M. A., Rolland, T., Grace, M., Dricot, A., Askenazi, M., Tavares, M., et al. (2012). Interpreting cancer genomes using systematic host network perturbations by tumour virus proteins. *Nature* **487**, 491–495.

Rucktäschel, R., Halbach, A., Girzalsky, W., Rottensteiner, H. and Erdmann, R. (2010). De novo synthesis of peroxisomes upon mitochondrial targeting of Pex3p. *Eur. J. Cell Biol.* **89**, 947–54.

Sacksteder, K. A., Jones, J. M., South, S. T., Li, X., Liu, Y. and Gould, S. J. (2000). PEX19 binds multiple peroxisomal membrane proteins, is predominantly cytoplasmic, and is required for peroxisome membrane synthesis. *J. Cell Biol.* **148**, 931–44.

Saito, T. and Gale, M. (2008). Differential recognition of double-stranded RNA by RIG-I-like receptors in antiviral immunity. *J. Exp. Med.* **205**, 1523–7.

Saito, T., Owen, D. M., Jiang, F., Marcotrigiano, J. and Gale, M. (2008). Innate immunity induced by composition-dependent RIG-I recognition of hepatitis C virus RNA. *Nature* **454**, 523–7.

Santos, M., Imanaka, T., Shio, H., Small, G. and Lazarow, P. (1988). Peroxisomal membrane ghosts in Zellweger syndrome - aberrant organelle assembly. *Science* **239**, 1536–1538.

Sarrazin, C., Hézode, C., Zeuzem, S. and Pawlotsky, J. (2012). Antiviral strategies in hepatitis C virus infection. *J. Hepatol.* **56**, S88–S100.

Satoh, T., Kato, H., Kumagai, Y., Yoneyama, M., Sato, S., Matsushita, K., Tsujimura, T., Fujita, T.,

VI. References

Akira, S. and Takeuchi, O. (2010). LGP2 is a positive regulator of RIG-I– and MDA5-mediated antiviral responses. *Proc. Natl. Acad. Sci. U. S. A.* **107**, 1512–1517.

Sauer, J.-D., Sotelo-Troha, K., von Moltke, J., Monroe, K. M., Rae, C. S., Brubaker, S. W., Hyodo, M., Hayakawa, Y., Woodward, J. J., Portnoy, D. A., et al. (2011). The N-Ethyl-N-Nitrosourea-Induced Goldenticket Mouse Mutant Reveals an Essential Function of Sting in the In Vivo Interferon Response to Listeria monocytogenes and Cyclic Dinucleotides. *Infect. Immun.* **79**, 688–694.

Scherz-Shouval, R. and Elazar, Z. (2011). Regulation of autophagy by ROS: physiology and pathology. *Trends Biochem. Sci.* **36**, 30–8.

Schlee, M. (2013). Master sensors of pathogenic RNA - RIG-I like receptors. *Immunobiology* **218**, 1322–35.

Schlee, M., Roth, A., Hornung, V., Hagmann, C. A., Wimmenauer, V., Barchet, W., Coch, C., Janke, M., Mihailovic, A., Wardle, G., et al. (2009). Recognition of 5′ Triphosphate by RIG-I Helicase Requires Short Blunt Double-Stranded RNA as Contained in Panhandle of Negative-Strand Virus. *Immunity* **31**, 25–34.

Schmidt, A., Schwerd, T., Hamm, W., Hellmuth, J. C., Cui, S., Wenzel, M., Hoffmann, F. S., Michallet, M.-C., Besch, R., Hopfner, K.-P., et al. (2009). 5′-triphosphate RNA requires base-paired structures to activate antiviral signaling via RIG-I. *Proc. Natl. Acad. Sci.* **106**, 12067–12072.

Schoggins, J. W., Macduff, D. A., Imanaka, N., Gainey, M. D., Shrestha, B., Eitson, J. L., Mar, K. B., Richardson, R. B., Ratushny, A. V, Litvak, V., et al. (2014). Pan-viral specificity of IFN-induced genes reveals new roles for cGAS in innate immunity. *Nature* **505**, 691–695.

Schrader, M. and Fahimi, H. D. (2006). Peroxisomes and oxidative stress. *Biochim. Biophys. Acta* **1763**, 1755–66.

Schrader, M. and Fahimi, H. D. (2008). The peroxisome: still a mysterious organelle. *Histochem. Cell Biol.* **129**, 421–40.

Schrader, M. and Yoon, Y. (2007). Mitochondria and peroxisomes: are the "big brother" and the "little sister" closer than assumed? *Bioessays* **29**, 1105–14.

Schrader, M., Baumgart, E., Völkl, A. and Fahimi, H. D. (1994). Heterogeneity of peroxisomes in human hepatoblastoma cell line HepG2. Evidence of distinct subpopulations. *Eur. J. Cell Biol.* **64**, 281–94.

Schrader, M., Burkhardt, J. K., Baumgart, E., Lüers, G., Spring, H., Völkl, A. and Fahimi, H. D. (1996). Interaction of microtubules with peroxisomes. Tubular and spherical peroxisomes in HepG2 cells and their alterations induced by microtubule-active drugs. *Eur. J. Cell Biol.* **69**, 24–35.

Schrader, M., Krieglstein, K. and Fahimi, H. D. (1998a). Tubular peroxisomes in HepG2 cells: selective induction by growth factors and arachidonic acid. *Eur. J. Cell Biol.* **75**, 87–96.

Schrader, M., Reuber, B. E., Morrell, J. C., Jimenez-Sanchez, G., Obie, C., Stroh, T. A., Valle, D., Schroer, T. A. and Gould, S. J. (1998b). Expression of PEX11beta mediates peroxisome proliferation in the absence of extracellular stimuli. *J. Biol. Chem.* **273**, 29607–14.

Schrader, M., King, S. J., Stroh, T. A. and Schroer, T. A. (2000). Real time imaging reveals a peroxisomal reticulum in living cells. *J. Cell Sci.* **113 (Pt 20)**, 3663–71.

Schrader, M., Costello, J., Godinho, L. F. and Islinger, M. (2015a). Peroxisome-mitochondria interplay and disease. *J. Inherit. Metab. Dis.* **38**, 681–702.

Schrader, M., Godinho, L. F., Costello, J. L. and Islinger, M. (2015b). The different facets of organelle interplay—an overview of organelle interactions. *Front. Cell Dev. Biol.* **3**, 1–22.

Schrader, M., Costello, J. L., Godinho, L. F., Azadi, A. S. and Islinger, M. (2016). Proliferation and fission of peroxisomes - An update. *Biochim. Biophys. Acta - Mol. Cell Res.* **1863**, 971–983.

Scott, I. (2009). Degradation Of RIG-I Following Cytomegalovirus Infection Is Independent Of Apoptosis Iain. *October* **11**, 973–979.

Seo, J.-Y., Yaneva, R., Hinson, E. R. and Cresswell, P. (2011a). Human cytomegalovirus directly induces the antiviral protein viperin to enhance infectivity. *Science* **332**, 1093–7.

Seo, J.-Y., Yaneva, R. and Cresswell, P. (2011b). Viperin: a multifunctional, interferon-inducible protein that regulates virus replication. *Cell Host Microbe* **10**, 534–9.

Seth, R. B., Sun, L., Ea, C.-K. and Chen, Z. J. (2005). Identification and Characterization of MAVS, a Mitochondrial Antiviral Signaling Protein that Activates NF-κB and IRF3. *Cell* **122**, 669–682.

Sharon-Friling, R., Goodhouse, J., Colberg-Poley, A. M. and Shenk, T. (2006). Human cytomegalovirus pUL37x1 induces the release of endoplasmic reticulum calcium stores. *Proc. Natl. Acad. Sci. U. S. A.* **103**, 19117–22.

Shi, S. T. and Lai, M. M. C. (2006). HCV 5' and 3' UTR: When Translation Meets Replication. In *Hepatitis C Viruses: Genomes and Molecular Biology* (ed. Tan, S.), pp. 49–87. Norfolk (UK): Horizon Bioscience.

Simmonds, P. (2013). The Origin of Hepatitis C Virus.pp. 1–15. Springer, Berlin, Heidelberg.

VI. References

Sinclair, J. and Sissons, P. (2006). Latency and reactivation of human cytomegalovirus. *J Gen Virol* **87**, 1763–79.

Smith, J. J. and Aitchison, J. D. (2013). Peroxisomes take shape. *Nat. Rev. Mol. Cell Biol.* **14**, 803–17.

South, S. T. and Gould, S. J. (1999). Peroxisome synthesis in the absence of preexisting peroxisomes. *J. Cell Biol.* **144**, 255–66.

Sparkes, I. and Gao, H. (2014). Plant Peroxisome Dynamics: Movement, Positioning and Connections. In *Molecular Machines Involved in Peroxisome Biogenesis and Maintenance*, pp. 461–477. Vienna: Springer Vienna.

Stern-Ginossar, N., Weisburd, B., Michalski, A., Le, V. T. K., Hein, M. Y., Huang, S.-X., Ma, M., Shen, B., Qian, S.-B., Hengel, H., et al. (2012). Decoding Human Cytomegalovirus. *Science (80-.).* **338**, 1088–1093.

Su, G., Morris, J. H., Demchak, B. and Bader, G. D. (2014). Biological Network Exploration with Cytoscape 3. In *Current Protocols in Bioinformatics*, p. 8.13.1-8.13.24. Hoboken, NJ, USA: John Wiley & Sons, Inc.

Sugiura, A., Mattie, S., Prudent, J. and McBride, H. M. (2017). Newly born peroxisomes are a hybrid of mitochondrial and ER-derived pre-peroxisomes. *Nature* **542**, 251–254.

Sun, W., Li, Y., Chen, L., Chen, H., You, F., Zhou, X., Zhou, Y., Zhai, Z., Chen, D. and Jiang, Z. (2009). ERIS, an endoplasmic reticulum IFN stimulator, activates innate immune signaling through dimerization. *Proc. Natl. Acad. Sci. U. S. A.* **106**, 8653–8658.

Sun, L., Wu, J., Du, F., Chen, X. and Chen, Z. J. (2013). Cyclic GMP-AMP Synthase is a Cytosolic DNA Sensor that Activates the Type-I Interferon Pathway. *Science (80-.).* **339**, 786–91.

Sychev, Z. E., Hu, A., DiMaio, T. A., Gitter, A., Camp, N. D., Noble, W. S., Wolf-Yadlin, A. and Lagunoff, M. (2017). Integrated systems biology analysis of KSHV latent infection reveals viral induction and reliance on peroxisome mediated lipid metabolism. *PLOS Pathog.* **13**, e1006256.

Tanaka, Y. and Chen, Z. J. (2012). STING Specifies IRF3 phosphorylation by TBK1 in the Cytosolic DNA Signaling Pathway. *Sci. Signal.* **5**, ra20.

Tanji, Y., Hijikata, M., Satoh, S., Kaneko, T. and Shimotohno, K. (1995). Hepatitis C virus-encoded nonstructural protein NS4A has versatile functions in viral protein processing. *J. Virol.* **69**, 1575–1581.

Tanner, L. B., Chng, C., Guan, X. L., Lei, Z., Rozen, S. G. and Wenk, M. R. (2014). Lipidomics identifies a requirement for peroxisomal function during influenza virus replication. *J. Lipid Res.* **55**,

1357–1365.

Targett-Adams, P., Boulant, S., Douglas, M. W. and McLauchlan, J. (2010). Lipid metabolism and HCV infection. *Viruses* **2**, 1195–217.

Theodoulou, F. L., Bernhardt, K., Linka, N. and Baker, A. (2013). Peroxisome membrane proteins: multiple trafficking routes and multiple functions? *Biochem. J.* **451**, 345–52.

Thiagarajan, V., Valdes, M., Elsby, R., Kakuta, S., Caceres, G., Saijo, S., Iwakura, Y. and Barber, G. N. (2007). Loss of DExD/H Box RNA Helicase LGP2 Loss of DExD/H Box RNA Helicase LGP2 Manifests Disparate Antiviral Responses. *J. Immunol.* **178**, 6444–6455.

Thomas, A. S., Krikken, A. M., van der Klei, I. J. and Williams, C. P. (2015). Phosphorylation of Pex11p does not regulate peroxisomal fission in the yeast Hansenula polymorpha. *Sci. Rep.* **5**, 11493.

Thompson, M. R., Kaminski, J. J., Kurt-Jones, E. a and Fitzgerald, K. a (2011). Pattern recognition receptors and the innate immune response to viral infection. *Viruses* **3**, 920–40.

Thrift, A. P., El-Serag, H. B. and Kanwal, F. (2017). Global epidemiology and burden of HCV infection and HCV-related disease. *Nat. Rev. Gastroenterol. Hepatol.* **14**, 122–132.

Tilokani, L., Nagashima, S., Paupe, V. and Prudent, J. (2018). Mitochondrial dynamics: overview of molecular mechanisms. *Essays Biochem.* **62**, 341–360.

Timpe, J. M., Stamataki, Z., Jennings, A., Hu, K., Farquhar, M. J., Harris, H. J., Schwarz, A., Desombere, I., Roels, G. L., Balfe, P., et al. (2007). Hepatitis C virus cell-cell transmission in hepatoma cells in the presence of neutralizing antibodies. *Hepatology* **47**, 17–24.

Toro, A. A., Araya, C. A., Córdova, G. J., Arredondo, C. A., Cárdenas, H. G., Moreno, R. E., Venegas, A., Koenig, C. S., Cancino, J., Gonzalez, A., et al. (2009). Pex3p-dependent peroxisomal biogenesis initiates in the endoplasmic reticulum of human fibroblasts. *J. Cell. Biochem.* **107**, 1083–1096.

Torres, L. and Tang, Q. (2014). Immediate–Early (IE) gene regulation of cytomegalovirus: IE1- and pp71-mediated viral strategies against cellular defenses. *Virol Sin* **29**, 343–352.

Twig, G. and Shirihai, O. S. (2011). The interplay between mitochondrial dynamics and mitophagy. *Antioxid. Redox Signal.* **14**, 1939–51.

UniProt Consortium (2015). UniProt: a hub for protein information. *Nucleic Acids Res.* **43**, D204-12.

Unterholzner, L., Keating, S. E., Baran, M., Horan, K. A., Jensen, S. B., Sharma, S., Sirois, C. M., Jin, T., Xiao, T., Fitzgerald, K. A., et al. (2010). IFI16 is an innate immune sensor for intracellular

VI. References

DNA. *Nat. Imunol.* **11**, 997–1004.

Valença, I., Pértega-Gomes, N., Vizcaino, J. R., Henrique, R. M., Lopes, C., Baltazar, F. and Ribeiro, D. (2015). Localization of MCT2 at peroxisomes is associated with malignant transformation in prostate cancer. *J. Cell. Mol. Med.* **19**, 723–33.

van der Meer, D. L. M., Degenhardt, T., Väisänen, S., de Groot, P. J., Heinäniemi, M., de Vries, S. C., Müller, M., Carlberg, C. and Kersten, S. (2010). Profiling of promoter occupancy by PPARα in human hepatoma cells via ChIP-chip analysis. *Nucleic Acids Res.* **38**, 2839–2850.

van der Veen, A. G., Maillard, P. V, Schmidt, J. M., Lee, S. A., Deddouche-Grass, S., Borg, A., Kjær, S., Snijders, A. P. and Reis e Sousa, C. (2018). The RIG-I-like receptor LGP2 inhibits Dicer-dependent processing of long double-stranded RNA and blocks RNA interference in mammalian cells. *EMBO J.* **37**, e97479.

Vanhove, G. F., Van Veldhoven, P. P., Fransen, M., Denis, S., Eyssen, H. J., Wanders, R. J. A. and Mannaerts, G. P. (1993). The CoA Esters of 2-Methyl-branched Chain Fatty Acids and of the Bile Acid Intermediates Di-and Trihydroxycoprostanic Acids Are Oxidized by One Single Peroxisomal Branched Chain Acyl-CoA Oxidase in Human Liver and Kidney. **268**, 10335–10344.

Wanders, R. J. A. (2014). Metabolic functions of peroxisomes in health and disease. *Biochimie* **98**, 36–44.

Wanders, R. J. A., Waterham, H. R. and Ferdinandusse, S. (2016). Metabolic Interplay between Peroxisomes and Other Subcellular Organelles Including Mitochondria and the Endoplasmic Reticulum. *Front. Cell Dev. Biol.* **3**, 83.

Waterham, H. R., Koster, J., van Roermund, C. W. T., Mooyer, P. a W., Wanders, R. J. a and Leonard, J. V (2007). A lethal defect of mitochondrial and peroxisomal fission. *N. Engl. J. Med.* **356**, 1736–41.

Wille, P. T., Wisner, T. W., Ryckman, B. and Johnson, D. C. (2013). Human Cytomegalovirus (HCMV) Glycoprotein gB Promotes Virus Entry In Trans Acting as the Viral Fusion Protein Rather than as a Receptor-Binding Protein. *MBio* **4**, 1–9.

Williams, C., Opalinski, L., Landgraf, C., Costello, J., Schrader, M., Krikken, A. M., Knoops, K., Kram, A. M., Volkmer, R. and van der Klei, I. J. (2015). The membrane remodeling protein Pex11p activates the GTPase Dnm1p during peroxisomal fission. *Proc. Natl. Acad. Sci.* **112**, 6377–6382.

Wolff, T., O'Neill, R. E. and Palese, P. (1996). Interaction cloning of NS1-I, a human protein that binds to the nonstructural NS1 proteins of influenza A and B viruses. *J. Virol.* **70**, 5363–72.

Wölk, B., Sansonno, D., Kräusslich, H. G., Dammacco, F., Rice, C. M., Blum, H. E. and Moradpour, D. (2000). Subcellular localization, stability, and trans-cleavage competence of the hepatitis C virus NS3-NS4A complex expressed in tetracycline-regulated cell lines. *J. Virol.* **74**, 2293–304.

Wu, J. Z. (2001). Internally Located Signal Peptides Direct Hepatitis C Virus Polyprotein Processing in the ER Membrane. *IUBMB Life (International Union Biochem. Mol. Biol. Life)* **51**, 19–23.

Wu, J., Sun, L., Chen, X., Du, F., Shi, H., Chen, C. and Chen, Z. J. (2013). Cyclic-GMP-AMP Is An Endogenous Second Messenger in Innate Immune Signaling by Cytosolic DNA. *Science (80-.).* **339**, 826–30.

Xu, L.-G., Wang, Y.-Y., Han, K.-J., Li, L.-Y., Zhai, Z. and Shu, H.-B. (2005). VISA is an adapter protein required for virus-triggered IFN-beta signaling. *Mol. Cell* **19**, 727–40.

Yagita, Y., Hiromasa, T. and Fujiki, Y. (2013). Tail-anchored PEX26 targets peroxisomes via a PEX19-dependent and TRC40-independent class I pathway. *J. Cell Biol.* **200**, 651–666.

Yamamoto, M. (2003). Role of Adaptor TRIF in the MyD88-Independent Toll-Like Receptor Signaling Pathway. *Science (80-.).* **301**, 640–643.

Yonekawa, S., Furuno, A., Baba, T., Fujiki, Y., Ogasawara, Y., Yamamoto, A., Tagaya, M. and Tani, K. (2011). Sec16B is involved in the endoplasmic reticulum export of the peroxisomal membrane biogenesis factor peroxin 16 (Pex16) in mammalian cells. *Proc. Natl. Acad. Sci. U. S. A.* **108**, 12746–12751.

Yoneyama, M., Kikuchi, M., Natsukawa, T., Shinobu, N., Imaizumi, T., Miyagishi, M., Taira, K., Akira, S. and Fujita, T. (2004). The RNA helicase RIG-I has an essential function in double-stranded RNA-induced innate antiviral responses. *Nat. Immunol.* **5**, 730–7.

Yoneyama, M., Kikuchi, M., Matsumoto, K., Imaizumi, T., Miyagishi, M., Taira, K., Foy, E., Loo, Y.-M. Y.-M., Gale, M., Akira, S., et al. (2005). Shared and Unique Functions of the DExD/H-Box Helicases RIG-I, MDA5, and LGP2 in Antiviral Innate Immunity. *J. Immunol.* **175**, 2851–2858.

Yoneyama, M., Onomoto, K., Jogi, M., Akaboshi, T. and Fujita, T. (2015). Viral RNA detection by RIG-I-like receptors. *Curr. Opin. Immunol.* **32**, 48–53.

Yoon, Y., Krueger, E. W., Oswald, B. J. and Mcniven, M. A. (2003). The Mitochondrial Protein hFis1 Regulates Mitochondrial Fission in Mammalian Cells through an Interaction with the Dynamin-Like Protein DLP1. **23**, 5409–5420.

You, J., Hou, S., Malik-Soni, N., Xu, Z., Kumar, A., Rachubinski, R. A., Frappier, L. and Hobman, T. C. (2015). Flavivirus infection impairs peroxisome biogenesis and early anti-viral signaling. *J. Virol.*

VI. References

89, JVI.01365-15.

Zhang, Y. and Chan, D. C. (2007). Structural basis for recruitment of mitochondrial fission complexes by Fis1. *Proc. Natl. Acad. Sci. U. S. A.* **104**, 18526–30.

Zhao, G., An, B., Zhou, H., Wang, H., Xu, Y., Xiang, X., Dong, Z., An, F., Yu, D., Wang, W., et al. (2012). Impairment of the retinoic acid-inducible gene-I-IFN-β signaling pathway in chronic hepatitis B virus infection. *Int. J. Mol. Med.* **30**, 1498–1504.

Zheng, C. and Su, C. (2017). Herpes simplex virus 1 infection dampens the immediate early antiviral innate immunity signaling from peroxisomes by tegument protein VP16. *Virol. J.* **14**, 1–8.

Zhong, B., Yang, Y., Li, S., Wang, Y.-Y. Y., Li, Y., Diao, F., Lei, C., He, X., Zhang, L., Tien, P., et al. (2008). The Adaptor Protein MITA Links Virus-Sensing Receptors to IRF3 Transcription Factor Activation. *Immunity* **29**, 538–550.

Zhou, M.-T., Qin, Y., Li, M., Chen, C., Chen, X., Shu, H.-B. and Guo, L. (2015). Quantitative Proteomics Reveals the Roles of Peroxisome-associated Proteins in Antiviral Innate Immune Responses. *Mol. Cell. Proteomics* **14**, 2535–49.

Zientara-Rytter, K., Ozeki, K., Nazarko, T. Y. and Subramani, S. (2018). Pex3 and Atg37 compete to regulate the interaction between the pexophagy receptor, Atg30, and the Hrr25 kinase. *Autophagy* **14**, 368–384.

Zignego, A. L., Macchia, D., Monti, M., Thiers, V., Mazzetti, M., Foschi, M., Maggi, E., Romagnani, S., Gentilini, P. and Bréchot, C. (1992). Infection of peripheral mononuclear blood cells by hepatitis C virus. *J. Hepatol.* **15**, 382–6.